Spring 1-1-2016

Modeling of Multi-Layered Protection Systems for Chloride Penetration in Concrete Bridge Decks

Ali A. Harajli
University of Colorado at Boulder, ali.harajli@state.co.us

Modeling of Multi-Layered Protection Systems for Chloride Penetration in Concrete Bridge Decks

By

Ali A. Harajli

B.S University of Texas at Austin, 1985

M.S University of Colorado at Boulder, 1987

A thesis submitted to the

Faculty of the Graduate school of the

University of Colorado for degree of

Doctor of Philosophy

Department of Civil, Environmental, and Architectural Engineering

2016

This thesis entitled:

Modeling of Multi-Layered Protection Systems for Chloride-Induced Rebar Corrosion in Bridge Decks

written by Ali Ayoub Harajli

has been approved for the Department of

Civil, Environmental, and Architectural Engineering

_____

Yunping Xi, Committee Chair

_____

Dan Frangopol, Committee Member

_____

Ross Corotis, Committee Member

_____

Mija Hubler, Committee Member

_____

Wil Srubar, Committee Member

Date_____

The final copy of this thesis has been examined by the signatories, and we find that both the content and the form meet acceptable presentation standards of scholarly work in the above mentioned discipline.

Ali Ayoub Harajli (Ph.D., Civil, Environmental, and Architectural Engineering)

Modeling of Multi-Layered Protection Systems for Chloride-Induced Rebar Corrosion in Bridge Decks.

Thesis directed by Professor Yunping Xi.

This paper covers the development of a new methodology for predicting the chloride concentration and corrosion initiation times for a multi-layer protection overlay system.

The first topic will be presenting an innovative method to predict the chloride concentrations using different diffusion coefficients for each protective layer. The new method covers the cases where the applied surface chloride concentrations are either a constant or linear functions with time.

The second topic will implement the results from field data about the chloride variations due to the presence of applied topical layers for comparison with the theoretical models. This section will also apply damage factors that are time-dependent to simulate external factors such as traffic loading or vibrations.

The third topic will investigate the sensitivity of the single and multi-layer systems due to diffusivity parameter changes.

The fourth topic will analyze the random variation of the diffusivity values to predict the mean and standard deviation of chloride concentrations. The diffusivity values are selected from published values by NIST and are based on certain water cement (w/c) ratios.

DEDICATION

To all my family

Ayoub Harajli

Khadijeh Sabra

Mohammed Harajli

Suheir Harajli

Amal Harajli

Rana Sharafeddine

Hussein Harajli

Zain Harajli

Fatima Harajli

Yasmine Harajli

Zachary Harajli

ACKNOWLEDGMENTS

My first and foremost thanks are to Allah The Almighty that had given me the strength and persistence to complete my research.

This would not have happened without the help of my advisor, friend and mentor Prof. Yunping XI. I would like to thank him for his sincere and continuous guidance, support and friendship.

My thanks also go to my co-advisor Prof. Dan Frangopol for his professional support and availability in this effort.

I want to express my sincere thanks to all the committee members for taking the time to be on my committee and provide their sincere and professional suggestions to make this effort come true. I would like to extend my thanks to Prof. Ross Corotis, Prof. Mija Hubler and Prof. Wil Srubar.

Moreover, I would like to thank my friends and colleagues for their help and support.

Also, I would like to thank my immediate family that has provided me the support and help by sacrificing precious time to make my research completion come to its final stages.

Table of Contents

List of Tables

List of Figures

Chapter 1

Organization

Most reinforced concrete members including bridge decks suffer from deterioration that is mainly caused by corrosion. Rust can form on the rebar due to oxidization and with time the volume of rust expands to develop a crack in the concrete member. This crack then grows to reach a crack width that can allow the ingress of chlorides ions to attack the concrete matrix, initiate rust on the rebar and reduce the performance of the member by decreasing its capacity due to cracking. It is the intent of this paper to develop new models for simulating the chloride concentration levels when multiple layers of protection are applied to the concrete base.

Currently, there are no available theoretical models to predict this concentration in the presence of topical application of multiple layers to the concrete surface. The chloride concentration could be constantly applied to the surface and Fick's second law of diffusion can only predict the concentration within any specific layer and there is no direct analytical solution for predicting the chloride concentration when additional topical layers are present.

Few linear models have been found in the literature where the concentrations vary linearly with time and are discussed in this paper. These models are limited to a single layer and can be deemed not suitable for the cases of multiple layer evaluations. However, the results from the new model and the existing models will be compared and discussed for the cases of a single layer application for verification.

It is the intent of this paper to present a new model where the chloride concentrations could be more effectively predicted to determine the service life of a particular concrete member that could be adversely affected by chloride induced corrosion.

This paper covers the development of a new methodology for predicting the chloride concentration and corrosion initiation time estimates in a concrete medium due to the presence of multiple topical layers of protection systems to mitigate the corrosion potential in the steel reinforcing typically present in concrete.

The first topic will be presenting an innovative method to predict the chloride concentrations using different diffusion coefficients for each protective layer. The new method covers the cases where the applied surface chloride concentrations are either a constant or linear functions with time.

The second topic will implement the results from field data about the chloride variations due to the presence of applied topical layers for comparison with the theoretical models. This section will also apply damage factors that are time-dependent to further improve the results of the models, and to simulate external factors such as traffic loading or vibrations that might accelerate the diffusion to match field data.

The third topic will investigate the sensitivity for the single and multi-layer system when certain diffusivity values do change to see which factors has the most influence on the results. The fourth topic will analyze the variation of the diffusivity values to predict the mean and standard deviation values for chloride profile at a specific time step. The diffusivity values are selected from published values by NIST and are based on certain water cement (w/c) ratios.

The diffusivity values selected are for a w/c of 0.45 and are uniformly distributed meaning there are unique values for any one value of the sample data. The diffusivity values of the topical layers will be randomly generated values based on uniform distribution of NIST data and will be used to estimate whether the corrosion initiation threshold has been reached.

Chapter 2 presents a basic overview of the importance of this corrosion damage to the transportation infrastructure and the relevant cost of corrosion to the US economy in general. This chapter summarizes the different deck protection types (membranes, sealers and monolithic concrete) that are used on highway bridge decks. It also explores the different state's experience with these methods, the associated cost and the expected service life.

Chapter 3 explores previous research efforts and available theoretical models in predicting the chloride concentration profiles against, (1) time or (2) distance from the surface, which serves as an indication of the corrosion initiation times.

Chapter 4 describes the development and the derivation of the new non-linear multi-layer model and presents the solutions to the problem. It also presents the capability of the new method to simulate the results from the currently available diffusion equations with no layers or only one layer being applied as a surface treatment.

Chapter 5 focuses on the development and derivation of a theoretical degradation model of materials that could then be used in the models for simulating topical layers as protective layers. A new time scale based on a damage factor will be applied to all topical layers instead of using the real time factor.

Chapter 6 presents the calibration of the model parameters based on field data obtained from test sections on a highway bridge structure. It includes the use of degradation models based on composite damage mechanics. This chapter presents the calibration and recommendation of the optimal product performance based on this theory.

Chapter 7 is a statistical analysis for the computation of the standard deviation for a multi-layer system. This method has been applied to single layer systems but not to a more

complex system with multiple layers. The new analytical method presented shows the methodology of the application to the new multi-layer system.

Chapter 7 presents a numerical method for the computation of the final standard deviation for a multi-layer system. This method assumes that these variables are independent variables and evaluates the slopes of the corrosion initiation time relative to some variables that are part of the multi-layer chloride function. For a given set of standard deviations for these variables, we use the new program to get these slopes relative to each independent variable and use the presented equation to get the aggregate standard deviation of the multi-layer system.

This chapter also presents the sensitivity of the new multi-layer model due to variations of the layer diffusivity. The apparent diffusivity equation includes variables such as the water cement ratio (w/c), the cure time (t_o) and the depth (x). We will investigate which of these variables has the most effect on the results for a wide range of material variations ranging from 10% to 50%. This effort has been done for single layer systems but not for a multi-layer system.

Also in this chapter, random values for the diffusivity of a three layer system have been used to evaluate the mean and standard deviation values for the multi-layer system.

Chapter 8 is reserved as a summary of the current research findings and the suggestions for future research.

Chapter 2

Literature Review of Topical Protection Systems

2.1 Overview

This part of the paper focuses on topical protection systems used on highway bridge decks, to provide a protective layer between the bridge deck and the environments. There are many different topical protection methods, such as low-permeability concrete overlays and waterproof membranes with asphalt overlays. Various types of sealers are also used on bridge decks and substructures in some states in an attempt to keep water and chloride ions from penetrating the concrete. The intent of this overview is to explain the need for better products that can protect concrete against damaging chemicals causing corrosion. The pros and cons of such systems will be later highlighted.

In light of all of the deficiencies regarding these systems, it is the intent of this paper to evaluate the effectiveness of thin bonded polymer overlays to protect bridge decks. These systems often can be applied as a single or multiple layers depending on the longevity of protection desired.

2.2 Cost of Corrosion

Corrosion is a big problem worldwide and is damaging to our infrastructure, mainly horizontal construction such as bridges. These structures are vital to our transportation industry and are a vital network for our economy and others likewise. In the past, cost of corrosion studies has been undertaken by several countries. The earliest study was reported in 1949 by Uhlig

(Uhlig 1952) who estimated the total cost of corrosion to the economy by summing material and procedure costs related to corrosion control. The 1949 Uhlig report, which was the first to draw attention to the economic significance of corrosion, was followed in the 1970s by a number of studies in various countries, such as the United States (NBS Special Publication 511-1 & 511-2), the United Kingdom (Hoar, 1971), and Japan (Okamoto, 1977). The national study by Japan conducted in 1977 followed the Uhlig methodology. In the United States, the Battelle-NBS study estimated the total direct cost of corrosion using an economic input/output framework.

The input/output method was adopted later by studies in two other nations, namely Australia in 1983(Cherry et al. 1983) and Kuwait in 1995 (Al-Kharafi et al. 1995). In the United Kingdom, a committee chaired by T.P. Hoar conducted a national study in 1970 (Hoar, 1971) using a method similar to the one used by Uhlig. The Hoar study estimated the total cost of corrosion by collecting data through interviews and surveys of targeted economic sectors. These previous studies are important in that they confronted the difficult problems in assessing the cost of corrosion and subsequently arrived at judgments regarding the most helpful approach to estimate the annual cost of corrosion relative to any country's GNP. They each contributed to the current knowledge of estimating the cost of corrosion.

2.3 Estimating Total Cost of Corrosion

The corrosion cost is an indication of the level of funding required to tackle this task. The knowledge of such costs and the estimation of the corrosion times can help agancies better plan their repair or replacement activities. According to FHWA records (FHWA-RD-01-156), the total cost of corrosion in the US is about $137.9 billion dollars of which the Transportation sector is $29.7 Billion. The annual cost per category is shown below in the following chart.

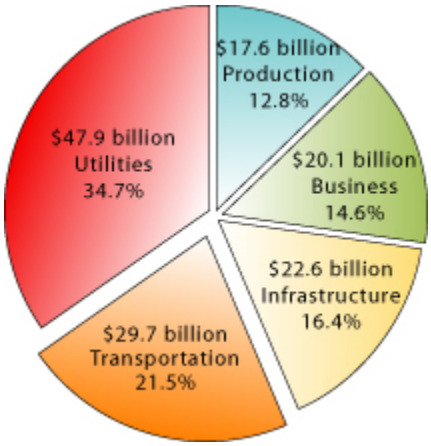

Figure-1 cost of corrosion per category (137.9 Billion, FHWA-RD-01-156).

The major sub sectors of these major subcategories are outlined in the following chart:

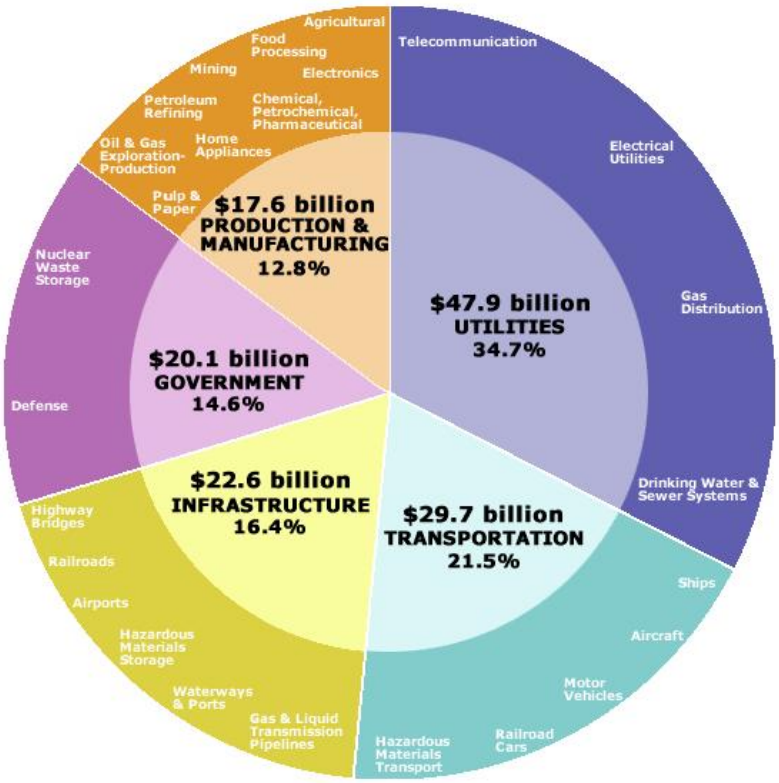

Figure-2 Major Industry categories and sub sectors FHWA-RD-01-156).

The cost of corrosion on highway bridges is considerable. The annual direct cost of corrosion for highway bridges is estimated to be $8.29 billion, consisting of:

- $3.79 billion for the annual cost to replace structurally deficient bridges over the next 10 years,
- $2.00 billion for maintenance and the cost of capital for concrete bridge deck, and
- $2.00 billion for maintenance and the cost of capital for substructures and superstructures (minus decks), and
- $0.50 billion for the maintenance painting cost for steel bridges.

Figure-3 below shows the cost of corrosion for highway bridges relative to the other industry sectors in the Infrastructure category.

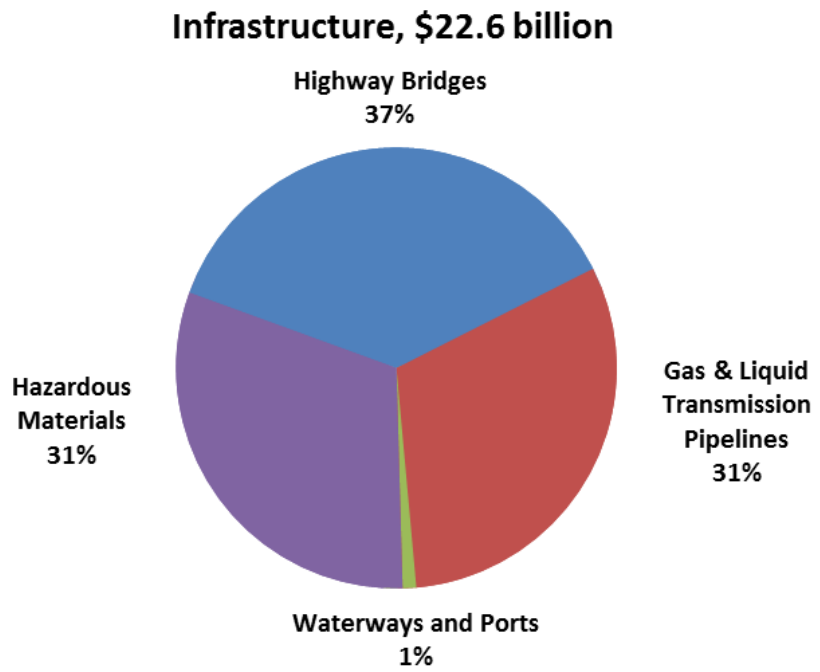

Figure-3 Annual cost of corrosion in highway bridges, (FHWA-RD-01-156).

According to FHWA records, the life-cycle cost analysis (LCCA) estimates indirect costs to the user due to traffic delays and lost productivity at 10 times the direct cost of corrosion (FHWA-RD-01-156). Although the user costs associated with bridge maintenance are greater than indirect costs in other sectors, it illustrates the significant indirect costs associated with corrosion.

The same FHWA report referenced above, presents the direct cost of corrosion per economic sector. Figure-4 below is a summary of direct cost per sector and of particular importance is the highway bridges sector being at 8.3 billion which is 37% of the total annual cost of corrosion for the Infrastructure category. The Highway bridges category cost is about 0.09 % of the 8.8 trillion gross domestic product (GDP) in 1998.

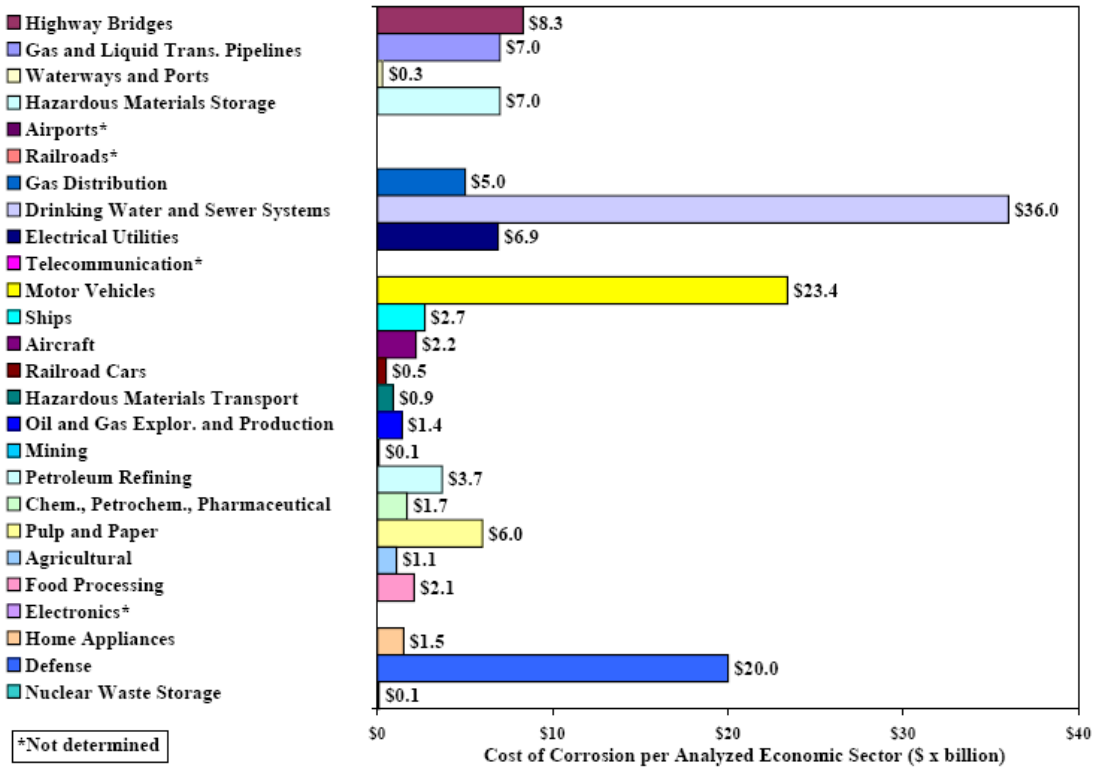

Figure-4 Direct cost of corrosion per industry sectors, (FHWA-RD-01-156).

The total direct cost of corrosion showed large differences between the Bureau of Economic Analysis (BEA) industry categories (see Figure-5). The largest impact is for the transportation and utilities, and manufacturing. Construction is large as well because it is extrapolated assuming the same corrosion cost as transportation and utilities. If the direct corrosion costs are expressed as a percentage of the GDP of the BEA industry category, the relative impact can be shown in Figure-7. The largest relative impact (in percent) is seen for the Transportation and Utilities, Construction, Federal Government, and Manufacturing BEA categories.

Figure-5 below shows the distribution of the GDP among the BEA industry categories studied.

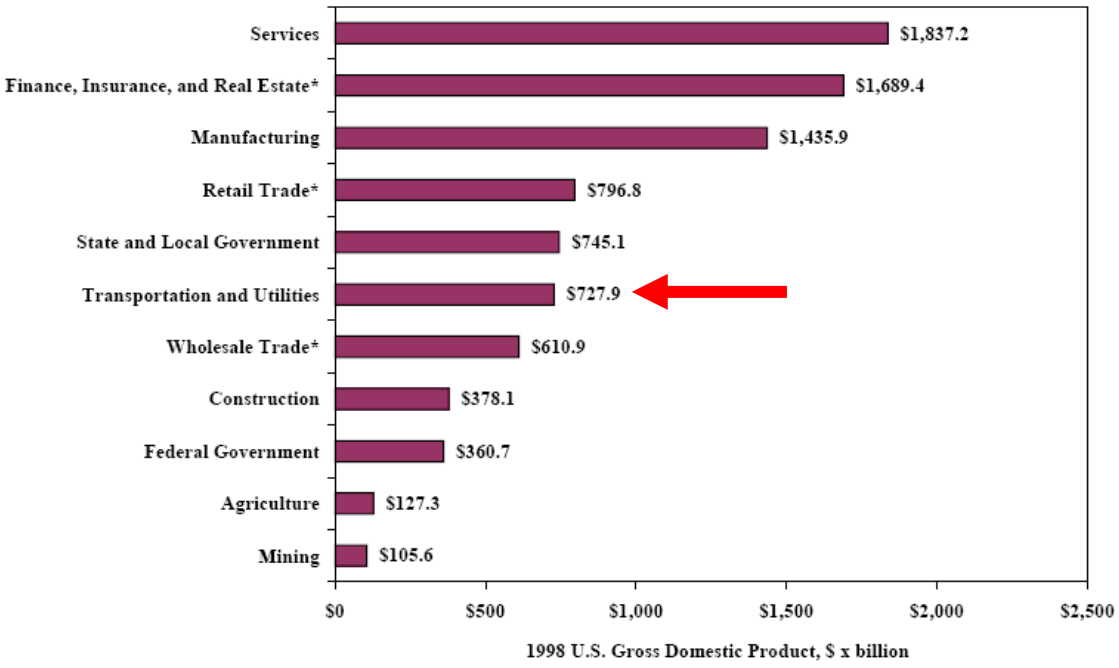

Figure-5 Distribution of 1998 U.S. gross domestic product for BEA industry categories, (FHWA-RD-01-156).

Even though the transportation and utilities category ranks as number 6in the GDP cost ranking in the above distribution, Figure-6 & Figure-7 show that it has the largest impact regarding the cost of corrosion.

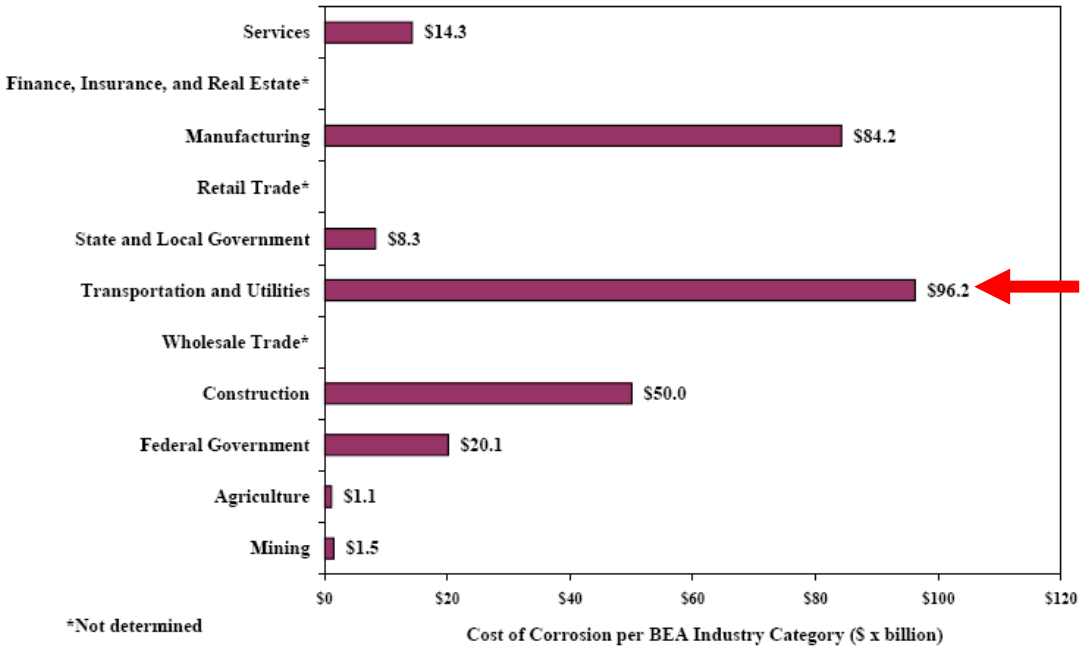

Figure-6 Direct corrosion costs per BEA industry category, (FHWA-RD-01-156).

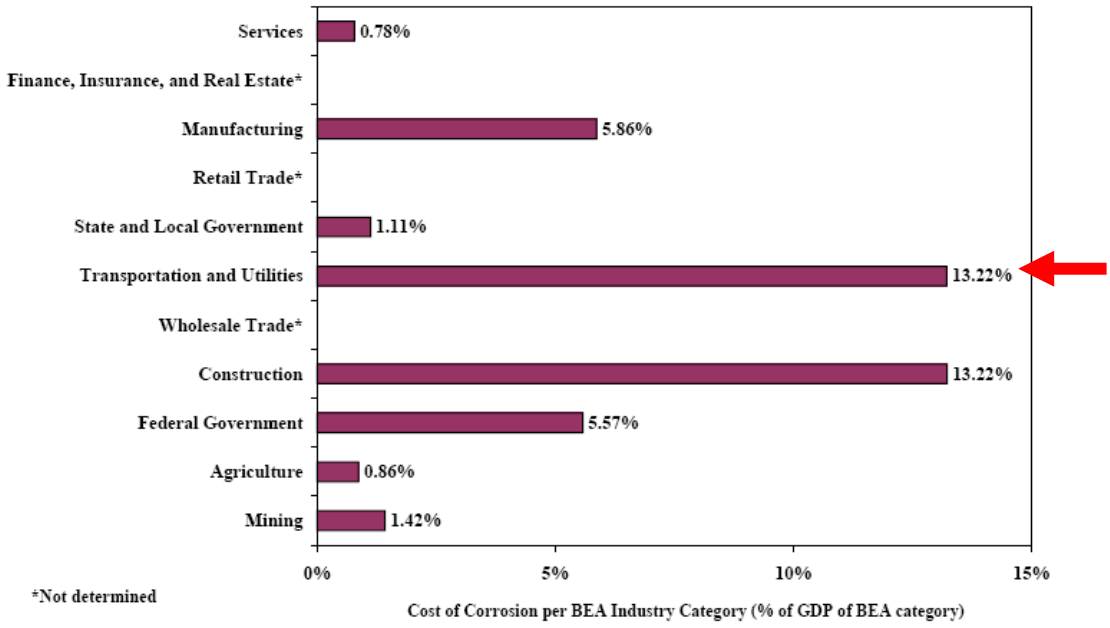

Figure-7 Corrosion costs as a percentage of GDP per BEA industry category, (FHWA-RD-01-156).

The total cost of corrosion in 26-industry sectors was $137.9 billion per year. This estimate was based on detailed analysis of industrial sectors that are known to have a significant corrosion impact. The sum of these sectors represented 27.5 percent of GDP. Based on the procedure for extrapolation, which used the percentage of cost of corrosion for BEA subcategories, an estimated total direct cost of corrosion of $275.7 billion US dollars per year was calculated. In 2013, this cost is about 500 Billion US dollars which is about 3.1% of the 2013 U.S. GDP.

Figure-8 illustrates the impact of corrosion on the nation's economy. The purpose of this figure is to show the relative corrosion impact (3.1 percent) with respect to the total GDP. In fact,

corrosion costs are as great as or greater than some of the individual categories, such as agriculture and mining (see Figure 5).

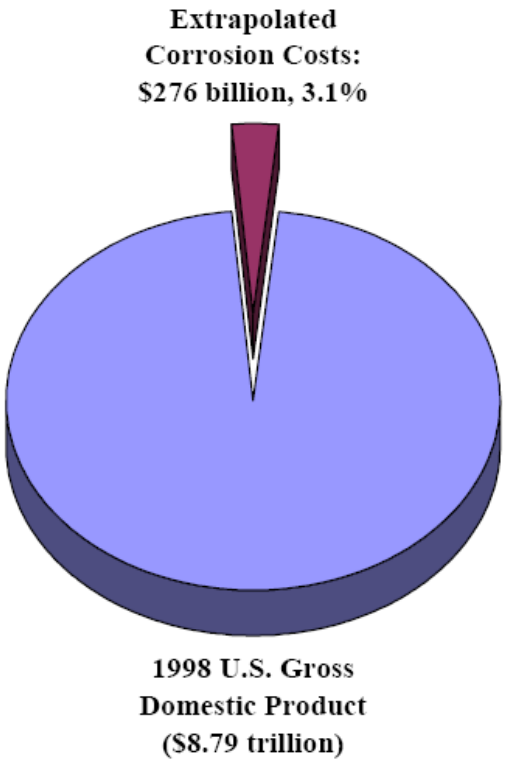

Figure-8 impact of corrosion on the U.S. economy, (FHWA-RD-01-156).

2.4 Background

Concrete bridge decks are long subject to corrosion of reinforcement due to chloride ion intrusion. When concrete decks are not protected with a waterproofing membrane or other protection methods, the chlorides ions used for deicing can take a toll on the protection that concrete provides to steel reinforcing bars. The concrete matrix will be contaminated with a critical level of chloride that can initiate corrosion leading to spalling the concrete cover and requiring rehabilitation. Economics sometimes requires that roads should be opened faster to

accommodate business activities and hence the need to apply deicing chemicals to accomplish this.

2.4.1 Use of Deicers

In recent years, the use of deicers or salts applied on roadways to open it to traffic seems to be a more attractive method to melt ice. This increase in use is usually driven by economic and political reasons to maintain a continuous flow of business that generates revenues for the localities. As a result, this increase in the amount of deicers leads to an increase in the potential of corrosion of most interest for the horizontal construction, and that is mainly for bridge decks. Below is a chart usage of rock salt for deicing in the U.S. in thousands of tons. (Data from the Salt Institute http://www.saltinstitute.org/). This detrimental effect on concrete decks due to the oxidization of the rebar which leads to the start of a corrosion initiation process in the bridge deck is of most interest for my research. This is due to the damage this expansion process creates affecting the service life of a bridge deck.

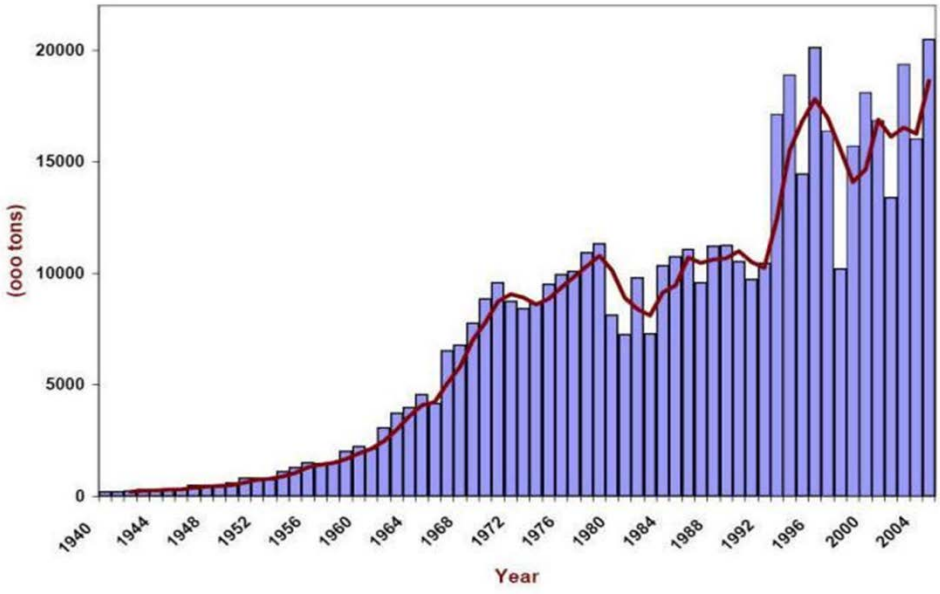

Figure-9 Salt Usage

2.5 Corrosion Initiation

The corrosion initiation is the early stages of deterioration and is of interest to capture this time to mitigate further damage to the asset in question. Since most of the deicing chemicals are mainly applied to bridge decks, I will concentrate on the corrosion initiation related to such assets in this research. To predict future performance of bridge decks, a mathematical model is developed for the corrosion initiation time of the rebar based on lab test samples or currently available bridge deck chloride profiles. When the concentration of chlorides at rebar level reaches the critical concentration, the corresponding time is the corrosion initiation time of the bridge deck.

The model could then be modified to have a time dependent concrete permeability. Among all structural components used for a highway bridge, bridge decks usually deteriorate at the fastest rate and require the most maintenance and repair actions (Yu-chang et al. 2010). This is mainly because bridge decks are exposed to severe environmental conditions such as temperature fluctuation and moisture variation and direct traffic loadings. In addition to the temperature and moisture variations, deicing salts are widely used in some states in the winter months for anti-icing and deicing of bridge decks and pavements, which causes the chloride-induced corrosion of steel reinforcement in bridge decks.

The corrosion of reinforcing bars has been a long-term problem for DOT's. For chloride-induced reinforcement corrosion, chloride ions penetrate into concrete from the environment, and reinforcement in concrete decks begins to corrode once the chloride concentration in the vicinity of reinforcement reaches a threshold value. Using concrete with low permeability is a natural choice of protection for the reinforcing steels. Cracks develop in concrete over time, and

cracked concrete provide a good avenues for chlorides to penetrate down to the rebar and expose the steel to corrosion effects.

2.6 Overlay Categories

There are several methods to protect a horizontal surface against damaging chemicals. The major methods used to prevent bridge decks from corrosion and prolong their longevity can be divided into four different categories:

(A) **Topical protection systems**

These systems are used as barrier methods to protect bridge deck rebar from corrosion damage by preventing water, oxygen, and chloride ions from reaching the reinforcement and initiating corrosion. These types of systems could be cementitious, polymer modified, epoxy, bituminous or polyester concrete.

(B) **Corrosion inhibitors**

Inhibitors are used as a topical application or added to the concrete mix to provide protection by raising the threshold of the critical chloride concentration level.

(C) **Cathodic protection/prevention techniques**

These methods are used either in the form of impressed current and/or external anode to protect the reinforcement. This type of method is effective even when the chloride ion concentration in the vicinity of reinforcement is above the threshold value.

However, while polarization must be high enough to prevent corrosion, cathodic overprotection must be avoided because exposure to excessive current has been shown to lower the bond strength between reinforcement and concrete and to cause hydrogen embrittlement (Kepler et al. 2000).

Hydrogen embrittlement and bond loss are significant concerns in prestressed steel, but they can also affect conventional steel reinforcement. A study by Vrable (1977) indicated the tensile strength of concrete cylinders was not affected by cathodic protection current. The study also indicated that the decrease in bond strength between reinforcement and concrete was affected more by total ampere hour/ft^2 of applied current than by current density.

(D) A**lternative reinforcement steel bars**.

They include materials that electrically isolate the steel from the concrete and create a barrier for chloride ions, materials that provide galvanic protection for the steel, and materials that have significantly higher corrosion thresholds than conventional reinforcing steel. Some of the most viable reinforcement types for mitigating corrosion include stainless steel, carbon or glass fiber reinforcement polymers (CFRP or GFRP) and low carbon micro-composite multi-structural formable (MMFX) rebar.

2.6.1 Waterproofing Membranes

Waterproofing membranes are a popular and a low initial cost alternative to protecting a bridge deck from moisture and deicing salts. These membranes are about 100mills thick and could be asphaltic or polymer based with the former being more popular due to the low initial cost. These membranes could be applies as a liquid or prefabricated sheets. However, some highway departments (Khossrow and Hawkins 1988) have had trouble with debonding of membranes and stripping of asphalt overlays, requiring the removal and replacement of the membrane in ten years or less, depending on both the traffic and the environment.

Other membranes deteriorate after about 15 years of service due to traffic stresses and age embrittlement. One of the major causes of debonding and stripping of the asphalt overlay is

water that is trapped on top of the membrane due to the porosity or cracking of the asphalt overlay itself.

2.6.1.1 Freeze Thaw

Freezing and thawing, along with pressure from traffic weaken the bottom part of the asphalt overlay and the bond between the overlay and the membrane (Khossrow and Hawkins 1988). To prevent this, proper drainage should be provided so that water can drain quickly from the deck, and seepage drains should be provided at low points to prevent water from sitting on top of the membrane (Manning 1995).

2.6.1.2 Blisters

Blisters in the membrane can also be responsible for performace problems. Some transportation departments have also experienced problems with poor wear resistance of asphalt concrete overlays. The properties of the asphalt overlay are important to prevent deterioration and stripping. A high-density overlay with quality aggregate is important, as well as proper seams, compaction, bonding techniques and adequate drainage (Khossrow and Hawkins 1988).

The dead load from an overlay of 2 to 3 inches may be effective in preventing such blisters (NCHRP 1979). Most agencies in North America apply asphalt overlays that are 65 to 80 mm (2.5 to 3.5 inches) thick. These overlays are usually applied in two lifts. The selection of these types of membranes requires a good performance of the overlay for good performance and thus the membrane system becomes a costly maintenance item both in terms of replacement and monitoring.

2.6.1.3 Quality control

Techniques that have been used to prevent blistering include applying the membrane when the deck temperature is higher than the ambient air temperature, such as in the evening or at night, sealing the concrete deck with silane prior to applying the membrane, and minimizing the time between membrane and asphalt placement. In most cases, using a minimum 50 mm (2 in.) asphalt overlay on top of the membrane has been sufficient to keep blisters from forming after the overlay has been placed.

Studies have also shown that protection board, such as a light weight sheets placed on top of the membrane, is effective in reducing damage to membranes during placement and compaction of the asphalt surface and under traffic loads. It is reported that only a few states in the United States require the use of protection board, but it is widely used in Europe and in Canada. It is also recommended that liquid membranes be more than 2 mm (0.08 in.) thick, and preformed membranes be more than 2.5 mm (0.10 in.) thick (Manning 1995).

2.6.1.4 Summary

Asphaltic membrane systems provide a good short term level of protection against chloride penetration but are susceptible to damage from asphalt milling operations when the life of the overlay is reached. The damage from the milling operation presents a threat to the concrete protection levels and can accelerate the rate of corrosion when the damaged membrane traps the moisture or the chlorides underneath and provides an avenue for the chlorides to penetrate via the damaged areas and accelerate the corrosion process. Damaged membranes are difficult and expensive to remove for a repair or replacement option.

2.7 Concrete Sealers

When sealers are used as corrosion protection of concrete highway structures, they have an advantage in the fact that they can be used to protect all of the exposed concrete surfaces of the structure, including bridge decks, substructure members, and deck undersides (Zemajtis and Weyers 1996).

The purpose of a sealer is to reduce corrosion of reinforcement in concrete by preventing capillary action at the surface, therefore preventing water and chloride ions from penetrating the concrete. Sealers can either be pore blockers, forming a microscopically thin (up to 2 mm) impermeable layer on the concrete surface, or they can penetrate into the concrete slightly (1.5 to 3 mm) and act as hydrophobic agents (Zemajtis and Weyers 1996). Most pore blockers are not appropriate for use on bridge decks because they do not offer good skid resistance and do not hold up under traffic wear (Sherman et al. 1993).

An important property of a sealer is its vapor transmission characteristics. Moisture within the concrete may need to be able to pass through the sealer and escape to prevent high vapor pressures from building up in the concrete during drying periods which could cause the sealer to blister and peal (Sherman et al. 1993).

2.7.1 Linseed Oil

In the United States, the first sealer to be used on concrete bridge decks was linseed oil. Linseed oil was first used as a method to reduce scaling of the deck surface as a result of deicer applications. Later, its use was expanded to corrosion protection when it was recognized that deicing salts were causing corrosion problems on bridge decks (Sherman et al. 1993).

Although its use has been discontinued in most states because of environmental reasons or because many engineers feel that it does not work well and is not cost effective (Meggers 1999), linseed oil is still used in some states. Missouri, for instance, applies a mixture of linseed oil and mineral spirits to all new decks before they are opened to traffic, and then again one year later. The linseed oil combination is applied at a rate of 0.23 l/m^2 (0.05 gal/yd^2). According to the Missouri Department of Transportation, other sealers have been tried, but none have worked as well as the linseed oil/mineral oil mixture (Wenzlick 1999).

Texas also uses a linseed oil/mineral spirits mixture as a standard surface treatment on many of its bridge decks. Results of research on the performance of the mixture have varied, but it has generally performed well in regions that are not exposed to frequent deicing salt applications (Cox 2000). Kansas has not used linseed oil on its decks for at least the past 10 years (Zemajtis and Weyers 1996).

Linseed oil works by preventing water and chloride ions from penetrating the concrete, while allowing water vapor to escape. Arguments for the use of linseed oil are that it is a well-known product, that most contractors have had experience with its application, and that it is one of the least expensive corrosion protection strategies available. However, linseed oil does need to be reapplied every 2 to 5 years to maintain its performance (Zemajtis and Weyers 1996), and some engineers question whether it actually provides any protection against corrosion.

Tests indicate that linseed oil requires exposure to ultraviolet light to produce a durable coating (Pfeifer and Scali 1981). Such exposure could be from direct sunlight for curing purposes to enhance performance.

2.7.2 Epoxy

Epoxies have been used as both penetrating sealers and as coatings. Epoxies were chosen for use as sealers because they have good adhesion to concrete, aggregate, and steel, are resistive to chemicals and weather, and cure quickly without requiring high temperatures or pressures (McCaskil et al. 1970).

Problems experienced with epoxy coatings include pinholing, blistering, and debonding from the deck. Epoxy coatings were applied to a number of Kansas bridge decks in a 1970 study (McCaskil et al. 1970). When the coatings were evaluated, they were found to be full of pinholes and to have not sealed the decks.

2.7.3 Silane and Siloxane

Silane and siloxane sealers are silica-based materials that function as hydrophobic agents. Silane and siloxane sealers do not block the pores of the concrete like most oil based sealers, but react chemically with the concrete surface to form a hydrophobic layer under the surface that repels water and chloride ions while allowing water vapor to pass through (McCaskil et al. 1970). Different types of concrete need different coverage rates and different sealers, depending on porosity and capillary size. Siloxanes are simply silanes that have been allowed to polymerize slightly, which makes them larger in size (Sherman et al. 1993).

Proper surface preparation is important when silanes or siloxanes are applied. The deck must be cleaned and be free of all oil, curing compounds, and general road grime to make sure

that the treatment material can actually reach the surface (Sherman et al. 1993). Prescreening tests for an NCHRP study found that concrete coated with silane had a water absorption value that was 30% of the absorption of untreated concrete when the saline was applied to clean concrete.

Absorption increased to 47% of the value for untreated concrete when the silane was applied on top of linseed oil (Pfeifer and Scali 1981). The deck must also be dry to allow the silane or siloxane to penetrate into the concrete and bond with it chemically. Prior applications of silane or siloxane do not need to be removed before reapplication, which is recommended every 5 years (Sherman et al. 1993).

The advantage of silane and siloxane sealers is that they are easy to apply, can be applied to any part of a structure, and can be applied at any time, during or after construction. Disadvantages include surface preparation requirements and the fact that the materials are difficult to screen for best performers without testing. They are also expensive when purchased in small amounts (Sherman et al. 1993).

Sealers are considered a good topical treatment to provide a barrier against chloride intrusion. However, structure like bridges often have cracks larger in size than the sealer can tolerate. Traffic often wear out the sealer mainly in the traffic lanes and require routine reapplication to be effective. A Wisconsin study indicated that only three types of sealers, Hydrozo Silane 40 VOC, Sonneborn Penetrating Sealer 40 VOC and Aquanil Plus 40 are not prone to damage due to freeze thaw action and thus would be acceptable to use (Pincheira and Dorhorst 2005).

2.7.4 Methacrylate

Another sealer that has been used extensively in California, Virginia and Alberta is high molecular weight methacrylate. Methacrylates can function as crack sealers or as fine overlays, using sand and other fine aggregate for skid resistance. Methacrylates are generally applied as a three component system consisting of a monomer, a promoter, and an activator, mixed together before application (Sprinkel 1992b). These types of sealers are usually low-viscosity materials, and are applied as a spray or with a broom or squeegee. (Sherman et al. 1993).

There are some significant problems associated with the use of high molecular weight methacrylates. Over time, cracks tend to reopen through the polymerized material, decreasing the effectiveness of the methacrylate. It should also be noted that treatment will not entirely refill cracks, and will not restore concrete strength that is lost with cracking. Field application problems are encountered with this sealer because most field crews are not familiar with application procedures of methacrylate, are bothered by the smell, and because the set and hardening of the material are highly sensitive to the environment (Sherman et al. 1993).

2.8 Concrete Overlays

With increased traffic costs that could make road closures prohibitive for extended periods of time, faster curing and longer lasting concrete overlays are becoming more economical than traditional methods for protecting concrete bridge decks. In this section, alternate methods are reviewed along with their advantages and disadvantages.

2.8.1 Reinforced Portland Cement Concrete (PCC) Overlay

A reinforced PCC overlay consists of a monolithic layer of PCC with one layer of longitudinal and transverse reinforcing steel. This type of overlay typically is placed with a

minimum thickness of 4.5 in., although a different thickness may be required for dimensional fit or structural adequacy. Typically, a Class D (4500 psi) concrete mix is used for reinforced PCC bridge deck overlays. TDOT specifications require that Class D concrete use Type 1 Portland cement, obtain a 4,000-psi minimum 28-day compressive strength, and maintain a maximum water-to-cement ratio of 0.43 (Knight et al. 2004).. A typical section used for this type of overlay is illustrated below.

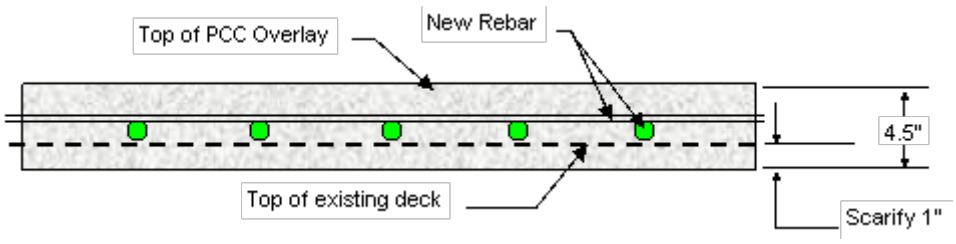

Figure-10 Reinforced PCC Overlay

After completion, this type of overlay and the existing concrete slab will behave in a composite manner. This type of overlay procedure protects the deck because of its thickness and low permeability and also provides additional strength. Based on TDOT practices, reinforced concrete overlays are used as preventive maintenance (sometimes structural repairs) in three general cases.

First, when additional construction activities such as rehabilitation, widening, or safety upgrades are being performed on the bridge structure, the reinforced concrete overlay provides good protection for the deck as well as structural stability and resistance for the upgrades being performed.

Second, concrete overlays are used when a large portion of the deck usually 50% or more is deemed to be in need of repair.

Third, an overlay of this type might need to be used on older bridges. Older bridge decks have four main characteristics that warrant the use of a reinforced concrete overlay: thinner cross sections than decks being designed and constructed today, less clear cover for the top mat of reinforcing steel than current standards require, existing rebar without epoxy coating that is more susceptible to corrosion, and only one layer (bottom) of reinforcing steel may be provided.

Therefore, for older but otherwise useful and adequate bridges, the concrete overlay can be used as preventive maintenance as well as to provide additional structural integrity.

2.9 Thin Bonded Overlays: Epoxy Urethane

Thin bonded overlays typically are proprietary products. Thin bonded overlays can be of two material types: polymer-modified cementitious or polymer modified epoxy. Both consist of a layer/layers of polymer-modified material applied to the prepared (shotblasing usually required) bridge deck and, in some cases (depending on the product being used), a rough fine aggregate applied on top of the compound. Typical overlays of both types are approximately 0.25 in. thick as shown in the figure below.

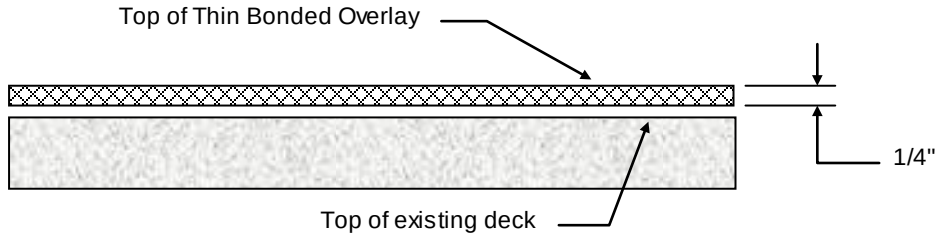

Figure-11 Thin Bonded Overlay system

Because of the polymer-modified material's low permeability and resistance to freeze–thaw and chemical degradation, these overlay options provide a protective layer for the bridge deck. They also provide additional skid resistance.

Thin bonded overlays might be chosen when additional skid resistance is desired, geometric considerations necessitate a thin overlay, or additional dead load is not suitable for the structure being considered.

2.9.1 Montana

In reviewing other states practice regarding the efforts made to assess the effectiveness of epoxy-urethane types of overlays, it is evident that most of these efforts are mainly experimental. There are no effective models to predict the effectiveness of these overlays in inhibiting the chloride ingress in bridge decks. For example, Montana Dot has received a 2 year contract with FHWA to install and monitor the performance of four different materials on a total of 13 bridges at 7 locations on Interstate 90 in south western Montana.

Three types of overlay materials, Thorotop HCR (polymer concrete), Flexolith 216 (epoxy/aggregate system), and MMA (Methacrylate resin/aggregate system) were placed in 1995. The fourth type of overlay material, silica fume concrete, was placed in 1996. In 1997, it was deemed that after one year of placement, the data collected had some conclusions on the poor performance of the Thorotop HCR (polymer concrete) at low temperatures and its low skid resistance. The other products used had an acceptable level of performance.

2.9.2 Alabama

The Alabama Department of Transportation [ALDOT] placed its first bonded bridge deck overlay in 1990, and over the ensuing 8 years has placed such overlays at 10 different locations

in the state. At 7 of these locations, each of 2 twin bridges was overlayed, and at 1 of these 7 locations, the twin bridges were overlayed twice. The service life performance of ALDOT's 19 bonded deck overlays as of 2003 (can be summarized as follows (Ramey and Derickson 2003) :

(1) Thin (6.4 mm or 1/4 in.) urethane polymer concrete (four overlays) provided a service life of 3 years and left much to be desired before the 3 years.

(2) Thin (9.5 mm or 3/8 in.) polyester polymer concrete (12 overlays) has provided highly variable performances. Four of the overlays had a service life of less than 1 year. The remaining 7 overlays are approximately 10 years old and continuing in service, however, most are near the end of their service life.

(3) Thin (9.5 mm or 3/8 in.) epoxy copolymer concrete (Flexogrid) (2 overlays) has provided excellent performance since its application in 1993. Both overlays were 8 years old, located on I-20 bridges, and remained in excellent condition as of the 2001 inspection period.

(4) Thin (12.7–19.1 mm or 1/2–3/4 in.) asphaltic based one layer material, NOVACHIP, was placed in 1998 and has only been in service for 3 years. During this short period, it has and is continuing to perform in an excellent manner.

Thus, a total of 19 overlays were placed during 1990–1998. Of the 19 bonded bridge overlays that the ALDOT has placed on its bridges prior to the summer of 2000, 8 have performed poorly and 11 have performed well. The failure mode for these overlays appears to be one of debonding of patches of the overlay with time.

Thus, when the overlays were inspected in the summers of 2000 and 2001, the only parameter monitored was the bonding of the overlay to the deck. A significant positive feature of both the NOVACHIP and Flexogrid overlays is that the overlay material manufactures and/or

specialty placement contractors work together in placing these currently available overlay materials. All parties are very familiar with the material, placement procedure, and have the specialty equipment needed to do a quality job in a minimal time.

2.9.3 Tennessee

Four types of overlay procedures used in Tennessee have been identified and shown in Table 1. Each of these overlay procedures provides similar benefits for bridge decks that is, the bridge deck is protected from water, chlorides, and other deleterious materials; in some cases, additional structural and skid resistance is added to the bridge deck. General descriptions and applications of each of the methods as well as information about their expected service life, average cost, and frequency of use on Tennessee bridges have been studied.

The results of this study indicate that the overlay methods discussed appear to be valuable preventive maintenance techniques that prolong the service lives of bridge decks in Tennessee. In this 2004 study, the expected life and average cost for these overlays are shown below.

Table-1 Expected Life and Average Cost of Overlay Types

Overlay Type	Expected Life (years)	Average Cost ($/yd^2)
Asphalt (both types)	15 – 20	30 – 40
Reinforced PCC	30+	70 – 80
Nonreinforced PMC	25 – 30	55 – 65
Thin Bonded (both types)	20 – 30	70 – 110

PCC=Polymer Modified Concrete

2.9.4 Michigan

The Michigan DOT has done a Field Performance of Polymer Bridge Deck Overlays in 2003 (Alger et al. 2003). This is an overview of the history of elastomeric coatings, a survey of

current use, and a field survey of existing coated structures is presented. Also, an extensive literature search was made to determine some of the past experiences and changes in the polymer overlay technology.

A survey of existing structures in Michigan is also made prior to a field investigation of several bridges within the state to determine how well these overlays are holding up as well as an investigation of possible "anti- icing" characteristics of the coatings.

The aforementioned Michigan study performed in 2003 covered a large range of efforts pertaining to the use of sealers on bridge decks. One of the most important observations of all of the studies performed during this scope is that research in this area over the previous 15 or more years has improved the development of these systems to a point where they are highly durable and will last long periods of time.

All of the pertinent reports and papers uncovered in this investigation revealed that there is a progression in the materials quality and methods of application. It was difficult to obtain information at the local state level, but enough information was obtained to get an idea of the state-of-practice, at least for most of Michigan.

Methods of application of the overlays have also been significantly fine-tuned by trial and error. Several failures have been observed and reported by others over the years that were a result of poor deck surface preparation prior to coating application.

The major failures examined during this project also appear to be caused by some form of poor surface preparation. This could be wetness or foreign material that was not properly cleaned off prior to application.

The elimination of this failure mode is dependent upon thorough cleaning of the pavement surface by sand or shot blasting, elimination of any prior surface coatings, and making sure that the surface is dry, all seem to aid in developing a good bond.

Double coats have become the norm in most instances. This appears to assure a good seal and good surface structure. It has been a field observation in Michigan that a coating that is too thin can wear out. Durable aggregates such as flint and quartz will prolong the surface life considerably (Alger et al. 2003).

The cost of a full 2 coat overlay on a bridge deck in Michigan has been roughly estimated as $1.25 per square feet for shotblasting, some amount for traffic control, $1.25 per square feet for epoxy, a small cost for aggregate, and a cost for labor. Methods of application are equipment or labor dependent and is being fined tuned to make the job quick and easy.

Currently, truck mounted equipment is designed to mix, meter and dispense material at controlled temperatures for highly predicable mass application at a rate of up to 10,000 square feet per hour or effectively about 50,000 square feet per an 8 hour shift. Previously, it was assumed that a good estimate of time is about 1000 ft2 per day using conventional labor.

Moreover, these systems are quite useful for increasing the friction as well as prolonging the life of a surface by sealing out unwanted moisture and chlorides. Service life must be monitored and performance measures (friction and plow damage) must be evaluated over a period of few years after time of first application. Such performance measures might include but not limited to skid values, visible delaminations and chloride levels at different depths.

These performance measures could be used to improve poor application methods since such newly applied or used materials must be closely monitored in the beginning stages to better

address the needs of proper bridge overlay. Looking at some of the most recent projects and the limited wear on those, it is not hard to envision a 15 year or longer service life.

2.9.5 Cost of Overlays

For designs in which an impermeable layer on the deck surface is wanted, the thin epoxy overlay deck protected strategy is by far the next most practical solution to using monolithic long term concrete overlays. Except for monolithic concrete, the low cost and ease of maintenance of thin bonded overlays make it ideal for all concrete deck bridges and especially post-tensioned segmental concrete bridges (Sprinkel 2002).

Table-2 Cost of deck protection systems for post-tensioned segmental bridges, $/yd^2

Strategy	Grinding	Shotblast	Protection	Skid	Initial	Life, yrs	Life Cycle
Thin Bonded Concrete Overlay	6	6	62	6	80	30	80
Membrane and Asphalt Overlay	6	0	27	18	51	15	96
Thin Bonded Epoxy Overlay (15 yr. Life)	6	6	21	0	33	15	60
Thin Bonded Epoxy Overlay (30 yr. Life)	6	6	21	0	33	30	33
Monolithic Concrete (30 year life)	6	0	24	6	36	30	36
Monolithic Concrete (90 year life)	6	0	24	6	36	90	12
Low Permeability Concrete (90 year life)	6	0	0	6	12	90	4

Advantages of using Thin Bonded overlay systems are:

1. Ease of application where local maintenance forces can easily be trained to do the application, thus reducing the cost of the overlay.

2. Lower prices when compared to similar overlay types as shown in Table above. Depending on the quantity used, the current 2016 prices are usually in the range of 40-60 ($/yd^2).
3. Minimize the additional dead weight imposed by other overlay typed shown above.
4. Minimize the time required for deck preparation as compared with more invasive removal procedures required to remove portions of existing deck surfaces.
5. Similar service life when compared to other overlay types.
6. Damaged Thin Bonded overlay systems can be repaired fairly quicker than other competitive systems.

2.10 Low-Slump Dense Concrete (LSDC) Overlays

2.10.1 Different State's Experience

A review of several states practice using LSDC overlays has revealed many problems related to performance. The following sections summarize the different state's experience (Washington interim report 1986).

2.10.1.1 Missouri

In Missouri, it was reported that percentages of cracks extending into the base concrete were 50% for Latex Modified Mortar (LMM), 29.6% for LSDC, and 14.3% for Latex Modified Concrete (LMC).

2.10.1.2 Washington State

The year of 1986 was the crossroads in the bridge deck overlay program. The seriousness of deterioration of decks did not require an extensive number of overlays until late 1970s and

1980s. LSDC overlays were the main type of overlay used in the early stages of the program although LMC was an option on most jobs. Currently, LMC is the exclusive choice for concrete overlays; however, some experimental applications of thin, polymer/epoxy overlays were performed or planed.

Later, a moratorium was placed on LSDC as an alternate method of overlaying based on some poor results in construction and measured higher permeability.

2.10.1.3 Minnesota DOT

For approximately the last 30 years, Minnesota-DOT has constructed the majority of its girder supported state highway bridge decks using a 7-inch thick structural slab topped with a 2-inch thick LSDC overlay (Rowekamp, 2004). The overlay mixture contains more than 800 pounds of cement per cubic yard, includes the maximum recommended dosage of water reducer, and is placed with a slump of ¾ inches. The mixture is batched at each bridge site by means of a mobile mixer using stockpiled sources of sand and igneous aggregates.

The present system also has some disadvantages, which make the use of alternative materials and methods more appealing. These disadvantages include:

(1) Constructing the slab in two separate lifts requires additional construction time since the structural slab must cure prior to placement of the overlay, and then additional time is needed to cast and cure the overlay concrete. This is sometimes further compounded by restrictions on overlay placement width.

(2) LSDC overlays require the use of specialized equipment (mobile mixer concrete mobile and a heavy-duty finishing machine) which may reduce competition.

(3) Specifications limit the width of a single pass overlay placement to 24 feet for quality control reasons.

(4) Specification cutoff dates limit late season overlay work and reduce the available construction season.

(5) A deck built with a structural slab and overlay costs approximately 5-10% more than a comparably sized 9” monolithic deck placement (comparison of deck cost only, not the cost of the entire bridge).

2.11 Latex-Modified Concrete (LMC)

2.11.1 Physical Properties

Latex-modified concrete (LMC) is a Portland cement concrete in which an admixture of styrene butadiene latex particles suspended in water is used to replace a portion of the mixing water. This type of concrete has been used on highway bridges over the past 45 years.

This type of overlay was first used on a bridge deck in Virginia in 1969. LMC is reported to be more resistant to the intrusion of chloride ions than concrete without latex and have higher tensile, compressive, and flexural strength; and to have greater freeze-thaw resistance (Sprinkel 1998).

The Virginia Department of Transportation’s (VDOT) specification for LMC overlays requires 13.2 l (3.5 gal) of styrene butadiene latex emulsion (46.5 to 49 percent solids) per bag of cement. The specification also requires a minimum cement content of 388 kg/m3 (658 lb/yd3); a maximum water content of 9.5 l (2.5 gal) per bag of cement; a water-cement ratio (w/c) of 0.35 to 0.40; an air content of 3 to 7 percent; a slump of 100 to 200 mm (4 to 6 in) when measured 4.5 minutes after discharge from the mixer; and a cement, sand, coarse aggregate ratio by weight of 1.0/2.5/2.0 (Sprinkel 1998).

2.11.2 Physical Benefits

LMC is reported to be more resistant to the intrusion of chloride ions; to have higher tensile, compressive, and flexural strength; and to have greater freeze-thaw resistance than concrete without latex (Sprinkel 1998). The advantages of using LMC overlays which is referenced to be one of the most popular ways to extend the life of bridge decks is that it inhibits the movement of chlorides to the reinforcement, delaying the initiation process of corrosion.

The resistance to chloride intrusion is mainly due to the lower w/c and the plastic film produced by the latex particles within the concrete. The higher strength is thought to be attributable to the lower w/c and the stronger bond between the paste and aggregate produced by the plastic film. The freeze-thaw resistance is greatly improved and is considered to be superior because the concrete is less permeable to water and is more flexible. These factors enable it to better withstand the expansion and contraction associated with frost action. The following describes the basic components of the different overlays studied.

Table-3 Physical and Chemical Properties of Cements

Type overlay	LMC-VE	LMC-VE	LMC-HE	LMC
Type cement	SB1	SB2	MT-III	MT-II
Chemical analysis (%)				
S_iO_2	15.5	14.55	20.82	21.3
Al_2O_3	12.45	13.15	4.44	4.4
Fe_2O_3	1.41	1.25	2.12	4.3
CaO	51.19	42.33	62.23	63.7
MgO	0.99	2.14	3.24	3
SO_3	14.16	14.96	4.4	2.7
Ignition loss	1.65	1.99	0.9	0.5
Physical analysis Blaine fineness (m2/kg)	642	775	504	365
Compressive strength, MPa (psi) (cubes)				
3 h	25.6 (3720)	14.7 (2130)	-	-
6 h	30.3 (4400)	25.0 (3630)	-	-
1 d	32.9 (4780)	33.1 (4810)	20.7 (3010)	-
3 d	-	-	33.5 (4860)	22.5 (3270)
7 d	44.4 (6440)	44.6 (6470)	40.9 (5930)	27.8 (4040)

Abbreviations:

LMC-VE=Latex Modified Concrete- Vey Early Strength.

LMC-HE=Latex Modified Concrete- High Early Strength.

SB=Special Blend of cements.

MT= Modified Concrete Type.

Very early strength is achieved with the special blended cement because of the fineness and the high Al_2O_3 and SO_3 content. High early strength is achieved with the LMC-HE because of the Type III cement and the higher cement content. However, the additional cost over the cost of Type I/II cements used in the conventional LMC overlays are 400 percent and 20 percent for the special blended cement required for the LMC-VE and the Type III cement used in the LMC-HE respectively. These cements increase the cubic meter cost of the concrete by approximately $120 and $9 (cubic yard, $90 and $7), respectively.

For highway projects where traffic need to be opened fairly quickly, these high early strength overlays might be a promising alternative. Table 4.4-2 below provides the VDOT cost data for four types of overlay systems. According to VDOT records, these costs are more than offset by the large savings in the cost of traffic control (Springel 1998). The cost for traffic control for LMC-VE overlays is the same as that for epoxy overlays. Departments of transportation that spend $5 million per year on deck rehabilitation can save up to $1.25 million per year by using LMC-VE overlays. LMC-VE and LMC-HE overlays can be done for approximately 25 percent less than conventional LMC overlays. Moreover, the epoxy overlays are the least expensive on a life cycle cost basis.

Table-4 Cost of Bridge Deck Protective Treatments, $/m2 ($/yd^2)

Overlay	LMC	Epoxy	LMC-VE	LMC-HE
Treatment	73 (61)	29 (24)	78 (65)	73 (61)
Miscellaneous	28 (23)	0 (0)	28 (23)	28 (23)
Traffic	55 (46)	9 (8)	9 (8)	9 (8)
Total	156 (130)	38 (32)	115 (96)	110 (92)
Life (years)	30	15	30	30
Life cycle	156 (130)	56 (47)	115 (96)	110 (92)
% control	100	36	74	71

2.11.3 Different State's Experience

In Washington State, it was observed that problems with LMC included cracks that ranged from minor to severe across different districts and scaling. In summary, weather conditions such as evaporation rates, contractor's experience and slump control had the most effects on performance (Washington interim report 1986).

In Colorado, field survey information on 10 LMC overlays reported cracking on all overlays within one year. There was a very high rate of salt usage. From a cost benefit perspective assuming a 40 year service life for concrete deck, LMC overlays are more expensive on an annualized cost basis. It was recommended that LMC overlays not be used in Colorado until further evaluation is performed.

2.12 Current Experimental Models

In this experimental study that is a research project managed by the Colorado Department of Transportation, several thin bonded overlay layers are to be investigated for their effectiveness in mitigating chloride ingress. For this study, several concrete slabs will be poured in the lab and will be overlaid with different types of products that are the same products applied on the subject bridge concrete deck. These products are called "thin bonded overlay protection layers" consisting of 3/8" thick single layers as a form of protection from chlorides.

Three field core samples will be collected from the application site located in the Denver area from that bridge deck to compare the non-protected sections and the protected section every six months during the research duration of 18 months to get data points for the analysis. Therefore only three data points are available for our research study to investigate the chloride profiles and the estimation of the corrosion initiation time.

The intent of this research is to measure effectiveness of different overlay products in preventing the ingress of chlorides into the slab and predicting the corrosion initiation times.

2.12.1 Overview Oregon Performance Testing Methods

Attempts in this field have been confined to field data observations by few states and the 2010 results of Oregon (Soltesz 2010) will be presented herein. The objectives of the Oregon investigation are to identify specific thin polymer overlay products that will provide good performance on Oregon bridges and to recommend a method for qualifying future products.

Eight thin polymer overlay systems were evaluated in the laboratory and on two bridge decks exposed to a mix of vehicles including those with studded tires. Among the epoxy type products included in the study were “Mark 154” by Polycarb, “Flex-O-Lith” by Euclid/Tamms Industries, “SafeLane HDX” by Cargill, Urefast PF60 by LiquidConcrete, s “Tyregrip” by Ennis/Prismo, and ProPoxyType III DOT by Unitex. Also, a methyl methacrylate type “Safetrack HW” by Stirling Lloyd, and a polyester concrete type “Kwik Bond PPC-MLS” by Kwik Bond polymers.

2.12.1.1 Water absorption

Water absorption tests were conducted on these resins. The tests were run for five weeks at which time the specimens showed little or no additional water absorption. Table 10 shows the

percent increase in weight due to water absorption after the five weeks. The following table shows the effectiveness of these products as being a potentially viable overlay type for concrete protection against chlorides.

Table 5-Water absorption results of the resins.

Product	Sample 1	Sample 2	Sample 3	Average
Mark 154	5.8	2.9	4.8	4.5
Flex-O-Lith	2.3	2.3	2.1	2.3
Safetrack HW	2.0	1.4	1.3	1.6
Kwik Bond PPC MLS	1.9	1.7	2.0	1.9
Tyregrip	0.9	1.1	1.0	1.0
SafeLane HDX	1.4	1.5	1.3	1.4
Urefast PF60	5.0	5.1	5.0	5.0
Unitex Pro-Poxy Type III DOT	1.3	1.3	1.4	1.3

Note: Values are the percentage increase in weight.

2.12.1.2 Abrasion testing

Abrasion testing in this referenced study was conducted on panels made on-site when the aggregate based overlay sections were installed. Two areas on the panels were tested. The rotating cutter samples were conditioned prior to testing by dragging a crowbar across the surface for three minutes. This procedure was able to knock off the aggregate that were weakly bonded to the overlay system.

This method requires the application of a force of 22 pounds on the cutter, and a rotation speed of 250 rpm to be used. Each test location was abraded for five 2-minute intervals, and the weight loss was measured after each interval. By the last interval, the rate of weight loss had

leveled off. Table 11.2 below reports the average weight loss for the last interval for each of the overlay systems.

Table-6 Abrasion test results.

Product	Aggregate Type	Sample 1	Sample 2	Average
Mark 154	Oklahoma Flint #8	0.7	0.8	0.8
Flex-O-Lith	3M Indag Basalt #8	0.7	0.5	0.6
Safetrack HW	Steilacoom Basalt	0.4	0.5	0.4
Kwik Bond PPC MLS (Newberg)	Steilacoom Basalt + #6-10 Oregon Emery	0.8	0.6	0.7
Tyregrip	Calcined bauxite	0.5	0.6	0.5
SafeLane HDX	Dolomitic limestone	1.3	1.1	1.2
Urefast PF60	Steilacoom Basalt	0.2	0.5	0.3
Unitex Pro-Poxy Type III DOT	#6-10 Oregon Emery	0.4	0.4	0.4

Note: Values are the weight loss in grams during the last two minutes of ten minutes of grinding.

2.13 Summary

The results of this Oregon study indicated the following:

- The Tyregrip and Safetrack HW overlays started to wear through to the concrete after actual exposure of approximately 1.3 million vehicles. Urefast PF60 wore through much sooner.
- For six of the eight products (Tyregrip and Urefast PF60 excluded), empirical equations were developed that could be used to predict friction number as a function of traffic exposure.

- For the five products that did not wear through, none of them performed well under moderate average daily traffic. At a traffic level of 10,000 vehicles per lane per day, the friction number of the best of these five products was predicted to decrease to 40 (average for a bare deck) within five months.
- Tyregrip was the only system that maintained friction numbers (50 and 54) greater than that of the concrete at the end of the field evaluation.
- Delaminations from the concrete were not a major problem with the products.
- Laboratory tests done in this study were not able to predict performance.

Chapter 3

Chloride Diffusion Models

3.1 Existing Linear & Non-Linear Models

Chloride diffusion models have been used to describe the diffusion of chloride ions through concrete samples. Diffusion models calculate the time from the initial chloride exposure to the time of corrosion initiation of the reinforcing steel. Fick's first law of diffusion is expressed below. It is the relationship between chloride ion flux and chloride ionic concentration gradient. The negative sign indicates that the flux J or Fx is positive when moving down the negative gradient. D (L^2/t) is the diffusivity of the material.

$$J = Fx = -D\frac{\partial C}{\partial x} \qquad \text{Eq. (3.1)}$$

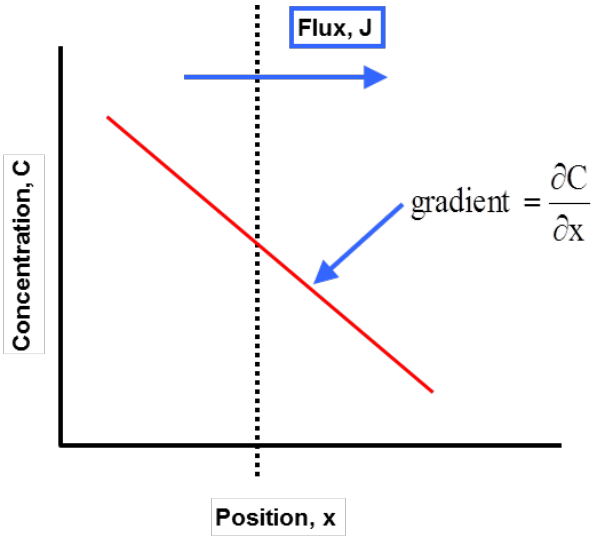

Figure-12 Fick's First Law of Diffusion

Fick's Second law is often used to describe the diffusion of the chloride ions in concrete and is also used to estimate the corrosion initiation time when the critical concentration of chloride (for the onset of steel corrosion) is available.

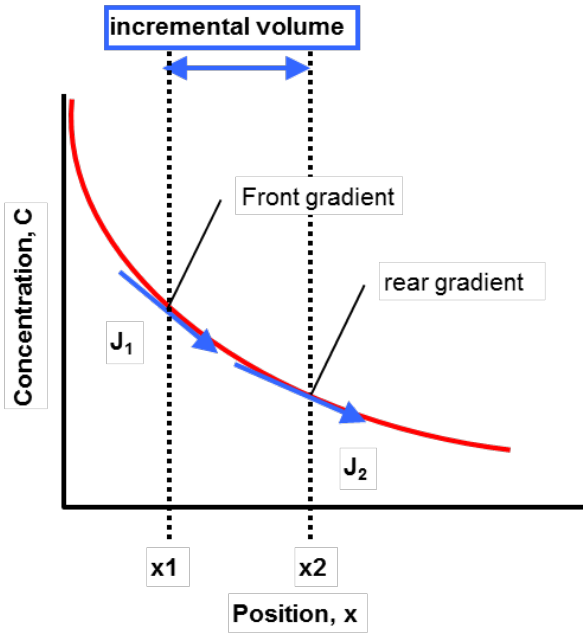

Figure-13 Fick's second Law of diffusion

3.2 General Transport Condition

Showing what was developed by Crank (Crank 1975), we show an element of volume in the form of a rectangular parallelepiped whose sides are parallel to the axis of coordinates and has length 2dx, 2dy, 2dz and the center of this element is located at point P with coordinates(x, y, z), where the concentration of diffusing substance is C. F_x is the rate of transfer through unit area of the corresponding plane through point P(x, y, z). Therefore, the rates at which the diffusing substance enters through the face ABCD and the rate of loss of diffusing substance through the face A'B'C'D' at x-dx & x+dx respectively are:

For face ABCD:

$$2dy.2dz.(Fx - \frac{\partial Fx}{\partial x}.dx) = 4dydz.(Fx - \frac{\partial Fx}{\partial x}.dx) \qquad \text{Eq. (3.2)}$$

&

For face A'B'C'D':

$$2dy.2dz.(Fx + \frac{\partial Fx}{\partial x}.dx) = 4dydz.(Fx + \frac{\partial Fx}{\partial x}.dx) \qquad \text{Eq. (3.3)}$$

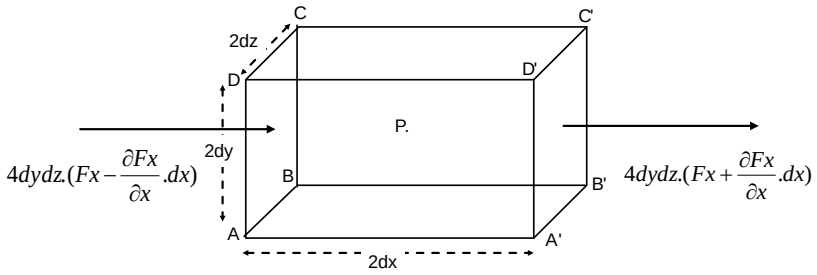

Figure-14 Element of Volume

The contribution to the rate of increase of diffusing substance in the element from these two faces is the difference between these two rates and shown below as:

$$4dy.dz.(Fx - \frac{\partial Fx}{\partial x}.dx) - 4dy.dz.(Fx + \frac{\partial Fx}{\partial x}.dx) = -8dx.dy.dz.(\frac{\partial Fx}{\partial x}) \qquad \text{Eq. (3.4)}$$

The result for the x-direction is shown as:

$$-8dx.dy.dz.(\frac{\partial Fx}{\partial x}) \qquad \text{Eq. (3.5)}$$

Similarly from the other two faces we get:

$$-8dx.dy.dz.(\frac{\partial Fx}{\partial z}) \qquad \text{Eq. (3.6)}$$

and:

$$-8dx.dy.dz.(\frac{\partial Fx}{\partial z}) \qquad \text{Eq. (3.7)}$$

Also, the rate at which the amount of diffusing substance increases in the element is given by:

$$8dx.dy.dz.(\frac{\partial C}{\partial t}) \qquad \text{Eq. (3.8)}$$

Substituting for the different faces and setting equation (3.8) equal to the rate from all faces, we get:

$$8dx.dy.dz.(\frac{\partial C}{\partial t}) = -8dx.dy.dz.(\frac{\partial Fx}{\partial x}) - 8dx.dy.dz.(\frac{\partial Fy}{\partial y}) - 8dx.dy.dz.(\frac{\partial Fz}{\partial z}) \qquad \text{Eq. (3.9)}$$

$$8dx.dy.dz.(\frac{\partial C}{\partial t}) + 8dx.dy.dz.(\frac{\partial Fx}{\partial x}) + 8dx.dy.dz.(\frac{\partial Fy}{\partial y}) + 8dx.dy.dz.(\frac{\partial Fz}{\partial z}) = 0 \qquad \text{Eq. (3.10)}$$

Simplifying, we get the main equation:

$$(\frac{\partial C}{\partial t}) + (\frac{\partial Fx}{\partial x}) + (\frac{\partial Fy}{\partial y}) + (\frac{\partial Fz}{\partial z}) = 0 \qquad \text{Eq. (3.11)}$$

For a given constant diffusion coefficient and applying the theory that the rate of transfer of diffusing substance through a unit area being proportional to the concentration gradient measured normal to the section and equal to:

$$F = -D.(\frac{\partial C}{\partial x}) \qquad \text{Eq. (3.12)}$$

$$\frac{\partial F}{\partial x} = -D.\frac{\partial^2 C}{\partial x^2} \qquad \text{Eq. (3.13)}$$

The general solution for an element of volume as determined from equation (3.11) is:

$$(\frac{\partial C}{\partial t}) + (\frac{\partial Fx}{\partial x}) + (\frac{\partial Fy}{\partial y}) + (\frac{\partial Fz}{\partial z}) = 0$$

Substituting equation (3.13) into equation (3.11), we get the following solution which is Fick's Law of diffusion:

$$\frac{\partial C}{\partial t} = -\frac{\partial}{\partial x}(-D.\frac{\partial C}{\partial x}) - \frac{\partial}{\partial y}(-D.\frac{\partial C}{\partial y}) - \frac{\partial}{\partial z}(-D.\frac{\partial C}{\partial z})$$

$$\frac{\partial C}{\partial t} = D.(\frac{\partial^2 C}{\partial x^2} + \frac{\partial^2 C}{\partial y^2} + \frac{\partial^2 C}{\partial z^2})$$

For a one-dimensional diffusion model where the gradient is only along the x-axis, the equation reduces simply to:

$$\frac{\partial C}{\partial t} = D.(\frac{\partial^2 C}{\partial x^2}) \qquad \text{Eq. (3.14)}$$

Where:

C = the chloride ion concentration at a distance x from the concrete deck surface at time t.

t = time (years)

D = is the apparent diffusion coefficient.

The 1D solution to Fick's second law is used to quantify the diffusion of chloride ions through an infinitely long bar with a boundary condition of constant concentration is shown below as:

$$C(x,t) = C_0 * \left[1 - erf\left(\frac{x}{2\sqrt{tD}}\right)\right] = C_0 * \left[erfc\left(\frac{x}{2\sqrt{tD}}\right)\right] \qquad \text{Eq. (3.15)}$$

This equation relates the chloride content at a distance x from the surface at time t if other variables are known.

The following terms are defined as follows:

C_o = the surface chloride concentration.

D = the apparent diffusion coefficient.

erfc = the complement to the error function,

This solution is for the case of constant surface chloride concentration and an infinite uniaxial diffusion space. In general, bridge decks do no typically follow these conditions in the field, and there are various protective layers on top of concrete deck as described in previous chapter. As a first approximation, let us use this solution to estimate the corrosion initiation time and then develop more accurate solutions.

Setting the distance x to be the depth of concrete cover D_c, the time t to be the initiation time t_o and the critical chloride concentration as C_r the solution to Fick's second law becomes:

$$C(D_c, t_0) = C_0 * \left[1 - erf\left(\frac{D_c}{2\sqrt{t_0 D}}\right)\right] = C_r \qquad \text{Eq. (3.15a)}$$

In general, the concrete deck deterioration consists of two phases, corrosion initiation (t_o) which is related to the penetration of chloride ions from the deck surface to the depth of rebars and crack propagation ($t_1 = t_{cr} + t_{sf}$) which is related to the accumulation of rust around rebars in years. A simple relationship between the "averages" of t_o and Dc for a large number of concrete bridge decks was presented by (Cady and Weyers 1983).

The mean values of D and C_o may be taken as 3.1E-9 in^2/s and 0.218 lbs/ft^3 (6.0 lb/cy) respectively. C_r may be assigned the value of 0.06 lbs/ft^3 (1.5 lb/cy).

The initiation time t_o, could be evaluated as follows:

$$t_0 = \frac{D_c^{\ 2}}{4.D}.\left[erf^{-1}\left(1 - C_r / C_0\right)\right]^{-2} \qquad \text{Eq. (3.15b)}$$

The inverse error function for a variable z could be approximated as follows:

$$erf^{-1}(z) = \frac{\sqrt{\pi}}{2}\left(z + \frac{\pi}{2}.z^3 + \frac{7}{480}\pi^2 z^5 + \frac{127}{40320}\pi^3 z^7\right)$$

Table-7 Coefficients for inverse function with $Z=1-C_r/C_0=0.75$

variable	coeff	coeff	coeff.Z^i
z	a	1.00000	0.75000
z^3	b	0.26180	0.11045
z^5	c	0.14393	0.03416
z^7	d	0.09766	0.01304
z^9	e	0.07330	0.00550

By using Fick's second law of diffusion and using the assumptions below,C_r as the assumed critical chloride threshold for corrosion, C_0=surface concentration, D =Apparent Diffusion coefficient, an estimate for the time to corrosion initiation could be numerically obtained for the cases of 2 and 3 inches of concrete cover, respectively as shown in the table below:

Table-8 Corrosion Initiation Time (Years)

Cr	Co	erf()$^{-1}$	z=1-Cr/Co	Dc.in	D(in^2/s)	T_o.yrs
1.50	6.00	0.8093	0.75000	2	3.10E-09	15.66
1.50	5.00	0.7311	0.70000	2	3.10E-09	19.19
1.50	4.00	0.6269	0.62500	2	3.10E-09	26.10
1.50	3.00	0.4769	0.50000	2	3.10E-09	45.10
1.50	2.00	0.2253	0.25000	2	3.10E-09	202.05

Cr	Co	erf()$^{-1}$	z=1-Cr/Co	Dc.in	D(in^2/s)	T_o.yrs
1.50	6.00	0.8093	0.75000	3	3.10E-09	35.24
1.50	5.00	0.7311	0.70000	3	3.10E-09	43.17
1.50	4.00	0.6269	0.62500	3	3.10E-09	58.73
1.50	3.00	0.4769	0.50000	3	3.10E-09	101.47
1.50	2.00	0.2253	0.25000	3	3.10E-09	454.61

These equations assume a constant diffusion coefficient values. In later sections, we will investigate the effect of damage on diffusivity in the new solution for the multi-layer system to predict the corrosion initiation times.

The total chloride content is comprised of the bounded chloride that are bound to the internal pore surface of cement paste and the free chlorides that can diffuse into the concrete. Since the free chloride is directly related to the transport of chloride into concrete, in this research, we will only consider the free chlorides in the formulation of the basic equation and to get a better estimate for the corrosion initiation time. As discussed earlier, the application of protective layers on the top of the concrete layer will slow down the migration of the chloride ions into the concrete decks, the protective layers and the concrete deck together can be considered as a multiple layered system. The transport parameter, the diffusivity for each layer will be different from other layer and different from the diffusivity of concrete.

Therefore, a theoretical model will be developed for the multiple layered system and will be verified against the solution for the single layer system. In the case that the diffusivity is considered as a constant, we called the solution as a linear model of the system, which could be a single layer or a multiple layer system. In order to consider the effect of aging (such as

environmental loading and/or traffic loading) on the transport properties of concrete and protective layers, the diffusivities can be considered as functions of time. In this case, we called the solutions as time dependent models meaning that the diffusivities are not constants.

3.3 Single and Multiple Linear Layer Systems (Steady State)

As part of our search for existing models, we will show existing steady state models that are deemed primitive when compared to our new model since they are not time dependent as shown in this section. Our new model will not be a steady state model and will be a better tool to estimate the corrosion initiation time. In order to estimate the corrosion initiation time when using a single layer of protection, a steady state model could be used when the following boundary conditions are satisfied in the following model.

3.3.1 Single Layer

In the figure below, the concentration C is shown with its variation against a time scale x. C_1 and C_2 represent the initial and final concentrations in this model. L is the thickness of the considered layer.

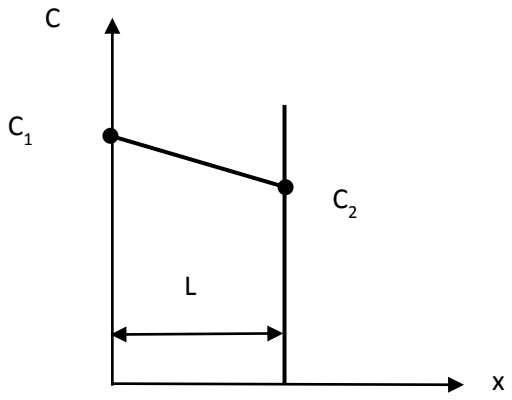

Figure-15 Single Layer

Since concentration varies only in x direction relative to the time scale, the partial-differential equation is the same as the ordinary differential equation (∂C=dC & ∂x=dx).

Therefore, for the case of a single layer and integrating we get:

$$\frac{\partial C}{\partial x} = A_1$$

$$\frac{dC}{dx} = A_1 \qquad \text{Eq. (3.15)}$$

Eq. (3.16)

$$C = A_1 x + A_2$$

If we apply the relevant boundary conditions, then we could solve for the constants A_1 & A_2:

If x=0 then $C=C_1$ and $A_2=C_1$

$$C = A_1 x + A_2 \qquad \text{Eq. (3.16a)}$$

$$x = 0, C = C_1, C_1 = A_2$$

If x=L then $C=C_2$ and solve for A_1

$$x = L, C = C_2 \qquad \text{Eq. (3.16b)}$$

$$C_2 = A_1 L + C_1$$

$$A_1 = \frac{(C_2 - C_1)}{L} \qquad \text{Eq. (3.16c)}$$

The main solution can be expressed as:

Eq. (3.17)

$$C = \frac{(C_2 - C_1)}{L} x + C_1$$

With:

$$\frac{\partial C}{\partial x} = \frac{dC}{dx} = \frac{(C_2 - C_1)}{L} \qquad \text{Eq. (3.17a)}$$

Substituting in the main equation of Fick's first law of diffusion, we get:

$$J = -D\frac{\partial C}{\partial x} = -\frac{(C_2 - C_1)}{\frac{L}{D}} = \frac{(C_1 - C_2)}{\left(\frac{L}{D}\right)}$$ Eq. (3.18)

3.4 Multiple Layers in Series

The following is a schematic of a system of layers in series for considering the chloride diffusion process. In the figure below, the concentration C is shown with its variation against a time scale x. C_i , C_{i+1} represent the initial and the final concentrations within a layer length L_i in this model.

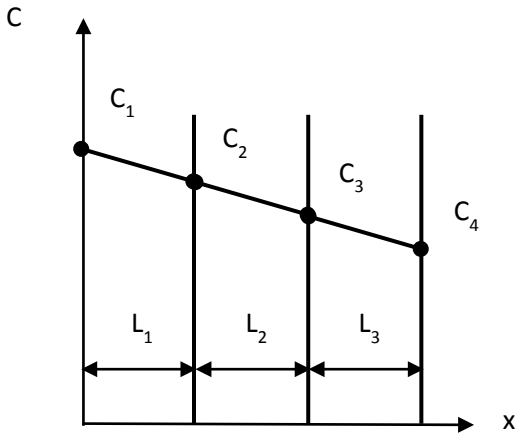

Figure-16 Composite Layers

If we apply this method to each layer in series with lengths and diffusion coefficients L_1, L_2 and L_3 and D_1, D_2 and D_3 respectively and where the flux is constant, then we can write the following equations:

Eq. (3.19)

$$J = \frac{(C_1 - C_2)}{\left(\frac{L_1}{D_1}\right)} = \frac{(C_2 - C_3)}{\left(\frac{L_2}{D_2}\right)} = \frac{(C_3 - C_4)}{\left(\frac{L_3}{D_3}\right)}$$

Eq. (3.20)

$$J = \frac{(C_1 - C_4)}{\left(\frac{L_1}{D_1}\right) + \left(\frac{L_2}{D_2}\right) + \left(\frac{L_3}{D_3}\right)}$$

This solution is not time dependent and a more realistic model where the time "t" is a variable that will be used in this study.

3.5 Existing Linear and Time Dependent Models

3.5.1 Linear Model#1

This method proposes to use a constant k (a sealer characteristic constant) representing the chloride ingress rate through the sealed surfaces. The solution for the semi-infinite medium with surface concentration that varies with time is obtained by the Laplace transform of the diffusion equation (Zemajatis et al. 1999). The solution equation is presented as follows:

$$C(x,t) = k\sqrt{t} * [e^{-x^2/4D_c t} - \frac{x\sqrt{\pi}}{2\sqrt{D_c t}}\left(1 - erf\ \frac{x}{2\sqrt{D_c t}}\right)] \qquad \text{Eq. (3.21)}$$

Where:

C = chloride concentration (pcy=pounds per cubic yard).

D_c = diffusion constant (in^2/year).

t = time (years).

x = depth in question (inch).

k = sealer characteristics constant (lb/cy/yr$^{0.5}$).

In this new study, a multi-layer system will be introduced where layer thicknesses and modified diffusion coefficients could be introduced and also varied based on damage theory for the analysis and conclusions. The above model using equation (3.21) will not be used for comparison with our new model and is shown herein for reference only.

3.5.2 Linear Model#2

Another available model developed (Liang et. al 1999) for predicting the chloride levels in concrete after the application of a protective layer is based on the following equation:

$$C(x,t) = kt\left[(1+\frac{x^2}{2D_c t})erfc(\frac{x}{2\sqrt{D_c t}}) - (\frac{x}{\sqrt{\pi D_c t}})e^{-\frac{x^2}{4D_c t}}\right] \qquad \text{Eq. (3.24)}$$

Where:

C = chloride concentration (pcy=pounds per cubic yard).

Dc = diffusion constant (in^2/year).

t = time (years).

x = depth in question (inch).

k = sealer characteristics constant (lb/cy/yr$^{0.5}$).

The above model using equation (3.24) will be used as model#2 for comparison with our new model that uses a linear boundary condition in later sections.

3.6 Constant Boundary Condition for Surface Chlorides

The existing theoretical models are not tailored for predicting the chloride levels in a concrete specimen when protected with more than one layer if subjected to a variable chloride concentration. The non-linear model developed by Fick and known as Fick's second law of diffusion will be used as the basis for developing a new multi-layer protection model. The newly developed model will be capable of predicting the chloride concentration at any level using different boundary conditions for the initial concentration.

In this paper, the newly innovative model presented herein, can model the scenario where another layer is applied to the concrete layer to prolong its life and act a barrier against chloride intrusion. The benefit of this model is that it could predict the time when the critical chloride concentration is reached for proper action by maintenance forces to mitigate the corrosive effect of the chlorides and apply specific mitigation strategies before the sample is far beyond repair.

For verification purposes of the newly developed model, below is a simulation for the case of a constant surface application of chlorides and the effect of increasing the diffusion coefficient in the top most layers. The depth of 1.25" is selected for comparison and to evaluate the difference in chloride concentrations between the case of applying additional layers for protection and that of no layers.

The top most layer is divided into two equal layers with a simulated diffusion coefficient as three times greater, D1=D2=6 (in^2/year), than the concrete or base layer which has a diffusion coefficient of D=2(in^2/year). These top two layers have a thickness of 3/8" each which makes up a total thickness of ¼" in this case. The figure below shows, as expected, the decrease in concentration relative to the case of no layer. The diffusion coefficient of the base or concrete layer is kept as constant and equal to 2.

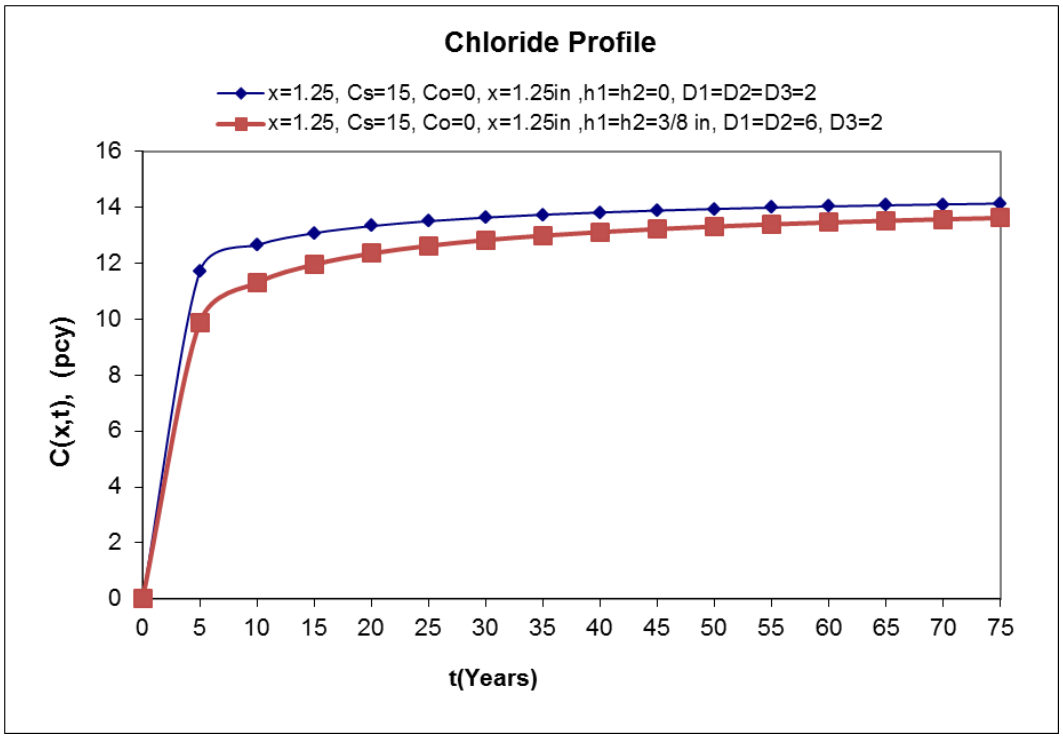

Figure-17 Effect of adding top layers.

The above figure terms are:

D_i= diffusion coefficient of an overlay layer ($in^2/yr.$).

h_i= thickness of an overlay layer (in.).

$C_s(x,t)$ = Surface chloride concentration in pounds per cubic yards (pcy).

$C_o(x,t)$ = Initial chloride concentration in pounds per cubic yards (pcy).

Therefore, a better model is now available to predict the chloride concentrations at any level for a system of protection with more than one layer and which did not exist before.

3.7 New Linear Model Comparison with Model#2

The figures below compare Fick's second law to the case of a time dependent force function presented as:

$$C(x,t) = kt\left[(1+\frac{x^2}{2D_c t})erfc(\frac{x}{2\sqrt{D_c t}}) - (\frac{x}{\sqrt{\pi D_c t}})e^{-\frac{x^2}{4D_c t}}\right] \quad \text{Eq. (3.24)}$$

The above equation is evaluated for the predicted chloride concentration with the following values:

D= Diffusion coefficient = 1.0 in^2/yr.

$C_{surface}$= C_0 =15 pcy (Fick's second Law with constant boundary condition)

t= 25 years (arbitrary).

For equation (3.24), using k = 1.25 & k=3.

$C_{surface}$= kt (Boundary condition for Eq. (3.24).

t = 25 years (arbitrary).

The following figure shows the variation of the chloride concentrations for different boundary conditions and models. This is to show the trend in each of the investigated diffusion models with the linear and constant boundary conditions.

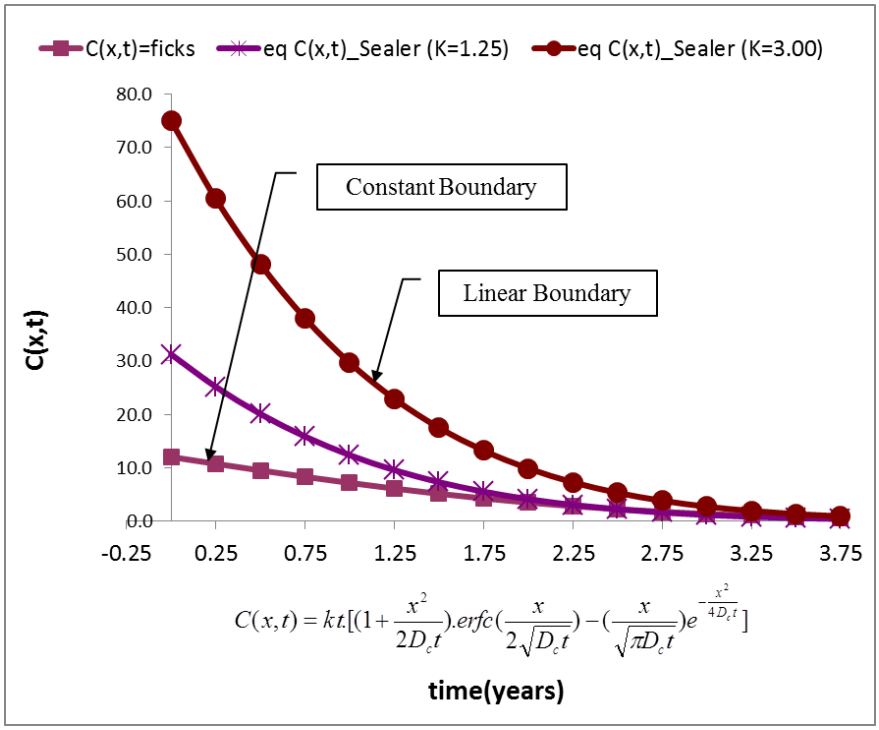

Figure-18 Chloride profile variation with depth

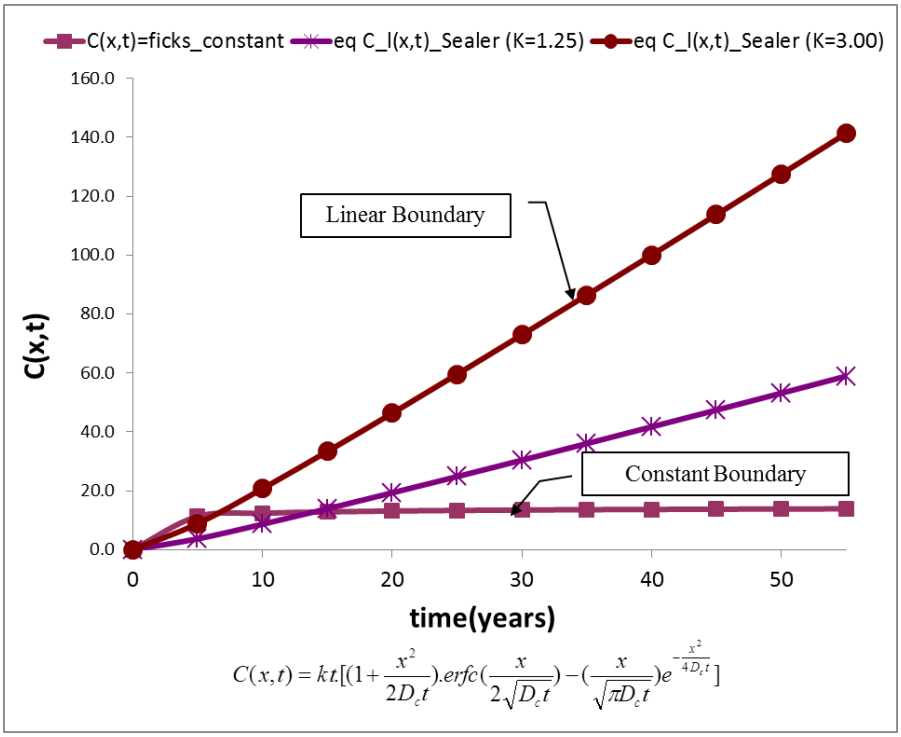

Figure-19 Chloride profile variation with time

Equation (3.24) yield similar results to equation (3.21) since there are both using a time dependent force functions. These models show a concentration that increases with time and Fick's second law with a constant concentration reaches a steady state after some years along the time axis.

These models lack the capability of explicitly using the properties of an applied topical layer or multiple layers that do have specific diffusivity and thickness values. These values will be used in our new model to predict the corrosion initiation times in porous media having reinforcement such as in bridge decks.

Later in this study, the newly developed models that are capable of modeling multiple layers and variable surface boundary conditions, constant or linear, will be evaluated against the aforementioned existing time dependent force function models. Our main research will focus on the constant boundary condition case.

We have shown herein that there are better methods to predict the chloride concentrations even with other boundary conditions for the multi-layer system.

Chapter 4

New Multi-layer Model

A new diffusion model based on Fick's law for a multi-layer system will be developed. Laplace transform will be used to obtain the analytical solution with given initial and boundary conditions. The main advantages of this new model are that it is a general solution that can be used for N-layered system, and that it can be used for any transport problem that can be characterized by the diffusion equation (heat conduction, moisture transfer, and diffusion of chemicals). The model prediction will be compared with the results from lab and field evaluations. The new model will be used to predict the chloride diffusion through multiple layers of overlays with different diffusion coefficients and thicknesses.

The new model can predict chloride concentration profiles in a system with the following features:

1) Multiple topical layers with different thicknesses
2) Individual layers having specific diffusion coefficients that are either:
    a. Constant in value or
    b. Time dependent with a damage factor to simulate deterioration of the material.
3) Layers that have specific material properties.

The following notations are designed to represent the material parameters and geometries of the layers in a multi-layer system:

Di =Diffusion coefficient for layer i,

Ci = Chloride concentration at the top of layer, i,

li = thickness of layer, i

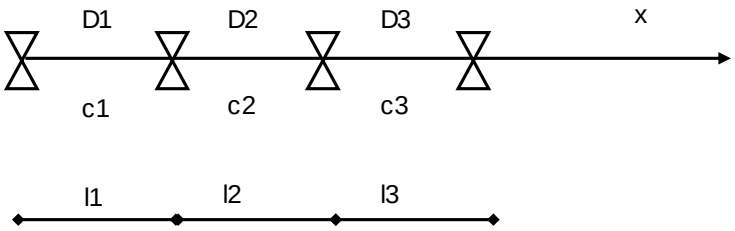

Figure-20 Layer layout

The following figure shows the field installation of a topical layer on top of a concrete bridge deck. It is possible to apply multiple layers for added protection and increased service life.

Figure-21 Topical layer application

4.1 Constant Boundary Condition

We will solve the problem of constant boundary condition first and then consider time dependent boundary conditions. The diffusion equations, the initial and boundary conditions are listed for three layers, and they can be extended to N-layered system if necessary.

4.1.1 Layer #1

For the first layer, we will formulate the diffusion equation, the boundary and initial conditions as follows:

$$\frac{\partial C_1}{\partial t} = D_1 \frac{\partial^2 C_1}{\partial x^2}, (l_1 \le x \le l_2) \qquad \text{Eq. (4.1)}$$

Boundary and initial conditions of_Layer#1

$$C(l_1, t) = C_s \qquad \text{Eq. (4.1a)}$$

$$C(x, 0) = C_0 \qquad \text{Eq. (4.1b)}$$

Where:

C_s= Surface concentration.

C_0= Initial concentration

4.1.2 Layer #2

For the second layer, the equation and the initial condition remain the same, and the boundary condition is different:

$$\frac{\partial C_2}{\partial t} = D_2 \frac{\partial^2 C_2}{\partial x^2}, (l_2 \le x \le l_3) \qquad \text{Eq. (4.2)}$$

Boundary Condition_Layer#2:

$$C_1(l_2,t) = C_2(l_2,t) \qquad \text{Eq. (4.2a)}$$

4.1.3 Layer #3

For the third layer, we will formulate the boundary conditions as follows:

$$\frac{\partial C_3}{\partial t} = D_3 \frac{\partial^2 C_3}{\partial x^2}, (l_3 \le x) \qquad \text{Eq. (4.3)}$$

Boundary conditions_Layer#3:

$$C_2(l_3,t) = C_3(l_3,t) \qquad \text{Eq. (4.3a)}$$

$$C_3(\infty,t) = C_0 \qquad \text{Eq. (4.3b)}$$

$$C_1(l_2,t) = C_2(l_2,t) \qquad \text{Eq. (4.3c)}$$

The ratios of diffusion coefficients are expressed as

$$\sigma_1 = \sqrt{D_1 / D_2} \qquad \text{Eq. (4.3d)} \qquad \sigma_2 = \sqrt{D_2 / D_3} \qquad \text{Eq. (4.3e)}$$

The differences in layer thicknesses are expressed as

$$h_1 = l_2 - l_1 \qquad \text{Eq. (4.3f)} \qquad h_2 = l_3 - l_2 \qquad \text{Eq. (4.3g)}$$

The solution process is lengthy and is listed in Appendix A, and can also be found in (Bai, Harajli, & Xi, 2015). The final solution for the concentration of chloride ions in the concrete (or the third layer) is expressed as:

$$C(x,t) = C_s - \frac{2(C_s - C_0)}{\pi}\int_0^{\infty} F_3(x,t,u)du \qquad \text{Eq. (4.4)}$$

Where:

$$W_3(u) = \frac{-1}{\sigma_1}\sin(u\sigma_1 h_2)\sin(uh_1) + \cos(u\sigma_1 h_2)\cos(uh_1)$$

$$V_3(u) = \frac{-1}{\sigma_1\sigma_2}\cos(u\sigma_1 h_2)\sin(uh_1) + \frac{1}{\sigma_2}\sin(u\sigma_1 h_2)\cos(uh_1)$$

$$F_3(x,t,u) = \frac{e^{-u^2Dt}[\cos(\sigma_1\sigma_2 u(x-l_3))V_3(u) + \sin(u\sigma_1\sigma_2 u(x-l_3))W_3(u)]}{u(W_3^{\,2}(u) + V_3^{\,2}(u))}$$

Where the following parameters are defined as follows:

σ_1 = (Diffusivity of Layer#1/ Diffusivity of Layer#2)$^{1/2}$= $(D_1/D_2)^{1/2}$

σ_2 = (Diffusivity of Layer#2/ Diffusivity of Layer#3)$^{1/2}$= $(D_2/D_3)^{1/2}$

h_1 = Thickness of layer#1= Distance of Layer#2- Distance of Layer#1= $l_2 - l_1$

h_2 = Thickness of layer#2 = Distance of Layer#3- Distance of Layer#2 = $l_3 - l_2$

C_s = Surface concentration (lb/yd^3).

C_0= Initial concentration present (lb/yd^3).

x = depth below the surface (inch)

t = time (years)

u= Gauss Integration variable (arbitrary).

The analytical solution was programed for this research effort with user defined input parameters such as the diffusion coefficients and layer thicknesses describing the properties for each layer. The program flow chart is presented in Appendix B. This model is innovative in the sense that it enables the prediction of the chloride levels and the corrosion initiation times for the cases where a protective layer or layers is applied on top of the concrete surface.

The figures below show the match of the new multi-layer model prediction with the solution of single layer system, Eq. (3.15a) at depths of 1.00 inches, 2.00 inches and 3inches from the surface of the concrete sample. The different layers are assumed to have the same diffusion values to resemble a one layer system for verification purposes.

The following tables show the new model prediction results where the heading shown as "Pgm C(x,t)_1"; D1=D2=D3" as the new results in (lb/yd^3) evaluated at a depth of 1.00 inch below the surface. The second column heading shown as "C(x,t)=Ficks_1"; D1=D2=D3" as the result from the one layer solution. The following is the result for a depth of 1 inch.

Table-9 Chloride levels: New multi-layer model vs. single layer at x = 1.00 in."

t	Pgm C(x,t)_1"; D1=D2=D3=1	C(x,t)=_Ficks_1"; D1=D2=D2=1
0	0.00	0.00
5	11.28	11.28
10	12.35	12.35
15	12.83	12.83
20	13.12	13.12
25	13.31	13.31
30	13.46	13.46
35	13.57	13.57
40	13.66	13.66
45	13.74	13.74
50	13.81	13.81
55	13.86	13.86
60	13.91	13.91
65	13.95	13.95
70	13.99	13.99
75	14.02	14.02

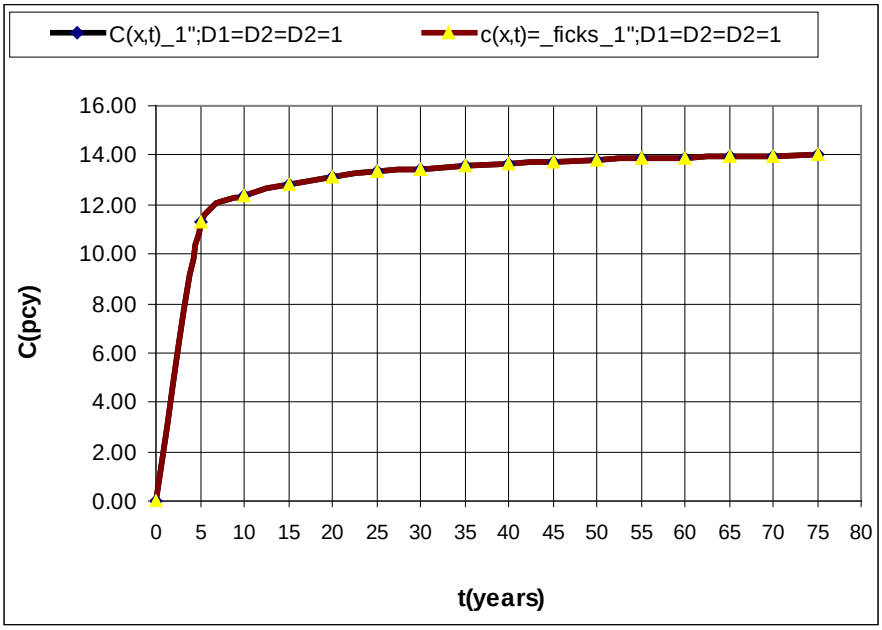

Figure-22 Comparison of results of the new multi-layer model and the single layer solution at x = 1.00 in.

The following table shows the results from using the new multi-layer model and the single layer known as Fick's second law of diffusion. The results are for the case of evaluating the concentration close to the location of the top rebar in a bridge deck.

Table-10 New multi-layer model vs. single layer at x = 2.00 in

t	Pgm C(x,t)_2"; D1=D2=D3=1	C(x,t)=_Ficks_2"; D1=D2=D2=1
0	0.00	0.00
5	7.91	7.91
10	9.82	9.82
15	10.73	10.73
20	11.28	11.28
25	11.66	11.66
30	11.94	11.94
35	12.17	12.17
40	12.35	12.35
45	12.50	12.50
50	12.62	12.62
55	12.73	12.73
60	12.83	12.83
65	12.91	12.91
70	12.99	12.99
75	13.05	13.05

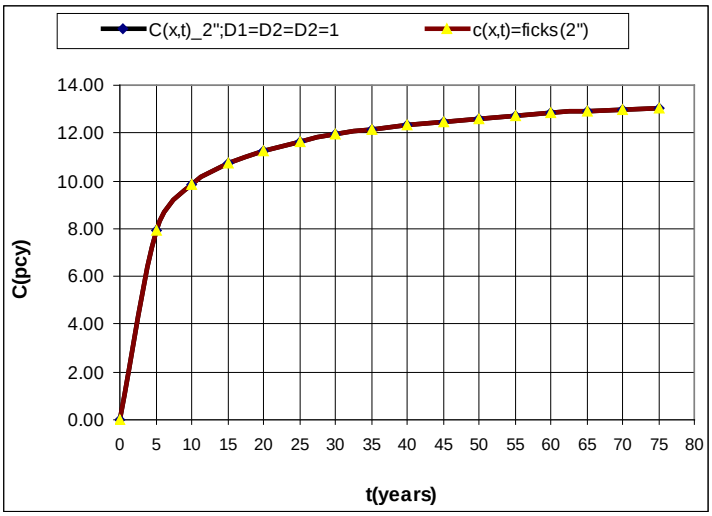

Figure-23 Comparison of new multi-layer model and the single layer solution at x = 2.00 in.

The following table is the result for the chloride concentration at a depth of 3 inch.

Table-11 Chloride levels: New multi-layer model and the single layer solution at x = 3.00 in

t	Pgm C(x,t)_3"; D1=D2=D3=1	C(x,t)=_Ficks_3"; D1=D2=D2=1
0	0.00	0.00
5	5.14	5.14
10	7.54	7.54
15	8.76	8.76
20	9.53	9.53
25	10.07	10.07
30	10.48	10.48
35	10.80	10.80
40	11.06	11.06
45	11.28	11.28
50	11.46	11.46
55	11.62	11.62
60	11.76	11.76
65	11.89	11.89
70	12.00	12.00
75	12.10	12.10

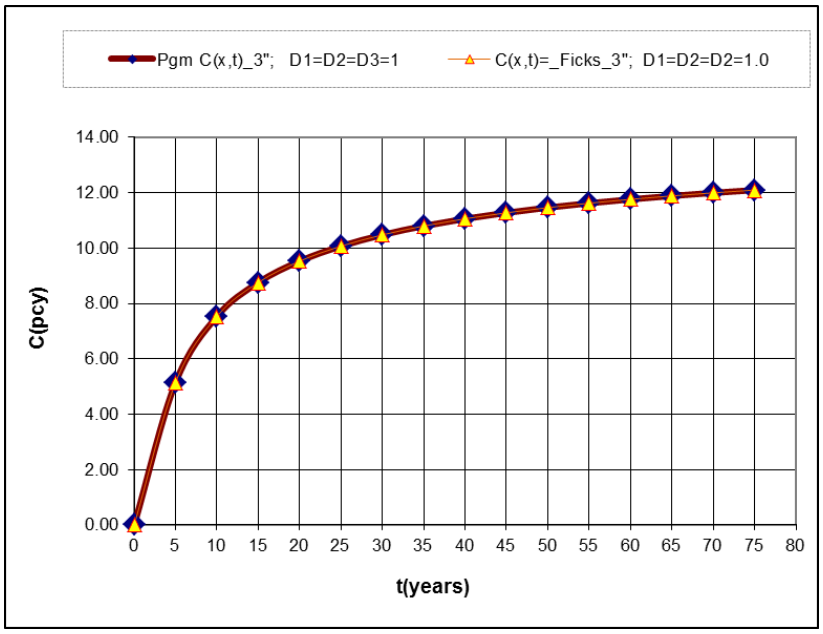

Figure-24 Comparison of results of the new multi-layer model and the single layer solution at x = 3.00 in.

A graphical summary of chloride concentrations predicted by the new multi-layer model at different depths while keeping the diffusion coefficient values, D_1 D_2 and D_3, constant in value and equal to 1.00 is presented in the following figure**.** The chloride concentrations increase with time but are lower in concentration values as the depth increases which is an expected result.

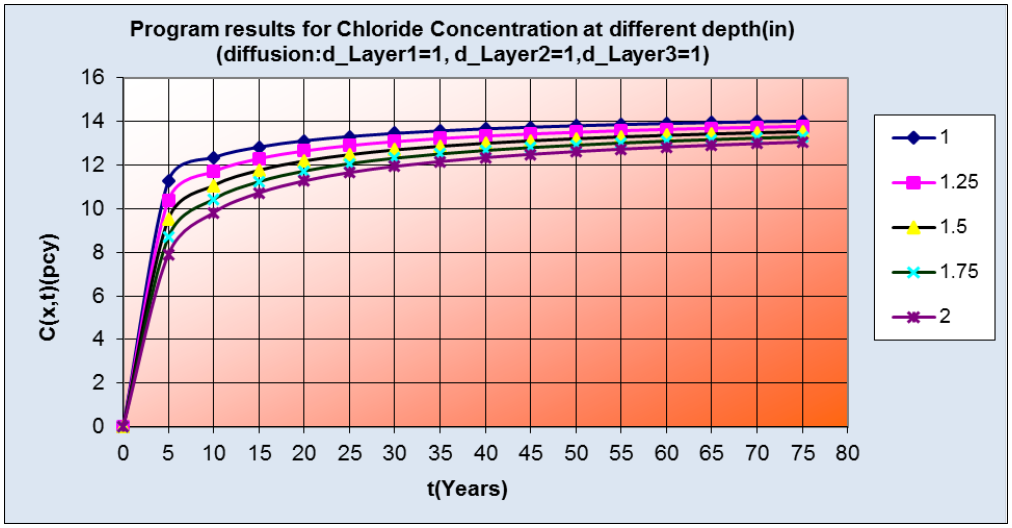

Figure-25 Chloride penetration with increasing time at different depths with a constant diffusivity for all layers

The following figure illustrates the results predicted by the new multi-layer model. One can see that chloride levels increase at a selected depth of 1.00 inch using increasing diffusion coefficients in each case evaluated. For each of the three cases evaluated, all of the diffusion coefficients were kept as a constant value but different constants for different cases(1.0 for the first case, 2.0 for the second case and 3.0 for the last case).

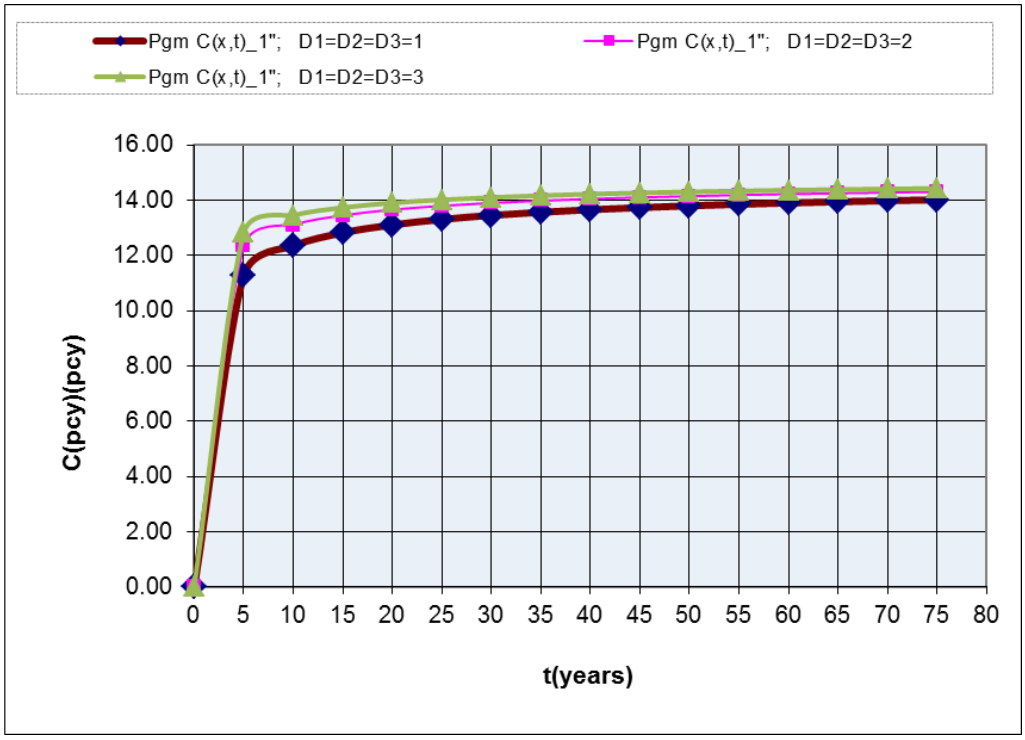

Figure-26 Chloride penetration with increasing time at different depths with different diffusivities for all layers

From the above figures and tables, one can see that the new multi-layer model and the computer program can give correct trends for the chloride concentrations in a multiple layer system with different properties and geometries. The values of the diffusivities of the material could be evaluated from field samples following a standard test procedure such as ASTM C1556.

4.2 Time Dependent Boundary Condition

In the previous section, we obtained the new model for a multi-layer system under a constant boundary condition, and the model predictions were studied using various model parameters. . In this section we will consider a time dependent boundary condition. The basic equation and boundary conditions for the second and the third layers are kept the same as before, however, the first layer boundary condition is changed.

For layer #1 (Linear boundary condition):

$$\frac{\partial C_1}{\partial t} = D_1 \frac{\partial^2 C_1}{\partial x^2}, (l_1 \le x \le l_2)$$

Boundary Condition_Layer1 (a_0, b_0 are arbitrary constants):

$$C(l_1, t) = a_0 t + b_0$$

$$C(x,0) = C_0$$

4.2.1 The solution (Linear boundary condition)

The final solution for this case is shown below and the details of the solution process can be found in (Bai, Harajli, & Xi, 2015):

Eq. (4.5)

$$C(x,t) = a_0 t + b_0 - \frac{2(b_0 - C_0)}{\pi} \int_0^\infty F_3(x,t,u)du + \frac{2a_0}{\pi D_1} \int_0^\infty \frac{1}{u^2} F_3(x,t,u)du - \frac{2a_0}{\pi D_1} \int_0^\infty \frac{e^{u^2 D_1 t}}{u^2} F_3(x,t,u)du$$

Where:

$$W_3(u) = \frac{-1}{\sigma_1} \sin(u\sigma_1 h_2)\sin(uh_1) + \cos(u\sigma_1 h_2)\cos(uh_1)$$

$$V_3(u) = \frac{-1}{\sigma_1 \sigma_2} \cos(u\sigma_1 h_2)\sin(uh_1) + \frac{1}{\sigma_2} \sin(u\sigma_1 h_2)\cos(uh_1)$$

$$F_3(x,t,u) = \frac{e^{-u^2 Dt}[\cos(\sigma_1\sigma_2 u(x-l_3))V_3(u) + \sin(u\sigma_1\sigma_2 u(x-l_3))W_3(u)]}{u(W_3^{\,2}(u) + V_3^{\,2}(u))}$$

Where the following parameters are defined as follows:

σ_1 = (Diffusivity of Layer$_{\#1}$/ Diffusivity of Layer$_{\#2)}$$^{1/2}$= $(D_1/D_2)^{1/2}$

σ_2 = (Diffusivity of Layer$_{\#2}$/ Diffusivity of Layer$_{\#3)}$$^{1/2}$= $(D_2/D_3)^{1/2}$

h_1 = Thickness of layer$_{\#1}$= Distance of Layer$_{\#2}$- Distance of Layer$_{\#1}$= $l_2 - l_1$

h_2 = Thickness of layer$_{\#2}$ = Distance of Layer$_{\#3}$- Distance of Layer$_{\#2}$ = $l_3 - l_2$

C_s = Surface concentration (lb/yd^3).

C_0= Initial concentration present (lb/yd^3).

x = depth below the surface (inch).

t = time (years).

u= Gauss Integration variable (arbitrary).

4.3 Comparison with Other Models

Previous efforts have been done to model the effect of providing a layer of protection to concrete bridge decks to increase the longevity against the corrosive effects of chemicals. These models cannot directly model these protection layers directly and might not be accurate. They will be presented here to show the shortfalls of such methods. In this section I will be presenting an effort done by previously done research (Zemajatis et al. 1999) that has been done to predict the amount of service life extensions for the corrosion damage initiation process. It is shown below that using the model based on equation (3.21); certain sealers can decrease the corrosion initiation times and extend the life as shown in the table below.

Table-12 Service life extensions (years)

Sealer Type	Application Method	VA	PA	NY
WBE	Brushed deck	39.5	42.9	17.3
SBE	Brushed deck	39.5	27.3	11.6
SIL	Low pressure Spray	39.5	53.8	49.7
SLX	Flood & Brush	39.5	53.8	39.5
t_{ini} (years)	Corrosion Initiation	12.0	19.0	32.0

The above research is valid only for the period studied since sealers tend to wear off mainly in the travel lanes and hence chloride concentrations might even be higher than expected. Therefor a damage mechanism should be included for these results to be sustainable and accurate. Also, corrosion initiation times are assumed times and sealer performance and longevity need a process of verification on per state basis via monitoring and laboratory testing as shown below.

Wisconsin DOT performed a sealer effectiveness study (Pincheira and Dorhorst 2005) and it found out that certain sealers do fail due to freeze thaw action and other lose their effectiveness after about 3 years. Therefore, a physical layer of protection applied to the top of the concrete deck is more practical and a better theoretical modeling approach and which will be followed in this research.

In this new study, a multi-layer system will be introduced where the diffusion coefficients could be introduced and varied based on damage theory for the prediction of the chloride profiles or the corrosion initiation times.

The new linear model uses a linear concentration $C=a_0t+b_0$ where a_0 is set equal to k which is used in equation (3.24) above. The following figure presents the chloride concentration results from the new developed model using equation (4.5) and the above equation (3.24) at time "teq".

Table-13 Results from program linear & existing model

eq C_l(x,t)_Sealer (K=1.25)	pgm_linear d1=d2=d3=1; at+b, a=1.25,b=0,x=1"	pgm_linear d1=d2=d3=1; at+b, a=1.25,b=0,x=2"	pgm _linear d1=d2=d3=1; at+b, a=1.25,b=0,x=3"	teq(yrs)
0.00	0.00	0.00	0.00	0
3.67	3.67	2.02	1.05	5
8.63	8.63	5.78	3.76	10
13.88	13.88	10.08	7.18	15
19.29	19.29	14.66	11.01	20
24.80	24.80	19.45	15.08	25
30.38	30.38	24.38	19.38	30
36.01	36.01	29.40	23.82	35
41.69	41.69	34.51	28.37	40
47.40	47.40	39.68	33.02	45
53.13	53.14	44.92	37.76	50
58.90	58.90	50.20	42.57	55
64.68	64.68	55.53	47.45	60
70.49	70.49	60.88	52.37	65
76.31	76.31	66.28	57.35	70
82.15	82.14	71.71	62.38	75

The headings in the above table represent:

- Eq_Cl(x,t)_sealer(k =1.25) is Eq. (3.24) with d=1; is equation (3.24) evaluated at k=a=1.25.
- pgm_linear is Eq.(4.5) with d1=d2=d3=1; (a=1.25, b=0, x=1”) is the new program at x=1inch.
- pgm_linear is Eq.(4.5) with d1=d2=d3=1; (a=1.25, b=0, x=2”) is the new program at x=2inch.
- pgm_linear is Eq.(4.5) with d1=d2=d3=1; (a=1.25, b=0, x=3”) is the new program at x=3inch.
- di=D= the diffusivity of layeri.

The above table results from these two methods match exactly for the case of a one layer system evaluated at 1inch depth. Also, we generate results at 2 and 3inches and these results are presented graphically in the figure below.

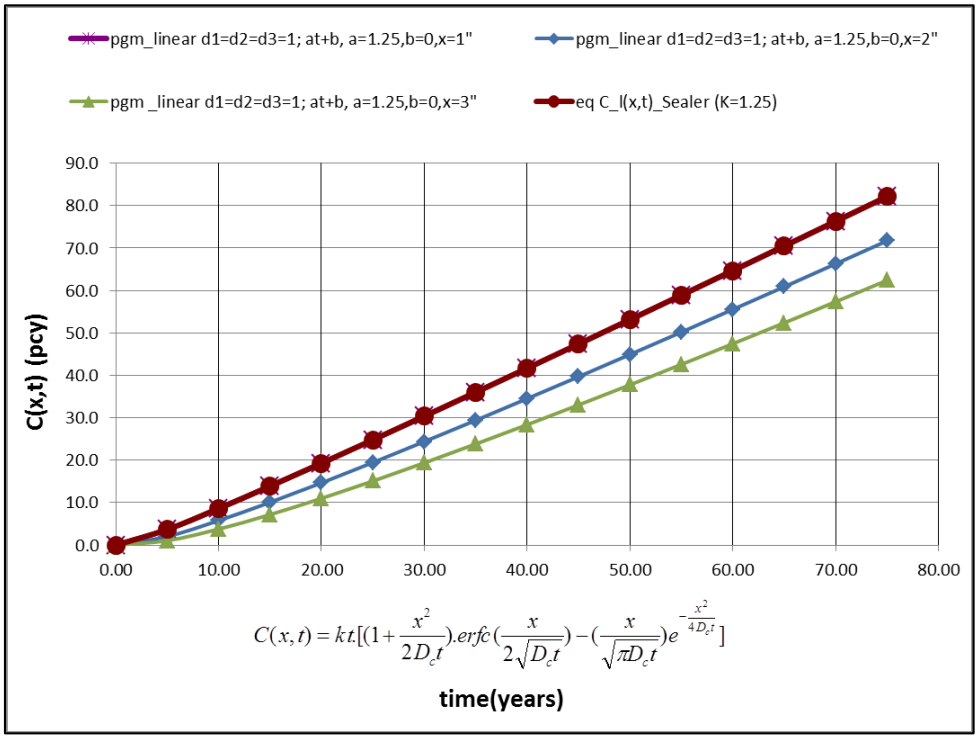

Figure-27 Comparing new model & existing kt model

The headings in the above chart represent:

- Eq_Cl(x,t)_sealer(k =1.25) is Eq. (3.24) with d=1; is Eq. 3.24 evaluated at k=a=1.25.
- pgm_linear is Eq.(4.5) with d1=d2=d3=1; (a=1.25, b=0, x=1") is the new program at x=1inch.
- pgm_linear is Eq.(4.5) with d1=d2=d3=1; (a=1.25, b=0, x=2") is the new program at x=2inch.
- pgm_linear is Eq.(4.5) with d1=d2=d3=1; (a=1.25, b=0, x=3") is the new program at x=3inch.
- d_i=D= Diffusivity values for a layer$_i$.

Notice in the above figure above that the curves from the two models, equation (3.24) and equation (4.5), do match exactly at x=1". However, the model with equation (3.24) cannot be used for the cases of multiple layers since we cannot directly input the diffusivity or the thickness values of any specific layer. Therefore, our program is a much more effective and flexible tool to use in the modeling process.

The chloride boundary condition for equation (4.5) could be changed to show the effect of increasing the chloride concentration levels. The general trend for an increasing linear boundary $C=a_0t+b_0$ will be used with lower and larger values of a_0. The tables and graphs are presented herein for illustration and show a predictable increasing concentration trend.

Table-14 Lower boundary condition

time (years)	pgm_linear d1=d2=d3=1; at+b, a=5.0,b=0,x=1"	pgm_linear d1=d2=d3=1; at+b, a=5.0,b=0,x=2"	pgm_linear d1=d2=d3=1; at+b, a=5.0,b=0,x=3"
0	0.00	0.00	0.00
5	14.68	8.09	4.22
10	34.50	23.11	15.05
15	55.53	40.31	28.72
20	77.17	58.66	44.03
25	99.20	77.81	60.33
30	121.51	97.53	77.53
35	144.04	117.62	95.28
40	166.75	138.04	113.47
45	189.59	158.72	132.09
50	212.55	179.67	151.05
55	235.59	200.78	170.30
60	258.74	222.13	189.80
65	281.95	243.52	209.48
70	305.24	265.12	229.39
75	328.58	286.83	249.50

Table-15 High boundary condition

time (yrs)	pgm_linear d1=d2=d3=1; at+b, a=15.0,b=0,x=1"	pgm_linear d1=d2=d3=1; at+b, a=15.0,b=0,x=2"	pgm_linear d1=d2=d3=1; at+b, a=15.0,b=0,x=3"
0	0.00	0.00	0.00
5	44.06	24.28	12.69
10	103.50	69.31	45.13
15	166.58	120.94	86.19
20	231.52	175.97	132.13
25	297.61	233.44	181.00
30	364.52	292.59	232.56
35	432.14	352.88	285.81
40	500.25	414.13	340.38
45	568.77	476.16	396.31
50	637.66	539.03	453.13
55	706.78	602.34	510.88
60	776.20	666.38	569.38
65	845.84	730.56	628.44
70	915.73	795.34	688.19
75	985.73	860.50	748.50

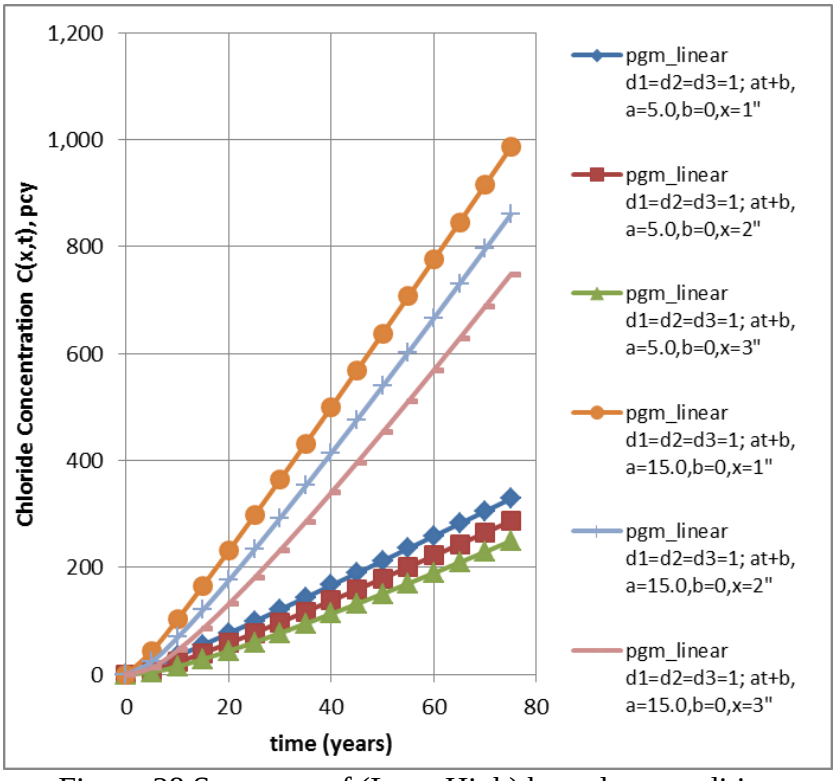

Figure-28 Summary of (Low, High) boundary condition

4.5 Summary

- Two new analytical models were developed for chloride penetration in multi-layer systems with a constant boundary condition and a linearly time dependent boundary condition.
- The analytical models were programed to show numerical results which were examined using different material parameters and compared with some available theoretical solutions. The basic trends predicted by the new models are correct.
- The new model predictions showed that our new models are advanced models in that they can simulate multiple layers with different material properties and layer thicknesses.
- In the following chapters, it will be shown that the new models can go a step further by simulating time-dependent damage in the layers and thus predict the chloride profiles and corrosion times in a distressed reinforced concrete structure.

Chapter 5

Degradation of Material

In Chapter 4, the transport properties of the materials in the multi-layer bridge deck system are considered as constants. They are the initial values of the transport properties of new bridge decks. During the life span of a bridge, the material properties deteriorate due to traffic loadings and environmental loadings such as temperature variation and humidity fluctuation. In particular, the diffusivities of the concrete and the overlays will increase and thus the rate of chloride penetration will also increase. This type of material degradation must be considered in the new multi-layer model in order to improve the accuracy of the model prediction for long-term performance of bridge decks. Since the degradation of materials depends on the age of bridge decks, the transport properties of the layered bridge decks must be treated as time dependent properties. The focus of this chapter will be made on how to consider time dependent transport parameters in the new multi-layer model developed in Chapter 4.

In this chapter, a new variable, m, is used to represent the rate of material degradation. The rate of degradation could be due to damage done to the layer due to external factors such as traffic loading or environmental temperature. Damage effects could be also due to internal factors such as Freeze/Thaw or micro-cracking in the concrete sample. This degradation factor will be scaled based on real chloride penetration data obtained from a bridge structure E-17-QM carrying I-270 over I-25 in Denver. This structure is being tested for the effectiveness of different kinds of protection layers applied to a bridge deck in the Denver Metro area. I will present the process of the different overlay application methods later. The diffusion coefficient

after (Xi et al. 2000; Mangat and Molloy 1994; Mangat and Limbachiya 1999) will be a function of time defined as:

$$D_i = \frac{D_{i0}}{t^m}$$

D_{i0} is the initial value for the diffusion coefficient of layer I and m is the factor for the rate of material deterioration, $m < 0$ meaning that with increasing time, D_i increases.

Substituting the new D_i into the diffusion equations for the multi-layer system, the new diffusion equations will be:

5.1 For Layer #1 (with degradation):

Old $\frac{\partial C_1}{\partial t} = D_1 \frac{\partial^2 C_1}{\partial x^2}, (l_1 \le x \le l_2)$

New $\frac{\partial C_1}{\partial t} = \frac{D_{10}}{t^m} \frac{\partial^2 C_1}{\partial x^2}, (l_1 \le x \le l_2)$

5.2 For layer #2 (with degradation):

Old $\frac{\partial C_2}{\partial t} = D_2 \frac{\partial^2 C_2}{\partial x^2}, (l_2 \le x \le l_3)$

New $\frac{\partial C_2}{\partial t} = \frac{D_{20}}{t^m} \frac{\partial^2 C_2}{\partial x^2}, (l_2 \le x \le l_3)$

5.3 For Layer #3 (with degradation):

Old $\frac{\partial C_3}{\partial t} = D_3 \frac{\partial^2 C_3}{\partial x^2}, (l_3 \le x)$

New $\frac{\partial C_3}{\partial t} = \frac{D_{30}}{t^m}\frac{\partial^2 C_3}{\partial x^2}, (l_3 \le x)$

The layers are assumed to undergo similar degradation and hence the same m variable will be applied to all layers in order to simplify the solution.

5.4 New Time Scale Transformation

In the three new equations, the diffusion coefficients are time dependent, and therefore the solutions developed in Chapter 4 cannot be used. We will be using a new time scale T and use the following relationship with the real time scale t for the first layer:

$$\partial T = \partial t.\frac{D_{10}}{t^m} \qquad \text{Eq. (5.1)}$$

Integrating we get: $T = \frac{D_{10}.t^{(1-m).}}{(1-m)}$

T can be considered as an adjusted time scale considering the degradation of materials. Using this relationship $\partial T = \partial t.\frac{D_{10}}{t^m}$ and replacing it in each equation we get:

For layer #1 (with the new time scale):

$$\frac{\partial C_1}{\partial t} = \frac{D_{10}}{t^m}\frac{\partial^2 C_1}{\partial x^2}, (l_1 \le x \le l_2)$$

Now becomes:

$$\frac{\partial C_1}{\partial T} = \frac{\partial^2 C_1}{\partial x^2}, (l_1 \le x \le l_2)$$

For Layer #2 (with the new time scale):

$$\frac{\partial C_2}{\partial t} = D_2 \frac{\partial^2 C_2}{\partial x^2}, (l_2 \le x \le l_3)$$

Now becomes:

$$\frac{\partial C_2}{\partial T} = \frac{D_{20}}{D_{10}} \frac{\partial^2 C_2}{\partial x^2}, (l_2 \le x \le l_3)$$

For Layer #3 (with the new time scale):

$$\frac{\partial C_3}{\partial t} = D_3 \frac{\partial^2 C_3}{\partial x^2}, (l_3 \le x)$$

Now becomes:

$$\frac{\partial C_3}{\partial T} = \frac{D_{30}}{D_{10}} \frac{\partial^2 C_3}{\partial x^2}, (l_3 \le x)$$

The ratio of the diffusion equations will be set to:

$\delta_i = \frac{D_{i0}}{D_{10}}$ For i=1, 2, 3

5.5 The Real Time Scale "T" and The New Time Scale "T"

Therefore, $\delta = 1$ for Layer#1, $\delta_2 = D_{20}/D_{10}$ for Layer#2, and $\delta_3 = D_{30}/D_{10}$ for Layer#3. With the new transformation, the diffusion coefficients in the three diffusion equations became constants and, as a result, the solutions developed in Chapter 4 for different boundary conditions can be used here. Of course, the new solutions will be in the new time scale T, which need to be converted back to the real time scale. The following figure illustrates the variation of the real time "t" with the new time scale "T".

From these figures, one can see that the smaller the degradation value m (must be negative) gets, the higher the new time scale gets and thus indicating that the diffusion process

will be faster With a given damage factor m, the new time T is actually a lot higher than the real time t indicating a higher chloride concentration for this case. It can be seen that when m=0, the real time is equal to the accelerated time. However, this time is accelerated to 60 years for a damage level with a value for m=-0.15 (m<0).

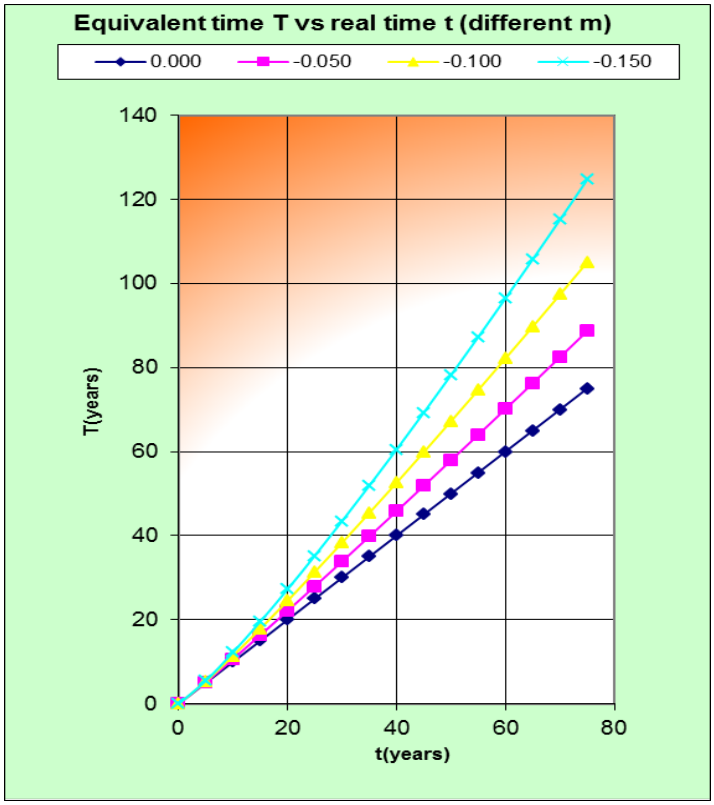

Figure-29 Comparing real time “t” with equivalent time “T”

Using the solutions in Chapter 4 and the transformation in this chapter, a numerical example is shown in the following figure. It is a comparison among the different chloride levels due to different degradation levels and comparing Fick’s second law of diffusion at m=0 and our new model with m=-1 and -2 respectively.

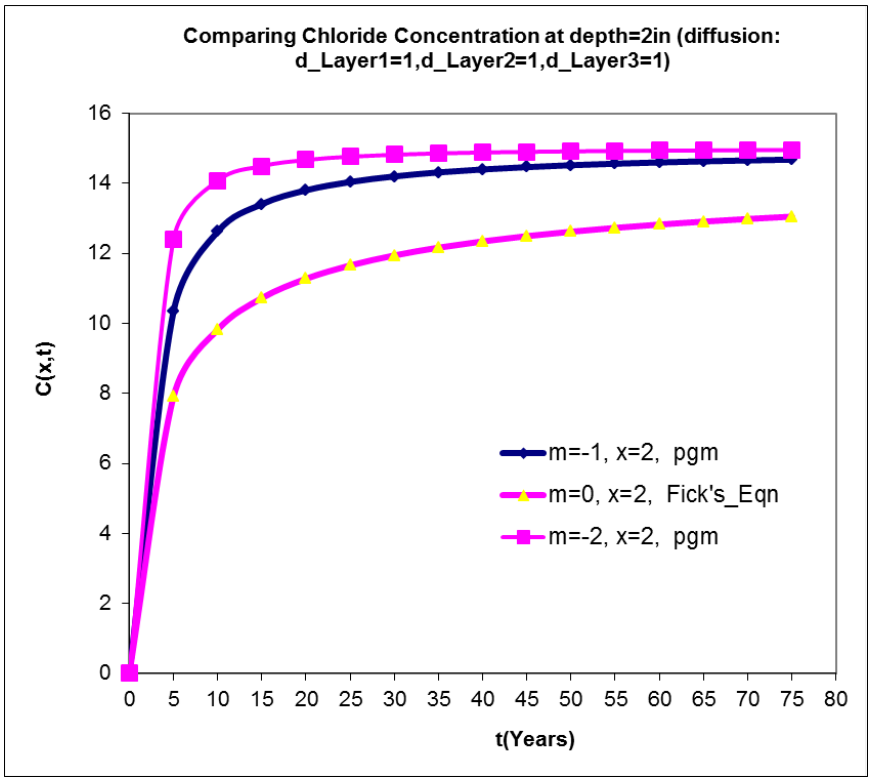

Figure-30 Comparing chloride levels with degradation applied

The terms in the above figure are:

d_layer_i= diffusion coefficient for $layer_i$.

C(x,t) = Concentration at depth x=2.0" using new model.

This is an innovative method where the new model can be used with minor modifications to predict the chloride concentrations using damage factors applied to all the layers simultaneously. The following table shows a numerical output comparing the model results for a single layer simulation of our new model and Fick's equation (3.14). The results agree quite well and we get an exact match for the case of m=0, meaning no acceleration of damage. Results for other values of damage factors are shown.

Table-16 New model Vs. Ficks

		m=-1,	m=-2,	m=0,	m=-0,
		x=2,	x=2,	x=2,	x=2,
T(years)	t(yrs)	pgm	pgm	Fick's_Eqn	pgm
0.0	0	0	0	0	0
12.5	5	10.34	12.40	7.91	7.91
50.0	10	12.62	14.07	9.82	9.82
112.5	15	13.41	14.50	10.73	10.73
200.0	20	13.81	14.67	11.28	11.28
312.5	25	14.04	14.77	11.66	11.66
450.0	30	14.20	14.82	11.94	11.94
612.5	35	14.32	14.86	12.17	12.17
800.0	40	14.40	14.88	12.35	12.35
1012.5	45	14.47	14.90	12.50	12.50
1250.0	50	14.52	14.92	12.62	12.62
1512.5	55	14.56	14.93	12.73	12.73
1800.0	60	14.60	14.94	12.83	12.83
2112.5	65	14.63	14.94	12.91	12.91
2450.0	70	14.66	14.95	12.99	12.99
2812.5	75	14.68	14.95	13.05	13.05

Chapter 6

Composite Damage Mechanics

In Chapter 5, the transport properties of the multi-layer system were considered as a function of time, and the factor m was introduced to characterize the aging rate of the system. In this chapter, the aging process of the deck system is modeled by using the concept of composite damage mechanics, in which the damage development in the materials is described by available composite models. The effect of the damage development is combined in the transport properties in the new solutions for the multi-layer bridge deck system.

6.1 Composite Damage Model

Previously, we discussed Fick's second law of diffusion with time dependent chloride diffusion coefficient as:

$$\partial C/\partial t = D(t) * \partial^2 C/\partial x^2 \Rightarrow \partial C/\partial t * D(t) = \partial^2 C/\partial x^2$$

in which D(t) is a general time dependent function, it was t^{-m} in chapter 5. In this chapter, it could be any time dependent function for considering the damage development in the materials.

6.1.1 A New Time Scale Concept

Similar to the transformation used in Chapter 5,, we use a new time scale, T represented as:

$$\partial T = D(t).\partial t \qquad \text{Eq. (6.1)}$$

Substituting the value of T in the above equation, we get:

$$\partial C/\partial T = \partial^2 C/\partial x^2$$

This is a diffusion equation with a constant diffusion coefficient.

6.1.2 The Composite Damage Theory

The composite damage mechanics approach can be used to develop a theoretical model for the diffusion equation (Xi and Nakhi 2005; Xi et al. 2006). In this model, the damaged concrete can be represented by many concentric spherical elements as is shown in the figure below.

Figure-31 conceptual composite damage model

The core or inclusions are the damaged portion of the model and the rings are the original material without any damage. It is assumed that the damage will occur and grow from the inner part for a specific state of damage.

The new time scale to be evaluated shown below as equation (6.1) is now a function of several constants and a new damage variable which must be positive (m_d>=0). The initial and damaged concrete diffusion rates are constants and shown as D_0 and D_d. where the subscripts indicate the initial and damaged state of the material. The damaged volume is represented by the variable d, which ranges from 0 to 1. For the case of the initial condition and when the time t=0, we use equation 6.4 to find d=0 meaning that there is no damage yet and equation 6.3 yields $D_{eff} = D_o$.

However, when t= ∞ (infinity) representing a very long period of time, then Equation (6.4) gives d=1 meaning there is 100 % damage or nothing is left of the original material and $D_{eff} = D_d$. In order to match any available data, these factors could be adjusted to predict the chloride concentrations at any given time by predicting the diffusivity with certain level of damage.

6.1.3 The Composite Damage Model with a Single Layer

The following expression represents the solution for the new time scale, T, based on the effective diffusion coefficient developed from the composite damage approach. The value of T using a new diffusivity expression shown in equation 6.3 can be evaluated as follows:

$$\partial T = D(t).\partial t$$

$$T = \int_0^t D(t).dt = \int_0^t D_{eff}\,dt = \int_0^T D_0 * \left[1 + \frac{d}{\frac{(1-d)}{3} + \frac{D_0}{(D_d - D_0)}}\right] dt \qquad \text{Eq. (6.2)}$$

The diffusion coefficients used are:

D_0= Initial diffusion coefficient

D_d= Damaged diffusion coefficient

D_{eff} = The effective diffusion coefficient

d = The damaged volume fraction.

$$D_{eff} = D_0 * \left[1 + \frac{d}{\frac{(1-d)}{3} + \frac{D_0}{(D_d - D_0)}}\right] \qquad \text{Eq. (6.3)}$$

I will propose a new damage model where:

$$d = 1 - \frac{1}{e^{t.m_d}} = 1 - e^{-t.m_d}, t.m_d \geq 0 \qquad \text{Eq. (6.4)}$$

The terms in the above equation are:

d = The damaged volume fraction.

m_d= the damage factor.

The chloride diffusion results shown below are based on the solution of equation (6.1). The basic diffusion equation was previously modified based on a new time T and has the form shown below as:

$$\frac{\partial C}{\partial T} = \frac{\partial^2 C}{\partial x^2} \qquad \text{Eq. (6.6)}$$

We now replace the value of the new time T calculated by a numerical integration function as shown in equation (6.1) into equation (6.7) to get the final chloride solution as:

$$C(x,t) = C_0 * \left[1 - erf\left(\frac{x}{2\sqrt{T}}\right)\right] \qquad \text{Eq. (6.7)}$$

For a single layer, the table below shows the results for the chloride profiles based on equation (6.7) using the new effective diffusion coefficient for the composite damage model, equation (6.3), and the new effective time “T” integrated as shown in equation (6.5).

Table-17 Chloride profile with damage factors m_d

t(years)	∫ :C(x,t)@ m_d= 0.100	∫ :C(x,t)@ m_d= 0.200	∫ :C(x,t)@ m_d= 0.300	∫ :C(x,t)@ m_d= 0.400
0	0.000	0.000	0.000	0.000
5	5.853	6.924	7.687	9.862
10	9.040	10.077	10.609	12.574
15	10.580	11.387	11.713	13.353
20	11.468	12.073	12.282	13.690
25	12.036	12.492	12.634	13.882
30	12.425	12.774	12.878	14.008
35	12.707	12.980	13.059	14.100
40	12.920	13.138	13.201	14.170
45	13.086	13.264	13.315	14.226
50	13.220	13.368	13.411	14.272
55	13.330	13.455	13.491	14.310
60	13.422	13.529	13.561	14.344
65	13.500	13.594	13.621	14.372
70	13.568	13.651	13.675	14.397
75	13.628	13.701	13.723	14.420

The chart below show the effect of increasing the damage factor, m_d, and the corresponding chloride profiles are shown as increasing in value which is expected for this single layer or concrete only layer simulation.

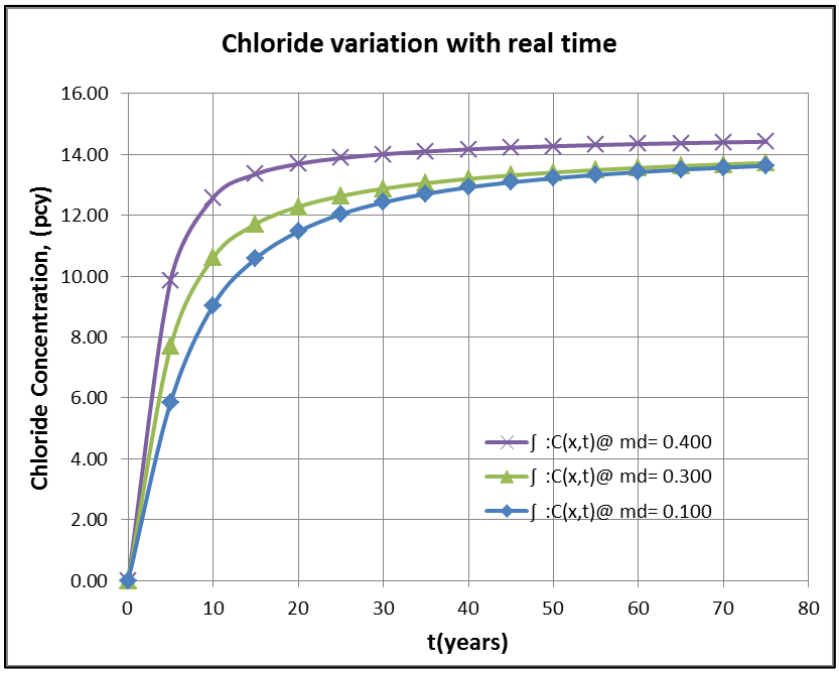

Figure-32 Single layer chloride profile

6.1.4 The Composite Damage Model with Multiple Layers

The solution published (Bai, Harajli, & Xi, 2015) for the following equation with the assumed constant boundary conditions will be used in the following evaluations and throughout the rest of the research for analysis. This is dependent on the ratios of the diffusion coefficients, the initial and final concentrations, depth from surface and the time as variables in the following equation:

$$C(x,t) = C_s - \frac{2(C_s - C_0)}{\pi}\int_0^{\infty} F(x,t,u)du \qquad \text{Eq. (6.7a)}$$

Where:

$$W_3(u) = \frac{-1}{\sigma_1}\sin(u\sigma_1 h_2)\sin(uh_1) + \cos(u\sigma_1 h_2)\cos(uh_1)$$

$$V_3(u) = \frac{-1}{\sigma_1\sigma_2}\cos(u\sigma_1 h_2)\sin(uh_1) + \frac{1}{\sigma_2}\sin(u\sigma_1 h_2)\cos(uh_1)$$

$$F_3(x,t,u) = \frac{e^{-u^2 D_l t}[\cos(\sigma_1\sigma_2 u(x-l_3))V_3(u) + \sin(u\sigma_1\sigma_2 u(x-l_3))W_3(u)]}{u(W_3{}^2(u) + V_3{}^2(u))}$$

Where the following parameters are defined as:

σ_I =square root of the ratio of the diffusivity of layer$_i$ to layer$_{i+1}$.

h_i = Depth of each layer.

C_s =Surface concentration.

C_0 = Initial concentration present.

x = depth from surface.

t = time.

u = Gauss Integration variable.

Using the effective diffusion coefficient and the damage volume fraction equations mentioned above in equations (6.3) and equation (6.4) shown below as:

$$D_{eff} = D_0 * \left[1 + \frac{d}{\frac{(1-d)}{3} + \frac{D_0}{(D_d - D_0)}} \right] \qquad \text{Eq. (6.4)}$$

Where:

$$d = 1 - \frac{1}{e^{t.m_d}} = 1 - e^{-t.m_d}, t.m_d \geq 0$$

We can now reformulate the basic diffusion equations as follows:

For layer #1 (with degradation):

$$\frac{\partial C_1}{\partial t} = D_{eff\,1} \frac{\partial^2 C_1}{\partial x^2}, (l_1 \leq x \leq l_2)$$

For layer #2 (with degradation):

$$\frac{\partial C_2}{\partial t} = D_{eff\,2} \frac{\partial^2 C_2}{\partial x^2}, (l_2 \leq x \leq l_3)$$

For layer #3 (with degradation):

$$\frac{\partial C_3}{\partial t} = D_{eff\,3} \frac{\partial^2 C_3}{\partial x^2}, (l_3 \leq x)$$

The significance of the new diffusion coefficient D_{effi}, is that it resembles the effective diffusion of a particular layer. The layers are assumed to undergo similar degradation and hence the same m_d variable will be applied simultaneously to all layers in order to simplify the solution. Different damage factors could be applied to each layer, however, this will be left for a future research topic.

Using the relationship $\partial T = \partial t.D_{eff\,1}$ and replacing it in each equation we get:

For layer #1 (new time scale):

$$\frac{\partial C_1}{\partial T} = \delta_1 \frac{\partial^2 C_1}{\partial x^2}, (l_1 \le x \le l_2) \qquad \text{Eqn. (6.8)}$$

For Layer #2 (new time scale):

$$\frac{\partial C_2}{\partial t} = D_{eff\,2} \frac{\partial^2 C_2}{\partial x^2}, (l_2 \le x \le l_3)$$

Now becomes:

$$\frac{\partial C_2}{\partial T} = \frac{D_{eff\,2}}{D_{eff\,1}} \frac{\partial^2 C_2}{\partial x^2} = \delta_2 \frac{\partial^2 C_2}{\partial x^2}, (l_2 \le x \le l_3) \qquad \text{Eqn. (6.9)}$$

For Layer #3 (new time scale):

$$\frac{\partial C_3}{\partial t} = D_3 \frac{\partial^2 C_3}{\partial x^2}, (l_3 \le x)$$

Now becomes:

$$\frac{\partial C_3}{\partial T} = \frac{D_{eff\,3}}{D_{eff\,1}} \frac{\partial^2 C_3}{\partial x^2} = \delta_3 \frac{\partial^2 C_3}{\partial x^2}, (l_3 \le x) \qquad \text{Eqn. (6.10)}$$

The ratio of the diffusion equations will be set to:

$$\delta_i = \frac{D_{effi}}{D_{eff\,1}} \text{ For i=1, 2, 3}$$

Therefore, δ =1 (layer#1), $\delta_2 = \frac{D_{eff\,2}}{D_{eff\,1}}$ (Layer#2), $\delta_3 = \frac{D_{eff\,3}}{D_{eff\,1}}$ (Layer#3).

This new transformation allows us to use the new model with simply replacing the required diffusivity values for each layer with a new ratio δ. The larger the degradation value m_d gets, the higher the new time scale gets indicating that the diffusion levels will be higher and so is the chloride concentration at any given level.

The figure below shows that our model is able to predict this increase in chloride concentration with increasing time and increasing the damage factor for the newly developed multi-layer system. This then could be used to predict the corrosion initiation times to estimate the time for taking action to prohibit further damage to a particular concrete member or element before reaching the critical chloride threshold.

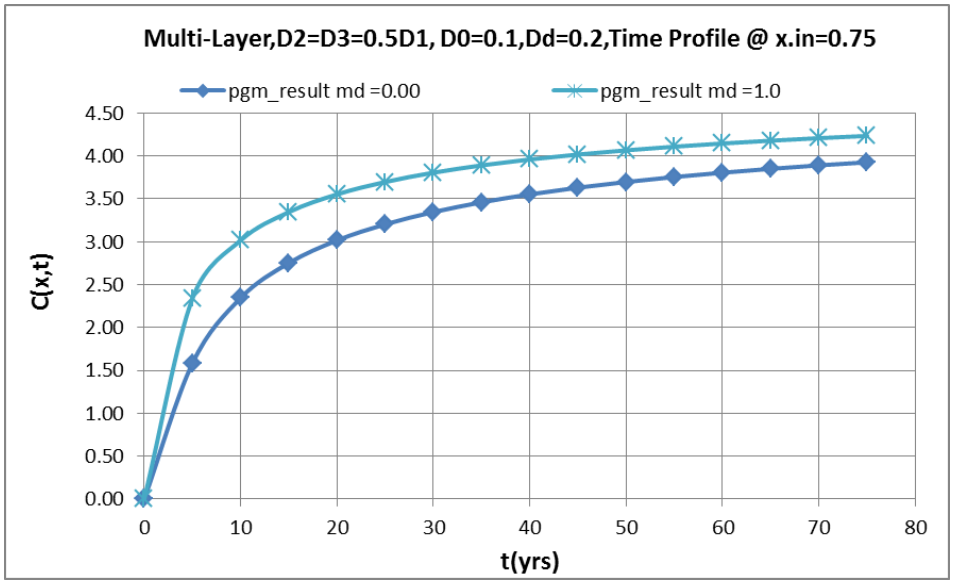

Figure-33 Time profile with degradation

In the figure above, D1 D2 and D3 are the assumed diffusivity values for each layer with in^2/year and m_d is the assumed damage factor applied for the simulation evaluated at depth x equal 0.75 inches. The initial and final damaged concrete diffusion rates are constants and shown as D_0 and D_d with values of 0.1 and 0.2 respectively.

6.2 Calibration curves based on field data

In this section, we will investigate the effectiveness of the model developed to calibrate field results obtained from bridge structure number E-17-QM. This structure was 15 years old at the beginning of the testing procedure and used to get core samples to obtain chloride variation throughout the concrete samples.

Three different overlay types were applied to protect the concrete deck from chloride ingress in this test section. Chloride levels are recorded at 0.25” intervals from the cores to obtain the chloride concentrations at different core depths from the surface at specific dates. The structure was visited three times to collect data during the testing period that lasted from July 2012 to July 2013.

The control section being the bare concrete deck section was left untreated and was used to compare the results and the effectiveness of these overlay products. Core samples were taken from all different overlay test sections after the initial application date on 7/15/2012. Core samples were taken again during two other visits on 4/10/2013 or after 9 months and on 7/15/2013 or after 12 months. The initial time of application is considered to be the start for the evaluation or time is equal to the age of the structure at that time. The table below shows the results of the chloride tests data obtained from these samples. The following figures show the typical installation procedure for these types of overlays.

Figure-34 Surface preparation & resin application

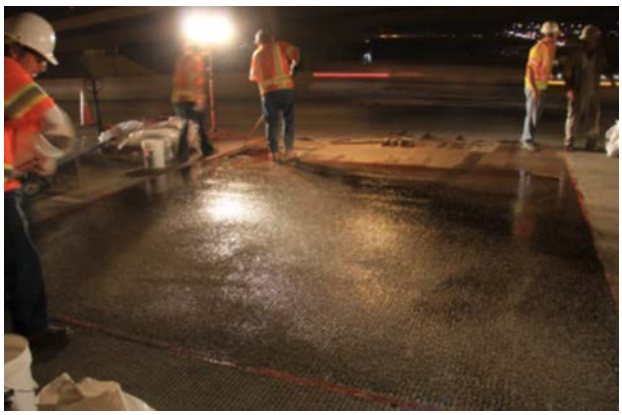

Figure-35 Apply wearing coarse or aggregates

Figure-36 Removal of excess material

Figure-37 Final product installed

Figure-38 Bond test for quality control

Table-18 Chloride test results

1st Visit	2nd Visit	3rd Visit	Overlay
7/15/2012	4/10/2013	7/15/2013	**Bare Deck**
% Chloride by Wt.	% Chloride by Wt.	% Chloride by Wt.	**Depth.in**
0.1345	0.2296	0.2290	0.00 Control
0.0880	0.1484	0.1390	0.50 Control
0.0331	0.0458	0.0130	1.00 Control
0.0128	0.0131	0.0020	1.50 Control
0.0059	0.0000	0.0020	2.00 Control
0.0037	0.0000	0.0030	2.50 Control
0.0033	0.0026	-	3.00 Control
			3.50 Control

6.3 Model fitting to field data

The figures below show the chloride profiles obtained from the samples shown in the above table. The critical concentration shown in the figures below is the level at which the corrosion of the rebar initiates and starts to cause concrete damage. Also, there is significant drop of concentration in the top 1” of the samples. This could not be due to external factors such as washing the bridge decks after winter because the agency does not implement such a process. Therefore, this could be attributed to other weather related issues causing this surface variation.

Therefore, there might be some error in the testing procedure due to the sensitivity of the results and the experience of the tester doing the tests

.

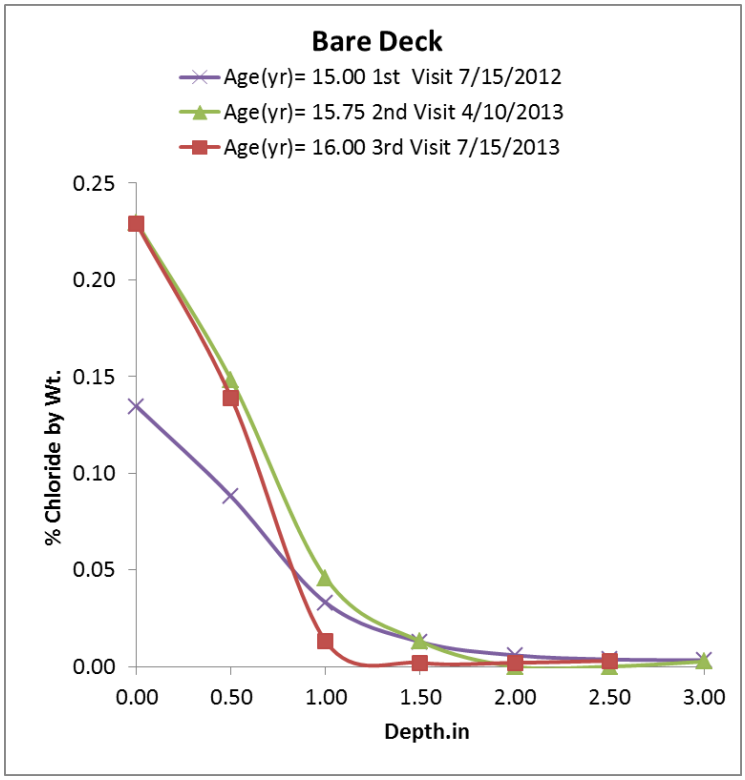

Figure-39 Bare Deck Test Data Profile

The initial chloride profile of the first set of data for the control sample is used for calibration and to calculate the diffusion coefficient of the existing concrete sample. Also, the 6 and 12 month samples will be investigated for an applicable damage factor for predicting the chloride samples at that age. The ratio of the damaged to the initial diffusion coefficient, D_d/D_0 to is equal to 10 for this case and using t=15 years (real time age of the core at that time) indicating no damage is allowed yet.

The figure below show the chloride profile match with a simulated real condition damage factor m_d=0.25 applied to the existing concrete for the data set using a time equal to15 years which is the age of the concrete on 7/15/2012. The effective diffusion coefficient, D_{eff} is calibrated to a value of 1.59E-10 (in^2/s) as a starting point for the bridge deck. The existing data does not follow a smooth profile as expected due to the variability of the ASTM C 1218 test

procedure used for the soluble chloride evaluation. The model predicts the actual conditions fairly well. The maximum error in the data points or the variation from the actual data is about 2%.

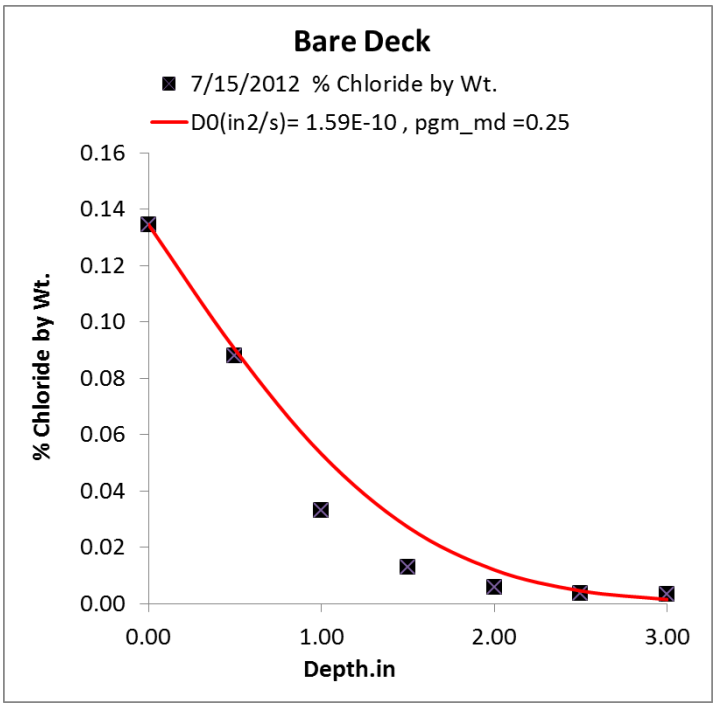

Figure-40 Bare Deck 1rst visit

When the concrete is 9 months old (t=15.75 years), the new time scale "T" for the period and the calibrated D_{eff} of the existing concrete is used to determine the best m_d scale factor for the new concrete profile. With a D_d/D_0 set to 10.0 and the effective m_d factor set to 0.25, a best fit curve to match the field data is created. The figure below shows these graphical results where the maximum variation in the data is about 4.8%.

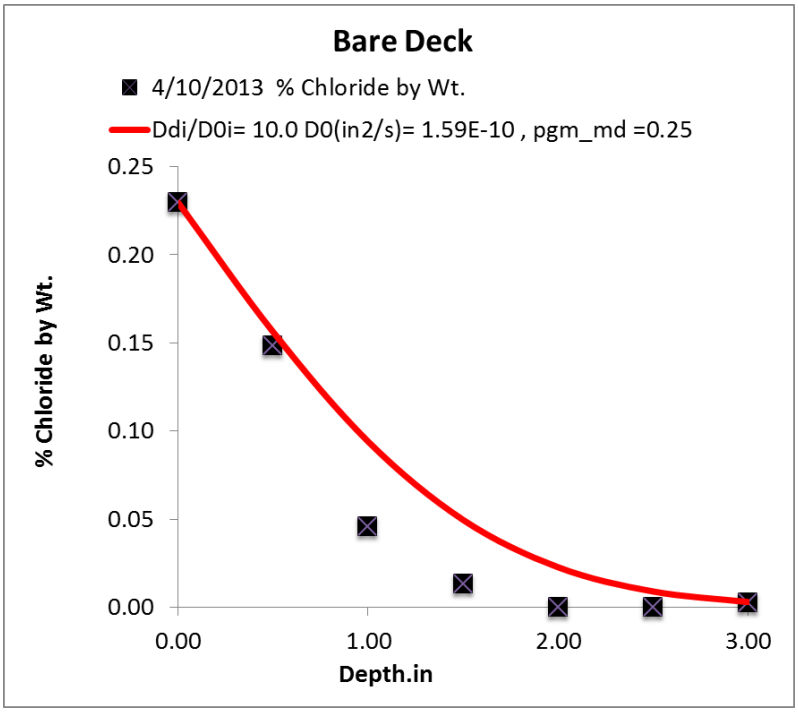

Figure-41 Bare Deck 2nd visit

When the concrete is 12 months old (t=16.00 years), the calibrated D_{eff} of the original concrete is also used to compare against the original concrete profile. With a D_d/D_0 set to 10, the effective m_d factor is calculated as 0.25 and the new time scale "T" used, the results follow closely the field data mainly in the upper and lower portions of the curve. The figure below shows these graphical results where the maximum variation in the data is about 8.2%.

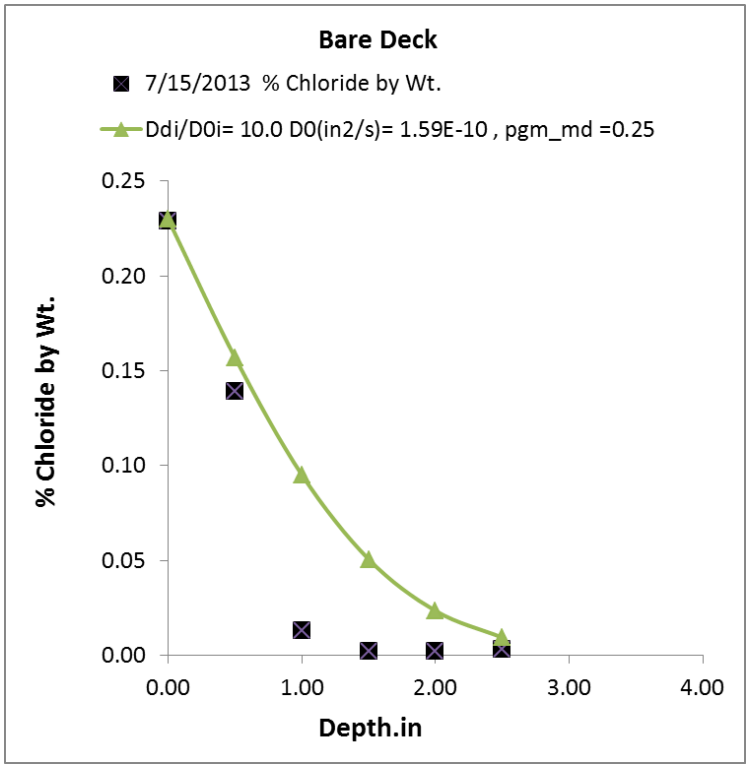

Figure-42 Bare Deck 3rd visit

The sharp drop in the chloride profile close to the 1 inch level is not typical of the chloride profiles could possibly indicate that the drilling has hit some of the aggregates which does not absorb chlorides causing such a drop in the concentration. The theoretical model however, does very well in approximating the upper and lower portions of the curve. Data in some cases was not available for the deeper levels as in the case of the 3rd visit for the 3.0" depth (Table-18). Therefore, the maximum depth for such cases is set to 2.5 inches for comparison.

6.4 Evaluation of a 3/8" Overlay on top of concrete

This sample is a thin bonded polyester concrete overlay that is 3/8" (0.375") thick and is placed over the existing concrete deck. The program has been used to match the field data by calibrating the damage factor m_d and the damaged diffusion coefficient D_d values. The bridge used for this research was built in 1998 and the data was extracted in 2013. The age of the bridge

at the time of testing is 15 years and this time is used as the starting time in an effort to match the field results.

Two tests were performed on the added overlay samples to determine the chloride levels. The diffusion coefficient of the concrete is calibrated in order to match the field results for the two test durations for this overlay. The calibration values are kept the same for both durations with the time being the only variable. As can be seen, the theoretical model follows closely the field data.

The new model incorporating the effect of additional protection layers has been used to predict the new theoretical profiles and compare to the field values. The new equations for the multi-layer model have been discussed previously and equations 6.8 through equations 6.10 are now used.

The concrete is now behaving as a lower diffusion material when compared to the case of no overlay. The figure shows the results obtained from this calibration and closely predicts the field data for most of the data points. The figure below shows the effect of adding a thin layer over the existing concrete and evaluated after 9 months of installation. The new calculated diffusion coefficient is 1.27E-10 as compared to the case of no overlay of 1.59E-10 indicating a 20% drop or gain of protection (see Figure-40, 34, 35).

6.5 Model Evaluation with Kwik Bond Overlay

6.5.1 Kwik Bond 2nd field visit data

The first field visit was to take control samples from the bare deck and apply the new overlays; hence no field data is available since no overlay was present at that time.

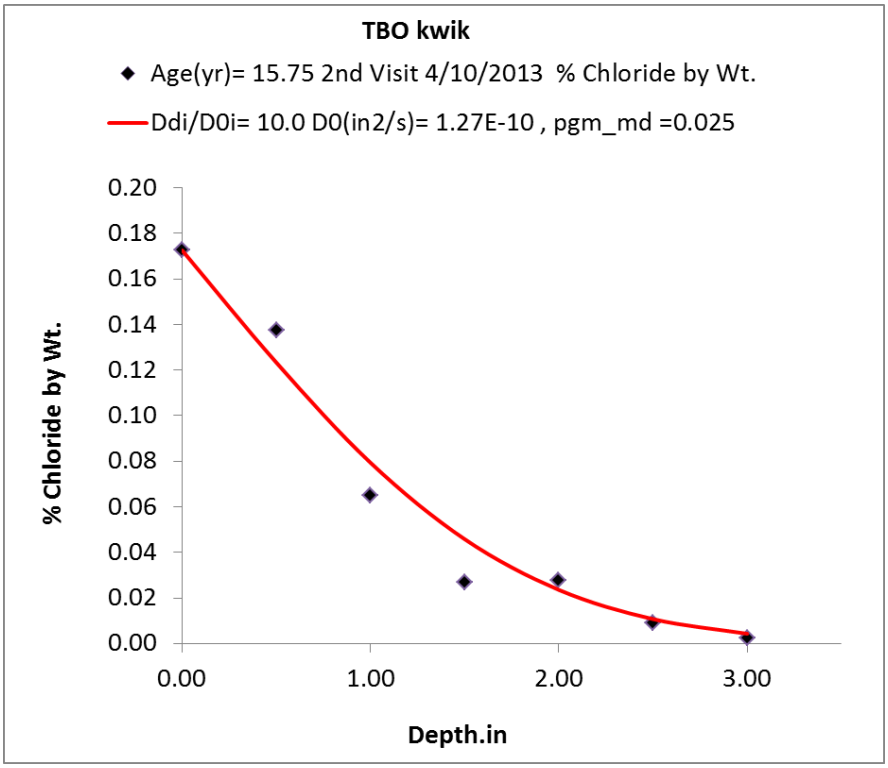

Figure-43 Kwik Bond Overlay (2nd visit)

The same damage diffusion ratios and factors, D_d/D_0 and m_d, were used along with new time scale for this period to predict the values of the new chloride concentrations. The new model results follow the actual field data fairly close and are a good approximation of the profile. The figure above shows the graphical results where the maximum variation in the data is about 1.9%.

6.5.2 Kwik Bond 3rd field visit data

The results at this level seem to have inconsistent results and will not be used for calibration. The chlorides seem to increase at lower depths which are not typical.

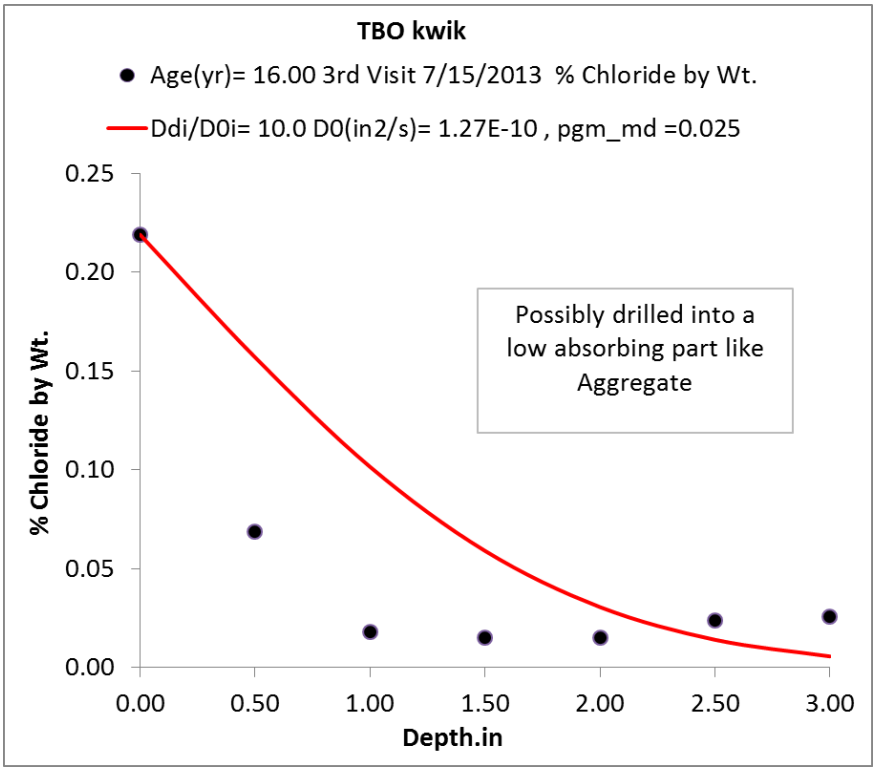

Figure-44 Kwik Bond Overlay (3rd visit)

6.5.3 Effectiveness of the Kwik Bond Overlay

The application of this overlay did decrease the level of chlorides mainly on the surface of the concrete.

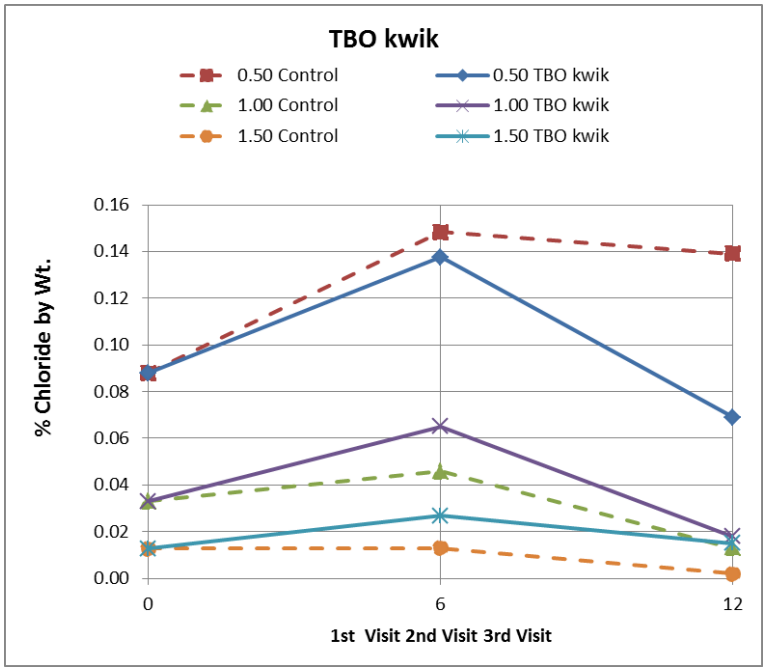

Figure-45 Field visit results

6.6 Model Evaluation with Euclid Overlay

6.6.1 Euclid 2nd field visit data

The following shows the profile for the 9 month age of the overlay placed. The model follows closely and approximates the field data fairly well with the calibrated factors. The figure below shows the graphical results where the maximum variation in the data is about 1.9%.

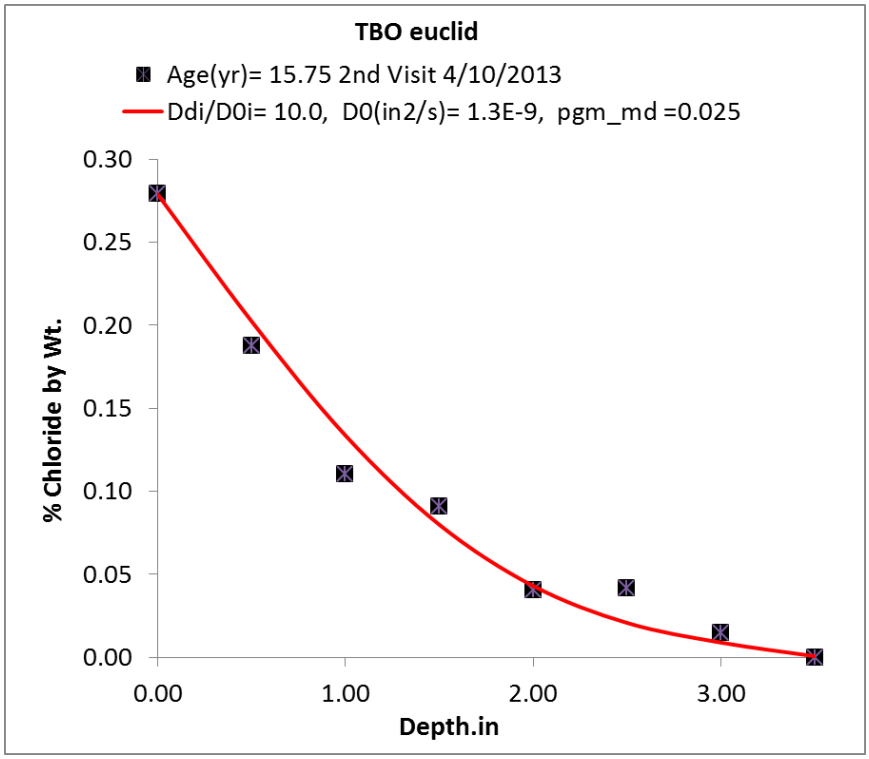

Figure-46 Euclid type Overlay (3rd visit)

6.6.2 Euclid 3rd field visit data

The 12 month evaluation period is not presented due to data inconsistency.

6.6.3 Effectiveness of the Euclid overlay

The application of this overlay did decrease the level of chlorides mainly on the surface of the concrete.

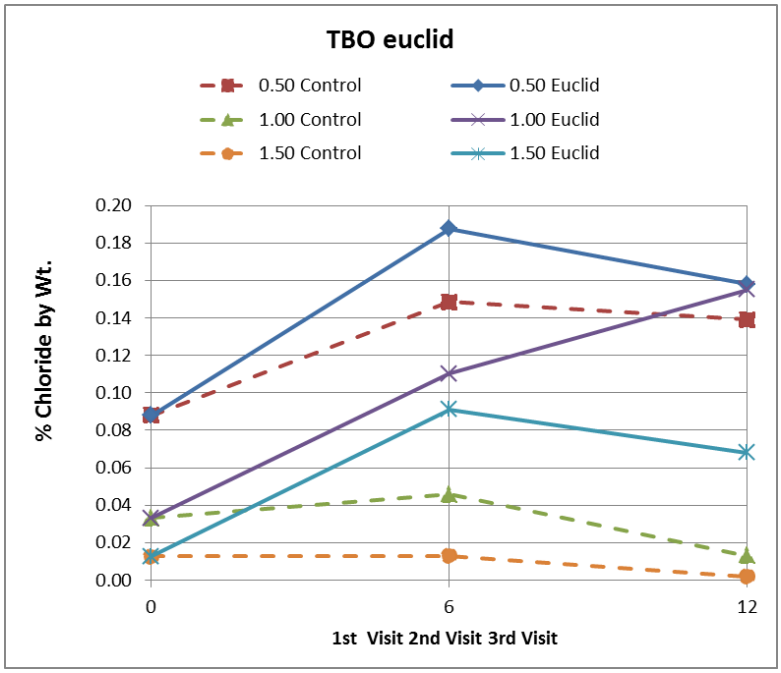

Figure-47 Field visit results

6.8 Conclusion

The TBO-Kwik overlay shows a lower coefficient of diffusion for the best fit for the field data indicating a better protection. The new program with multiple layer functionality and a new time scale "T" method incorporating damage factors, m_d, was used to predict the effective diffusivity of these thin bonded overlay layers that could be used to predict the corrosion time initiation. The margin of error was minimized to get a closer match to predict the diffusion coefficient for each product and is an effective tool to predict the corrosion initiation times.

Both overlays seems to lower the surface chloride levels at some point, however, the most adverse effect or increase in chloride concentration is observed for the TBO-Euclid at all depths and mainly at the 1.00 inch level at the 12 month period as shown in Figure-45 Field visit results above. Therefore, we can recommend that the most effective overlay for this bridge deck

application is the TBO-Kwik overlay type based on the developed method and equations for a multi-layer system.

Therefore, our new developed model modified to accommodate the new time scale methodology and a specific damage factor has been used to calibrate the diffusivity value.

This innovative method allows us to better evaluate the corrosion time and is a major improvement from previous single layer models.

Chapter 7

Statistical Analysis

Using the new multi-layer model and a critical chloride concentration at a rebar depth, the corrosion initiation time can be calculated. The calculated time will be an estimation because there are many parameters in the model are random variables. The focus of this chapter is to analyze statistically the variation of the estimation on the corrosion initiation time based on available knowledge of the random variables in the model.

7.1 Estimating the Standard Deviation of Corrosion Initiation Time

The general equation (Benjamin and Cornell, 1970; Clifton, 1993; Kirkpatrick et al., 2002b) below is used to evaluate the standard deviation of a function C(x,t) that depends on a set of independent random variables, σ_i, i = 1, 2, …N and N is the number of random variables in the function C. In the function C(x,t), x is the coordinate in space, and t is time. The partial derivatives of the function C(x,t) with respect to the random variables could be calculated analytically or numerically for simple or single layer systems and for the complicated multi-layer function.

In this study, the main random variable is the corrosion initiation time, which is expressed by the function C(x,t), the new multi-layer model. The random variables shown below are σ_1, σ_2 and σ_3 used in the main equation for the multi-layer model. These random variables will be selected and defined later in detail. The partial derivatives and the standard deviations of these random variables are required to calculate the standard deviation of the chloride concentration C(x,t) as follows:

$$\sigma_{c(x,t)}^{2} = (\frac{\partial C(x,t)}{\partial \sigma_1}.\sigma_{\sigma 1})^2 + (\frac{\partial C(x,t)}{\partial \sigma_2}.\sigma_{\sigma 2})^2 + (\frac{\partial C(x,t)}{\partial \sigma_3}.\sigma_3)^2 \qquad \text{Eq. (7.1)}$$

7.2 Single Layer Model:

The standard deviation of any variable X can be calculated using the equation below shown in a different form. We will ignore the higher order terms of the Taylor series in this case and use this general form of the equation as:

$$\sigma^2{}_X = \sum_{j=i}^{j=k}\left(\frac{\partial X}{\partial j} * \sigma_j\right)^2 \qquad \text{Eq. (7.2)}$$

Where:

σ_j: is the standard deviation of the variable "*j*".

$\frac{\partial X}{\partial j}$: is the partial derivative or slope of the variable X with respect to the variable "*j*".

For a single layer, the equation for diffusion is as follows:

$$C(x,t) = C_0 * \left[1 - erf\left(\frac{d}{\sqrt{4Dt}}\right)\right] = C_0 * \left[erfc(\frac{d}{\sqrt{4Dt}})\right] \qquad \text{Eq. (7.3)}$$

Where:

d: is the depth below the surface.

D: is the diffusion coefficient

t: is the time

efr, erfc: are the error and complementary error functions.

Solving for the value of the corrosion initiation time variable from the above equation, we get the following equation for t_{corr}:

$$t_{corr} = \frac{d^2}{4D.\left(erfc^{-1}(C/C_0)\right)^2} \qquad \text{Eq. (7.4)}$$

7.2.1 Slope of Corrosion Time Relative to Depth

If we further rearrange the terms, we find that the ratio of the corrosion initiation time, t_{corr}/d, is as follows:

$$\frac{t_{corr}}{d} = \frac{d}{4D.\left(erfc^{-1}(C/C_0)\right)^2} \qquad \text{Eq. (7.5)}$$

Now, we take the derivative of the function t_{corr} Eq. (7.4) with respect to d to get:

$$\partial t_{corr}/\partial d = \frac{2d}{4D.\left(erfc^{-1}(C/C_0)\right)^2} \qquad \text{Eq. (7.6)}$$

Now we replace the ratio or equation (7.5) in the derivative equation which is equation (7.6) to get a numerical determination of the slope as:

$$\partial t_{corr}/\partial d = \frac{2d}{4D.\left(erfc^{-1}(C/C_0)\right)^2} = 2\frac{t_{corr}}{d} \qquad \text{Eq. (7.7)}$$

The above slope value is for a single layer model without any topical protection. In this section, we will confirm these results by using our model for a single layer where the slope will be calculated at a specific depth and compared to the value from the equation above. This slope along with its standard deviation will be one of the terms used to get the final standard deviation

of the corrosion time. Other dependent factors could be determined similarly. The critical chloride threshold is set to 1 pound per cubic yard (pcy). The slope (the partial derivative) of the corrosion time relative to the depth variable is shown below.

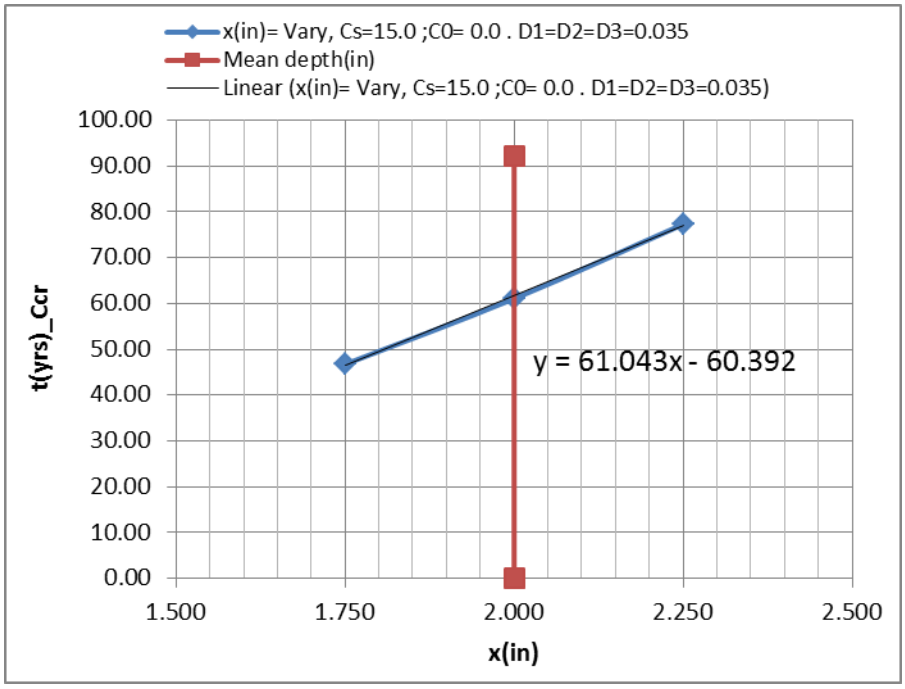

Figure-48 slope of relative to depth: “Single Layer”

It can be seen from the chart above that the slope of the corrosion time can be easily calculated and used in equation 6.17 to complete the first part of the evaluation for obtaining the standard deviation of the corrosion time. This slope is verified to be the same numerically and analytically at 61.043 as can be seen from the equation below describing the best fit for data used. The slope across a range of depth values remains a constant.

7.2.2 Slope of Corrosion Time Relative to Diffusivity

The value found earlier for t_{corr} is as follows:

$$t_{corr} = \frac{d^2}{4D.\left(erfc^{-1}(C/C_0)\right)^2} \qquad \text{Eq. (7.4)}$$

Now, we take the derivative of the function t_{corr} Eq. (7.4) with respect to the diffusivity, D, to get the following:

$$\partial t_{corr}/\partial D = \frac{-d^2}{4D^2.\left(erfc^{-1}(C/C_0)\right)^2} \qquad \text{Eq. (7.8)}$$

Now we replace the ratio or equation (7.5) in the derivative equation which is equation (7.7) to get a numerical determination of the slope as:

$$\partial t_{corr}/\partial D = -2\frac{t_{corr}}{D} \qquad \text{Eq. (7.9)}$$

The above slope value is for a single layer model without any topical protection. In this section also, we will confirm these results by using our model for a single layer where the slope will be calculated at a specific depth and compared to the value from the equation above. This slope is verified to be the same numerically and analytically at 3802.1 as can be seen from the equation below describing the best fit for data used.

This slope along with its standard deviation will be one of the terms used to get the final standard deviation of the corrosion time. Other dependent factors could be determined similarly. The slope of the corrosion time relative to the diffusivity of the first layer, D_1 is shown below.

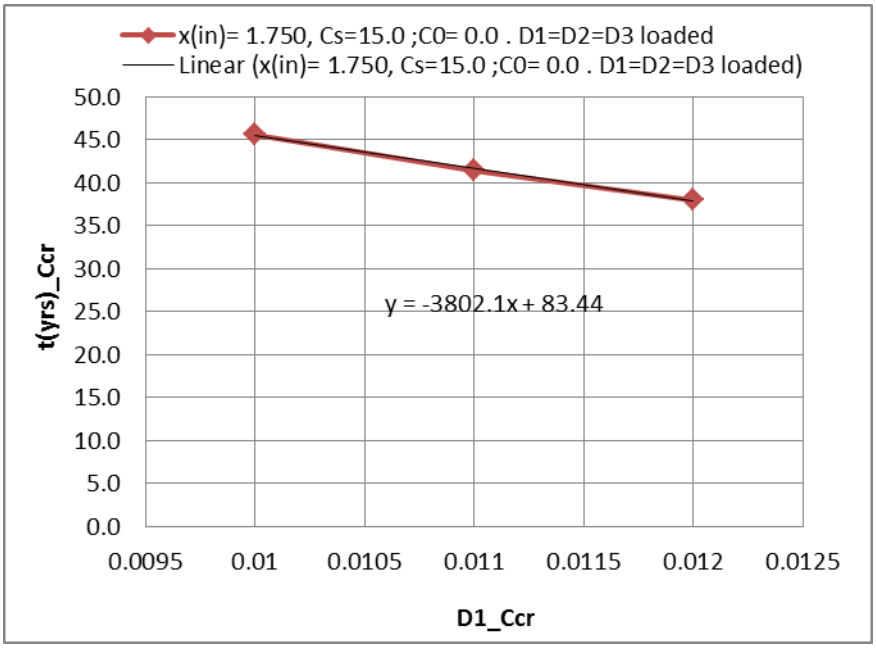

Figure-49 C(x,t) slope of relative to diffusivity: “Single layer”

Now, equation (7.2) can be used to get the final standard deviation using each of the considered variables standard deviation and slope as shown in the table below. The final standard deviation is calculated and shown below under column SD for C(x,t).

Table-19 Standard deviation for Single Layer

1-layer			
Variable	Mean	SD	slope=dy/dx
x(in)	2	0.50	61.04
$D_1(in^2/yr)$	0.02	0.01	-3802.00
t_{corr}	-	48.76	

7.3 Multiple Layer Model:

For a multiple layer system, the single layer equation or equation (7.3) cannot be used and the new multi-layer equation or equation (4.22) needs to be evaluated. Rearranging this new

equation to get the corrosion time as a function of the other variables numerically is a very complicated if not impossible.

Therefore, the evaluation of any contributing variable will be evaluated numerically. This will involve calculating the slope which is the derivative of the function with respect to the contributing variables. The function to be used for a multi-layer system is as follows:

$$C(x,t) = C_s - \frac{2(C_s - C_0)}{\pi}\int_0^{\infty} F(x,t,u)du \qquad \text{Eq. (4.22)}$$

$$W_3(u) = \frac{-1}{\sigma_1}\sin(u\sigma_1 h_2)\sin(uh_1) + \cos(u\sigma_1 h_2)\cos(uh_1)$$

$$V_3(u) = \frac{-1}{\sigma_1\sigma_2}\cos(u\sigma_1 h_2)\sin(uh_1) + \frac{1}{\sigma_2}\sin(u\sigma_1 h_2)\cos(uh_1)$$

$$F_3(x,t,u) = \frac{e^{-u^2 D_1 t}[\cos(\sigma_1\sigma_2 u(x-l_3))V_3(u) + \sin(u\sigma_1\sigma_2 u(x-l_3))W_3(u)]}{u(W_3^{\,2}(u) + V_3^{\,2}(u))}$$

The variation of the standard deviation of the chloride profile can be evaluated if the mean and standard deviation of the relevant variables in the above equation is considered. The main contributing variables are the depth x, the corrosion time t and the diffusivity of each individual layer. We will only consider the slopes relative to the depth and diffusivity in this research.

7.3.1 Analytical vs. Deterministic

The random variables that could be considered for the evaluations are the depth and the diffusivity of the corresponding used layers. In this section, we will evaluate the slope of the corrosion time relative to the depth (x) and the diffusivity of a specific layer as in the case of the single layer. For all the evaluations, the following parameters are used:

- h1, D1= thickness, diffusivity of the top most overlay layer.
- h2, D2= thickness, diffusivity of the second top most overlay layer.
- h3, D3= thickness, diffusivity of the concrete porous layer.
- x= depth into the concrete or the porous layer.
- C_s, Co= Surface and initial chloride concentration values.

The figure below is a representation of the slope variation for a multi-layer system with a concrete diffusivity value equal of 0.04 and is set to be higher than the upper protective layer. The critical chloride threshold is set to 1 pound per cubic yard (pcy). It is typical of a protective layer to have lower diffusivity values but that could be set to a lower value if it is determined that this layer is damaged.

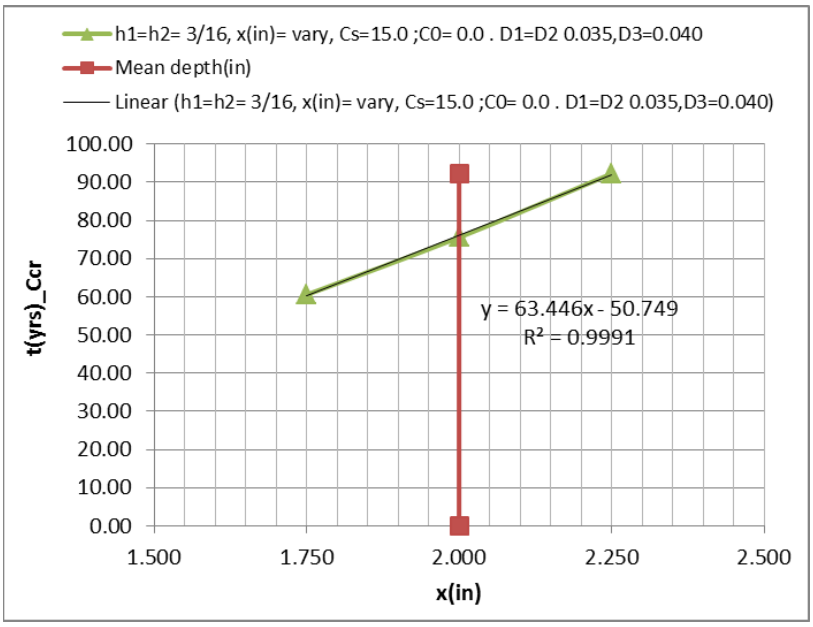

Figure-50 slope relative to depth: “Multi-Layer”

The slope of this variation is calculated from a best fit and has a value of 63.44 which is higher than the single layer which is expected indicating more time to reach the corrosion

threshold. The slope representing the partial derivatives along with the standard deviation for a certain variable could be used in the equation above to calculate the final standard deviation for that variable per equation (7.2).

As the above figure could be used to get the slope for the time variation with respect to depth, other variable variations could be easily calculated to get the slope. The second variable to be evaluated is the diffusivity of the upper overlay layer, D1 as shown in the figure below. It is assumed that the top overlay layers have the same thicknesses and diffusivity properties for this case even though they could be set to different values. This will be set as a task for future research topics.

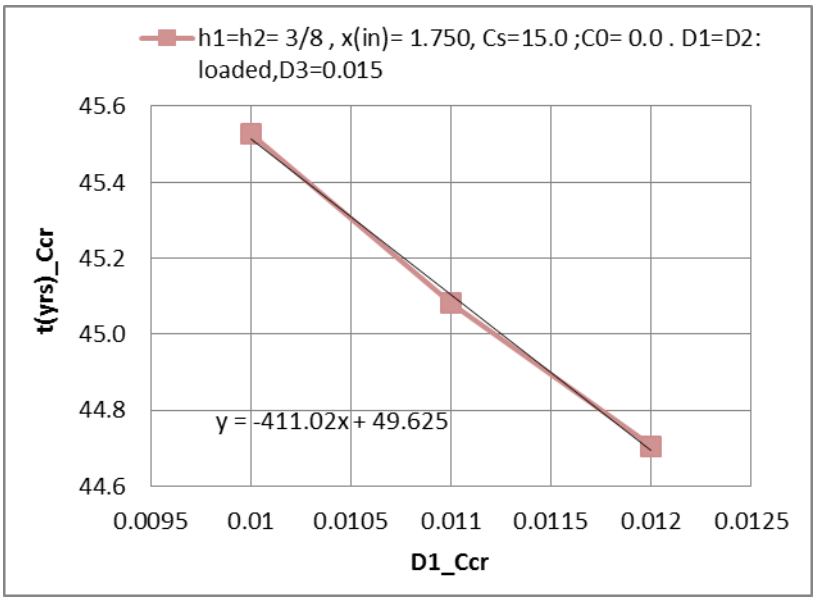

Figure-51 C(x,t) slope relative to diffusivity: ”Multi-Layer”

Now, equation (7.2) can be used to get the final standard deviation using each of the considered variables standard deviation and slope as shown in the table below. The final standard deviation is calculated and shown below under column SD for C(x,t).

Table-20 Standard Deviation for Multi-layer

Multi-layers			
Variable	Mean	SD	slope
x(in)	2	0.50	63.45
$D_1(in^2/yr)$	0.02	0.01	-411.02
t_{corr}	-	31.99	

It can be seen and concluded that not only the application of an overlay system increases the time to reach the corrosion threshold; it also decreases the standard variation by about 35% for the corrosion time as a secondary benefit. This can lead to better estimation of corrosion initiation times when using a multi-layered system of protection.

7.3 Sensitivity Analysis

In this section, we will evaluate the effect of the changes of several variables on the corrosion initiation times. The effect of the depth of the porous (concrete) layer, the water cement ratio (w/c) and the curing time t_o for a multi-layered system. The apparent diffusion coefficient developed by (Xi & Bazant) will be used for the analysis and is shown below as:

$$D_a = \left[\left(\frac{1}{4}+\frac{28-t_0}{300}\right)(w/c)^{6.55}+\frac{28-t_0}{62{,}500}\right].2\left[\frac{1-(V_p-V_p{}^c)}{S^2}\right](V_p-V_p{}^c)^f\left[1-K_{ion}(C_f)^m\right]$$

In this section, we will set the following term to be equal to 1:

$$\left[\frac{1-(V_p-V_p{}^c)}{S^2}\right](V_p-V_p{}^c)^f\left[1-K_{ion}(C_f)^m\right]=1 \qquad \text{Eq. (7.10)}$$

Thus the equation that will be used in generating the corrosion initiation time will be based on changing the w/c ratio and the curing time t_o. The apparent diffusivity is:

$$D_a = \left[\left(\frac{1}{4} + \frac{28 - t_0}{300}\right)(w/c)^{6.55} + \frac{28 - t_0}{62{,}500}\right].2 \qquad \text{Eq. (7.11)}$$

7.3.1 Single Layer Systems

For a single layer system, the sensitivity analysis is quite simple and will be evaluated for a 10% change in the selected variables mentioned earlier. For the variations in the water cement ratios and the curing time, the depth is kept a constant. Previous efforts have been done and published for a single layer evaluation. Our analysis also shows that the w/c ratio has the most effect on the results for the change in corrosion initiation as shown in the figure below:

For all the evaluations in this section, the following parameters are used:

- h1, h2= 0=thickness of overlay.
- C_s (Surface Chloride Concentration) = 15 (pcy).
- Co= (Initial Chloride Concentration) = 0 (pcy).
- $D_1 = D_2 = 0.01$, $D_3 = 0.035$. D_i= diffusivity of $layer_i$ when x is variable.
- x=1.75, $D_1 = D_2 = 0.01$ for the top most layers when D_3 ($D_{a)}$ is a variable.
- D_a= Diffusivity of the porous concrete layer based on w/c & t_o.

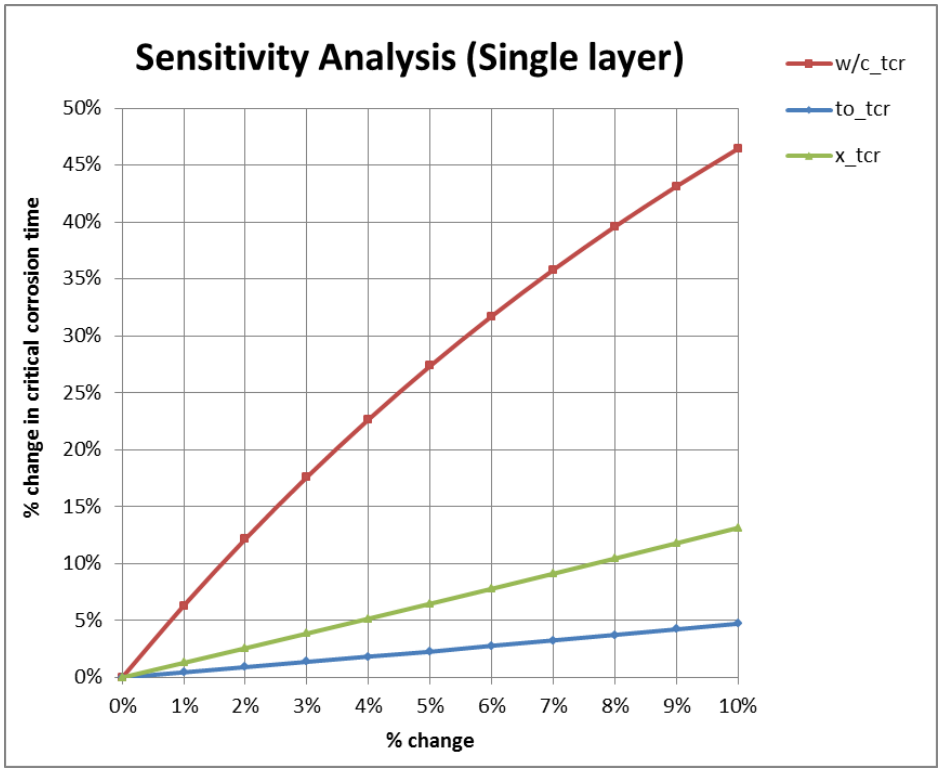

Figure-52 Single Layer Sensitivity Analysis

7.3.2 Multi-Layer Systems

For the multi-layer analysis, a maximum of 50% variation will be used for these variables in this study to determine which variable has the most effect on the results. Only one variable will be changed while keeping the others as constant. It is apparent from the figure below that the w/c shows the most impact on the results for the critical corrosion time for the multi-layer system also.

For all the evaluations in this section, the following parameters are used:

- h1, h2= 0=thickness of overlay.
- C_s (Surface Chloride Concentration) = 15 (pcy).
- Co= (Initial Chloride Concentration) = 0 (pcy).
- $D_1 = D_2 = 0.01$, $D_3 = 0.035$. D_i= diffusivity of layer$_i$ when x is variable.
- x=1.75, $D_1 = D_2 = 0.01$ for the top most layers when D_3 (D_a) is a variable.

- D_a= Diffusivity of the porous concrete layer based on w/c & t_o.

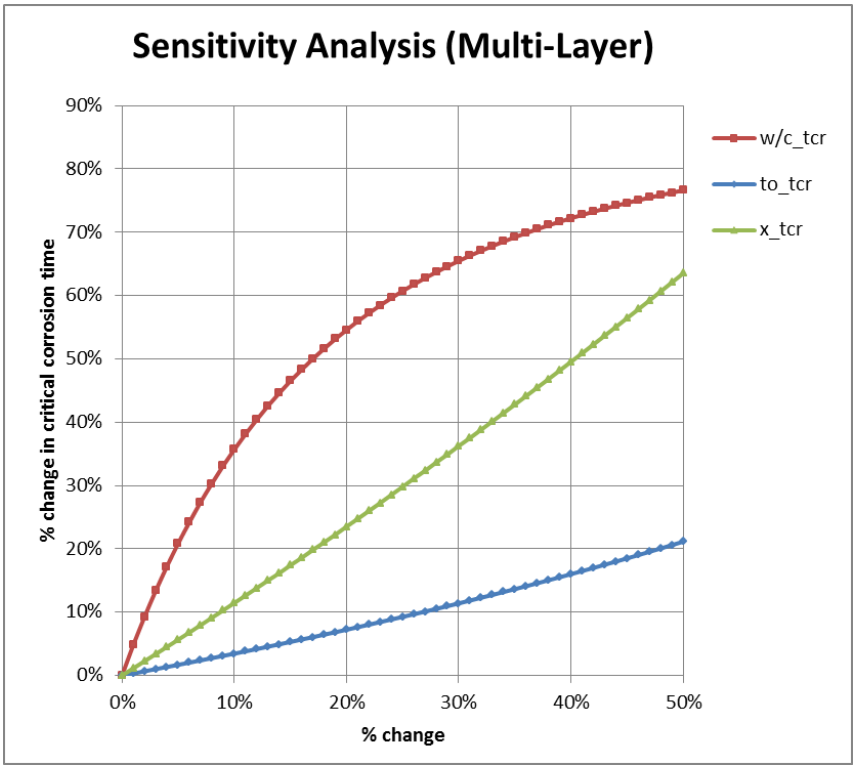

Figure-53 Sensitivity Analysis for Corrosion Initiation Time

It can be seen that for a multi-layer system that the w/c has the most influence on the results followed by the depth from the surface and lastly the cure time. This information is very valuable in the evaluation of the change in the corrosion initiation time for this system as seen in the table below. The % change is the improvement or reduction in values relative to the one layer system is shown below.

Table-21 Comparison at 10% change

t_{corr}	t_o	w/c	depth
1layer	4.7%	46.4%	13.1%
2layer	3.4%	35.7%	11.4%
% Change	27.1%	23.2%	12.9%

Even though the equations do show that the w/c has more influence on the results, the new multi-layer system allows us to predict the amount of change in the corrosion initiation

times. This has a significant benefit on corrosion cost and planning for best times to design a repair plan before it is too costly to do so.

7.4 Random Variables for Mean and Standard Deviation

The chloride concentration is based on the different diffusivity values of the different layers and these diffusivity values will be considered as random variables. The nature of the diffusivity values considered are unique and will be considered to be uniform in nature based on published data in (NIST, 1972-1995) records for the porous concrete layer.

The topical layers are assumed to have similar uniform variations and will be evaluated as such. Therefore the uniform distribution values will have a minimum and maximum values and randomly generated values in the range between minimum and maximum. The formula for generating these variables will be as follows:

$D_i = D_{min} + (D_{max}-D_{min})*[\text{random values between } (0, 1)]$. Eq. (7.11)

- D_{min}= the minimum diffusivity of a layer.
- D_{max}= the maximum diffusivity of a layer.

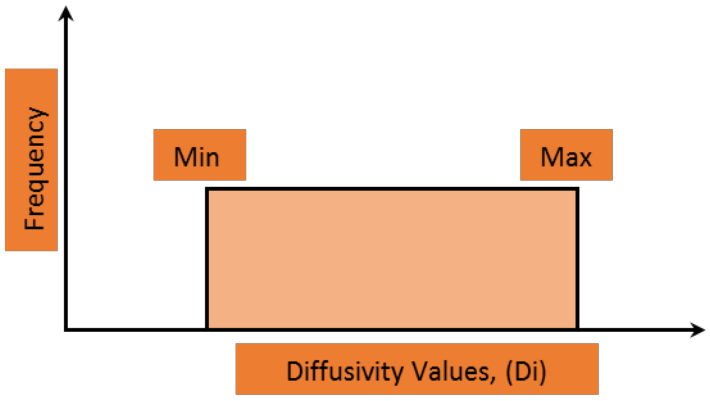

Figure-54 Uniform diffusivity

The table below shows the values to be used to study the effect on the mean and the standard deviation of the chloride concentration values for a randomly generated diffusivity values. Based on the NIST data available (NIST, 1972-1995) with the age of the samples of being less than 3 months, it is assumed that a ratio of 5 exists between the maximum and minimum ratio which will be used in this case.

Table-22 Diffusivity values

w/c =0.45		
in^2/yr	Min.	Max.
D_1	0.0500	0.2500
D_2	0.0600	0.3000
D_3	0.0700	0.3500

The above D_3 data represent data values that will be used and are generated for concrete samples having a w/c of 0.45. The diffusion values are assumed to occur randomly at the same time and loaded into the program to generate the set of data.

The top two overlay layers are the layers closer to the surface, D_1 and D_2, are assumed to have a lower diffusivity values initially to simulate real applications. The figure below shows a sample from a set of 100 generated points to evaluate the average chloride concentration value and the associated standard deviation for such a simulation.

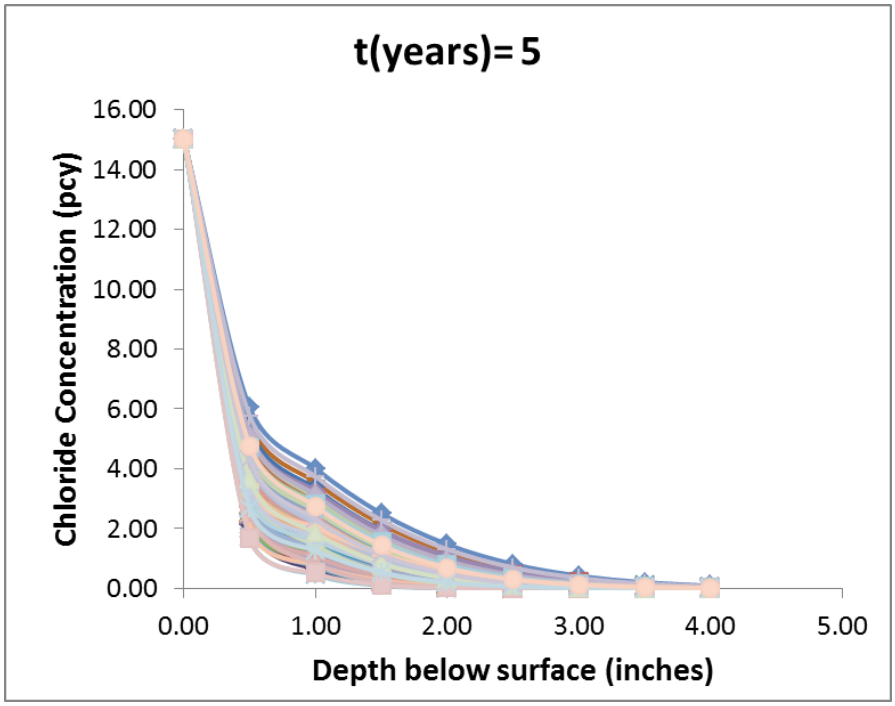

Figure-55: Data set for 100 points

These values could be used for a multi-layer system as a set of values to get more reliable results for the corrosion initiation time evaluation. The figure below shows the result for the average chloride profile and the critical threshold line to locate the depth where the corrosion initiation might start for the multi-layer system at a given time step taken as 5 years for this situation.

Depending on the location of the reinforcing steel, we can look at the concentration profile and recommend a state of damage for a given concrete specimen. For example, if the reinforcing steel depth is at 1.5 inches below the surface, then we could say that the corrosion initiation has reached the threshold we have set to take action, otherwise we could be facing more severe deterioration in the future. If the reinforcing is located 2 inched below the surface, then we could see that the risk of corrosion initiation is low and has not reached the threshold level yet.

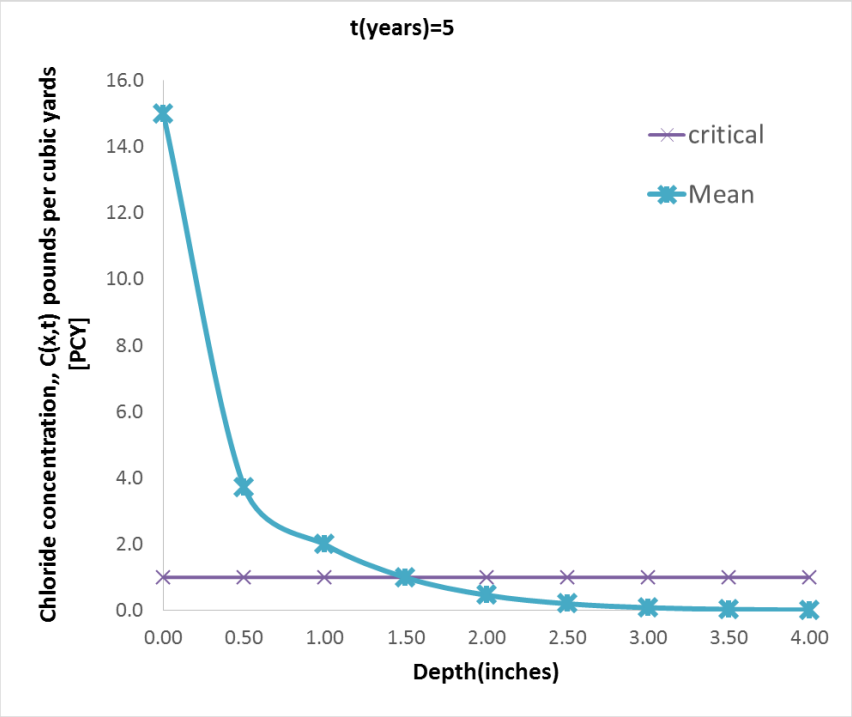

Figure-56 Chloride Concentration Average Profile

The figure below shows the result of the average and the standard deviation values generated for this data set. Given the set of data for the diffusion coefficients, we can estimate a reliable value for the mean and standard deviation to be used in the corrosion initiation time estimates.

We can recommend from these results installing the reinforcing steel at a depth with a low standard deviation to predict more reliable corrosion time estimates.

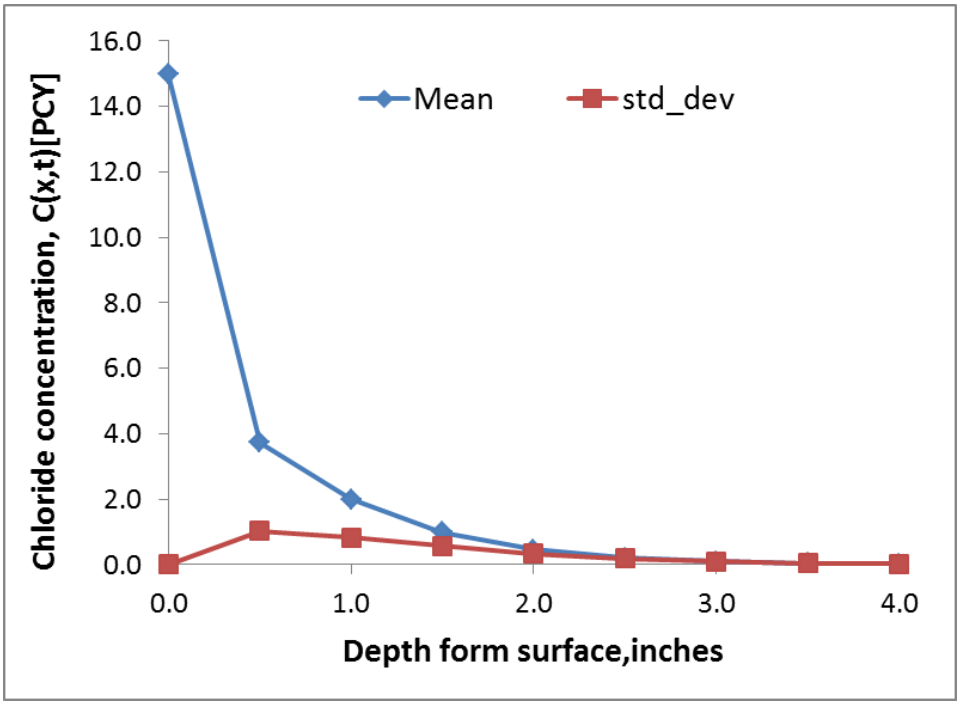

Figure-57 Sample Mean and Standard deviation

It is evident from the figure above that the standard deviation tends to be much lower at the 2 inch depth that is a typical depth of reinforcing steel used in most bridge designs. Therefore we could recommend that for a chloride threshold of a maximum of 1.0 pounds per cubic yards (pcy), we should place the steel at a minimum depth of about 1.5 inches below the surface.

7.5 Distribution of Random Variables

When investigating the distribution functions of the diffusion coefficients, we could see that the distribution does not follow a normal distribution. The figures below shows the distribution of the values used in our analysis. The distributions are shown for different depths in the last or concrete layer. It can be seen that when increasing the depth into the last layer, the distributions tend to deviate from a normal type of distribution. Therefore, a uniform type of distribution is applicable in this case.

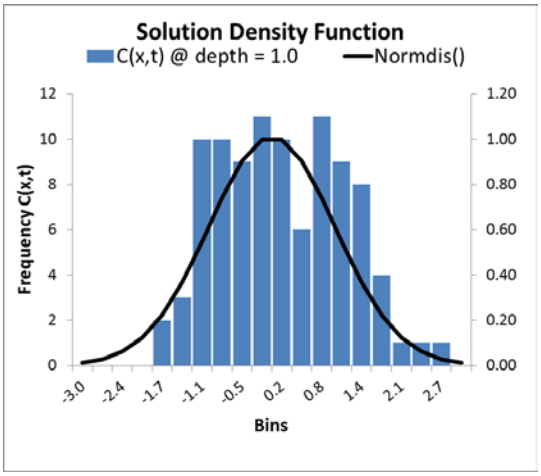

Figure-58 Distribution, x=1

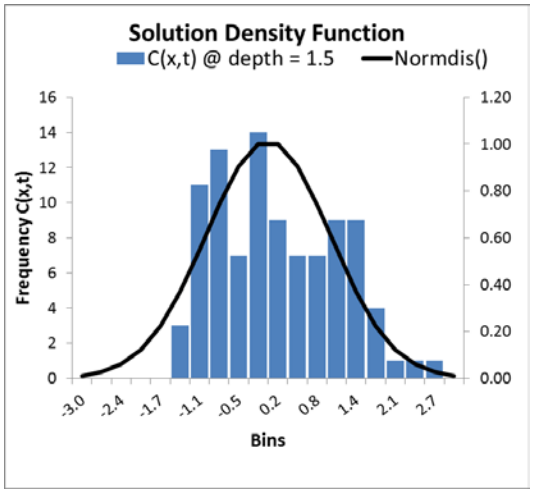

Figure-59 Distribution, x=1.5

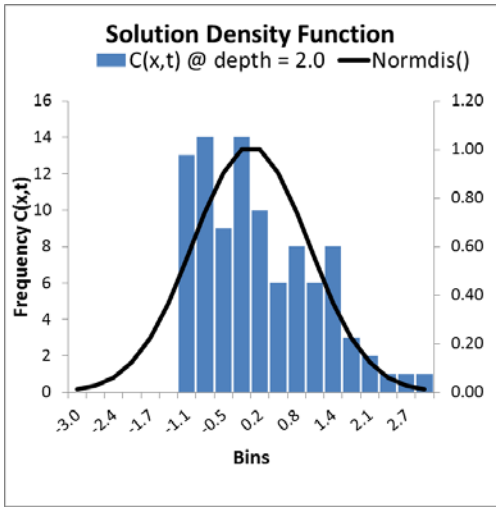

Figure-60 Distribution, x=2.0

Chapter 8

Summary and Suggestions for Future Work

8.1 Summary

It can be seen that the current diffusion models have solutions that are geared towards a single layer of porous media with a single diffusivity value but the new developed model can accommodate multiple layers to predict the corrosion initiation times.

We have developed and compared our multi-layer with linear boundary condition case to some of the existing systems used to predict the increase of corrosion initiation times. These systems do not have the capability to utilize the diffusivity of different layers but instead use a calibration method and they only work for a single layer.

In chapter 5, a new time scale, “T”, and a damage factor are used for the new model to predict the corrosion imitation acceleration with time. The new model is used by simply replacing the real time, t, with the new time scale factor, “T” and substituting the new values of the diffusivity values with new ratios to get the new chloride profiles. The new model successfully shows this increase in chlorides due to this damage effect.

In Chapter 6 we investigated a new composite damage method to use for the calibration of field samples taken from an actual site and make a recommendation on the most effective product to use for protecting the candidate bridge deck for the evaluation period and given data samples.

In chapter 7, we presented a numerical method to evaluate the slopes of some of the dependent variables considered to be part of the multi-layer chloride function. For a given set of standard deviations for these variables, we use the new program to get the slopes of the new

function relative to any variable and use the presented equation to get the aggregate standard deviation of the system.

We have also shown the sensitivity of the new multi-layer model due to variations of concrete diffusivity that has variables such as the water cement ratio (w/c), the cure time (t_o) and the depth (x). We have shown that for this multi-layer system, the w/c has the most effect on the results for a wide range of material variations ranging from 10% to 50%. This has been shown to be the case for a single layer model also.

Also, random values for the diffusivity of a three layer system have been used to evaluate the mean and standard deviation values for this sample. We have presented the results that show the mean and the standard deviation values that could be used to evaluate the standard deviation of the system as done in previous sections. This means that for any variable, the standard deviation could be evaluated as such and if the slope is evaluated as described in previous sections, the standard deviation for the system could be evaluated for better estimates of the corrosion initiation times.

Overall, our new models with linear and constant boundary conditions are considered to be new and innovative methods to predict the corrosion initiation times. The new models can be easily modified to accommodate damage factors using new time scale methods that can take into account damage factors.

8.2 Future Research

1. In Chapter 6, we have assumed the same composite damage factor for all the layers. However, this could be improved to investigate different m_d factors for the evaluation.
2. In Chapter 6, the number of samples used in this research for the calibration of the effective diffusivity values was limited. For better recommendations, it is best if more

field samples could be collected to get more data for the chloride concentrations and that will yield a more refined final evaluation.

3. In Chapter 7, we have calculated the slope of the chloride function due to the variation of a single diffusivity value. Since this is a multi-layer system, more than one diffusivity value could be varied to get a more refined estimate for the final standard deviation of the system.
4. In Chapter 7, we have assumed that there are no correlations between the diffusivity values of each of the topical layer. There might be some correlation that could be included as a future research task.

Bibliography

Bai,Y., Harajli, A., Xi,Y., (2015, November 4). Analytical Solutions of Ionic Diffusion and Heat Conduction in Multilayered Porous Media. *Journal of Applied Mathematics*, 12.

Benjamin, J.R. and Cornell, C.A. (1970) Probability, Statistics,and Decision for Civil Engineers, McGraw-Hill, New York.

Cady, P.D., and Weyers, E.R. (1983). "Deterioration rates of concrete bridge decks",
" *Journal of Infrastructure Systems*, ASCE, 4(4).

Crank, J. (1975)."The Mathematics of Diffusion", Oxford University Press, Oxford.

Clifton, J.R. (1993) 'Predicting the service life of concrete', ACI Mater. J., Vol. 90, No. 6, pp.611–617

Dave Johnson & Jerry Stephens, Interim Report Montana DOT, "Monitoring and evaluation of thin bonded overlays and Surface laminates for bridge decks".

Drumm, R. D. (1992). "Determination of the Service Life of Concrete Sealers on Horizontal and Vertical Bridge Members". M.S. thesis.

G. Okamoto (1977). “A Survey of the Cost of Corrosion in Japan”. Report of the Committee on Corrosion and Corrosion Protection. Japan Society of Corrosion Engineering and Japan Association of Corrosion Control.

George E. Ramey and John P. Derickson, P.E.(2003). “Performance of Bonded Bridge Deck Overlays in Alabama”, 20-21.

Gerhardus H. Koch, Michiel P.H. Brongers, Neil G. Thompson,Y. Paul Virmani, Joe H. Payer (2001). “Corrosion Cost and Preventive Strategies in the United States”, Report No. FHWA-RD-01-156.

H.H. Uhlig (1952). “The Cost of Corrosion in the United States, *Corrosion*, Vol. 6, 29.

Jennifer L. Kepler David Darwin Carl E. Locke, Jr, (2000). “Evaluation Of Corrosion Protection Methods For Reinforced Concrete Highway Structures”,112.

José A. Pincheira, Ph.D., and Melissa A. Dorhorst (2005). “Evaluation of Concrete Deck and Crack Sealers “, Report No. WHRP 06-09, 120-121.

Khossrow, Babaei and Hawkins, Neil M. (1988). “Evaluation of Bridge Deck Protective Strategies, *Concrete International*, Vol. 10, No. 12, 56-66.

Kirkpatrick, T.J., Weyers, R.E., Sprinkel, M.M. andAnderson-Cook, C.M. (2002b) ‘Impact of specification changes on chloride-induced corrosion service life of bridge deck’, *Cement and Concrete Research*, Vol. 32, No. 8,pp.1189–1197.

Li, L.Y., Damrongwiriyanupap, N., and Xi, Y. (2011) “A Probabilistic Prediction Model for the Corrosion Initiation Time of Steel Reinforcement in Concrete Structures”, *International Journal of Modelling, Identification and Control*, 14(1/2), 112-120.

Liang,M.T., Hong,C.L., and Liang, C.H. (1999). “Service Life Prediction of Existing Reinforced Concrete Structures Under Carbonation Induced Corrosion”, J. Of the Chinese Institute of Civil and Hydraulic Engineering, Vol. 11, No. 3, 485-492.

Mangat, P.S., and Molloy, B.T. (1994) ”Prediction of long term chloride concentration in concrete,” Materials and Structure 27, p338-346.

Mangat, P.S., and Limbachiya, M.C. (1999) “Effect of initial curing on chloride diffusion in concrete repair materials,” Cement and Concrete Research 29, 1475–1485.

Manning, David M. (1995). “Waterproofing Membranes for Concrete Bridge Decks”, NCHRP Synthesis of Highway Practice, 220.

Marcus L. Knight, G. Scott Wilson, Wayne J. Seger, and Sankaran Mahadevan (2004). “Overlay Types Used as Preventive Maintenance on Tennessee Bridge Decks”, 79-84.

McCaskil, Geo. A., Crumpton, Carl F., and Wendling, Wm. H. (1970). “Epoxy Resin Seal Coats and Epoxy Mortar Patching for Bridge Decks”, State Highway Commission of Kansas and Federal Highway Administration.

Michael M. Sprinkel (1998).” Very-Early-Strength Latex-Modified Concrete Overlay”. Technical Assistance Report.

Meggers, David (1999). Kansas Department of Transportation, personal communication.

Michael M. Sprinkel (2002). “Deck Protection Systems for Post-Tensioned Segmental Concrete Bridges”.

NCHRP (1979). “Synthesis of Highway Practice 57: Durability of Concrete Bridge Decks”. Transportation Research Board.

NIST. (1971 & 1995). *NIST*. Retrieved from http://ciks.cbt.nist.gov/~bentz/clpencon.html

Paul A. Rowekamp, PE, (2004). “The Minnesota Department of Transportation’s Experience with High Performance Concrete Bridge Decks”,146-155.

Pfeifer, D. W. and Scali, M. J. (1981). “Concrete Sealers for the Protection of Bridge Structures”, NCHRP Report 244, 138.

Russ Alger, Scott Gruenberg, Joe Wegleitner (2003). Field Performance of Polymer Bridge Deck Overlays in Michigan", Report No.Research Report RC-1422.

Sherman, Matthew R., Carrasquillo, R. L., and Fowler, D. W. (1993). "Field Evaluation of Bridge Corrosion Protection Measures", Report No. FHWA/TX-93+1300-1, Texas Department of Transportation.

Sprinkel, Michael M. (1992). "Twenty-Year Performance of Latex-Modified Concrete Overlays", Conference Paper, Transportation Research Board.

Steven Soltesz (2010). "Evaluation of Thin Overlays for Bridge Decks", Oregon Department of Transportation, Research Report No. FHWA-OR-RD-11-05.

Stewart, G.M., and Rosowsky, V.D. (1998). "Structural safety and serviceability of concrete bridges subject to corrosion." Journal of Infrastructure Systems, ASCE, 4(4), 146-155.

T.P. Hoar (1971). Report of the Committee on Corrosion Protection. " A Survey of Corrosion Protection in the United Kingdom".

Washington interim report (1986). "Concrete Overlay for Bridges". Washington State Transportation Center.

Wenzlick, J. D. (1999, 2000). Missouri Department of Transportation, personal communication.

Xi,Y., and Bazant, Z.P. (1999) "Modeling chloride penetration in saturated concrete", *J. Mater. Civ. Eng.*, Vol. 11, No. 1, pp. 58-65.

Xi,Y., and Bazant, Z.P., Molina, L. and Jennings, H.M. (1994a) " Moisture diffusion in cementitious materials: adsorption isotherm', *Adv. Cem. Based Mater.*, Vol. 1, No. 6, pp. 248-257.

Xi,Y., and Bazant, Z.P., Molina, L. and Jennings, H.M. (1994b) " Moisture diffusion in cementitious materials: moisture capacity and diffusivity', *Adv. Cem. Based Mater.*, Vol. 1, No. 6, pp. 258-266.

Xi, Y., Eskandari-Ghadi, M., Suwito, and Sture. S. (2006) "A Damage Theory Based on Composite Mechanics", *J. of Eng. Mech., ASCE*, 132(11), 1-10.

Xi, Y., Willam, K., and Frangopol, D. (2000) "Multi-scale Modeling of Interactive Diffusion Processes of Concrete," Journal of Engineering Mechanics, ASCE, 126(3), 258-265.

Xi, Y. and Nakhi, A. (2005) "Composite Damage Models for Diffusivity of Distressed Materials", *J. of Materials in Civil Engineering*, ASCE, May/June, 17(3), 286-295.

Yu-chang Liang, Weiping Zhang, Yunping Xi (2010). “Strategic Evaluation of Different Topical Protection Systems For Bridge Decks And The Associated Life-Cycle Cost Analysis”, pp. 6.

Zemajatis, Jerzy, Weyers, Richard E., and Sprinkel, Michael (1999). “Performance of Corrosion Inhibitors and Galvanized Steel in Concrete Exposure Specimens,” Report No. VTRC 99-CR4, Virginia Transportation Research Council.

Zemajtis, J., and Weyers, Richard (1996).“Concrete Bridge Service Life Extension Using Sealers in Chloride-Laden Environments”. Transportation Research Record 1561, 1-5.

Appendix A

Derivation for Constant Boundary condition

Derivation: Layer #1:

$$\frac{\partial C_1}{\partial t} = D_1 \frac{\partial^2 C_1}{\partial x^2}, (l_1 \le x \le l_2)$$

Multiply both sides by e^{-pt} and integrate:

$$\int_0^\infty \frac{\partial C_1}{\partial t}.e^{-pt} = \int_0^\infty D_1 \frac{\partial^2 C_1}{\partial x^2}.e^{-pt} \qquad \text{Eq. (A.1)}$$

Evaluate the left term using

$$\int u.dv = u.v - \int v.du \qquad \text{Eq. (A.2)}$$

Appling integration by parts where:

$$u = e^{-pt} \;\&\; dv = \frac{\partial C_1}{\partial t}$$
$$v = C_1(x, p), du = -p.e^{-pt}dt$$

We get

$$\int_0^\infty \frac{\partial C_1}{\partial t}.e^{-pt} = e^{-pt}.C_1(x, p) - \int_0^\infty C_1(x, p).-p.e^{-pt}dt$$
$$\int_0^\infty \frac{\partial C_1}{\partial t}.e^{-pt} = e^{-pt}.C_1(x, p) - p\int_0^\infty C_1(x, p).e^{-pt}dt \qquad \text{Eq. (A.3)}$$

Using Laplace transform of C as $\overline{C}$, we define:

$$\overline{C}_1(x, p) = L(C_1(x, p)) = \int_0^\infty C_1(x, p)e^{-pt}dt \qquad \text{Eq. (A.4)}$$

Applying the boundary condition for layer 1 where C(x,o)= C_o, we get

$$\int_0^\infty \frac{\partial C_1}{\partial t}.e^{-pt} = e^{-pt}.C_1(x,p) - \int_0^\infty C_1(x,p).-p.e^{-pt}dt = p.\overline{C_1}(x,p) - C_0 \qquad \text{Eq. (A.5)}$$

The new form of the differential equation is:

$$\frac{d^2}{dx^2}\overline{C}_1(x,p) = \frac{p}{D_1}.\overline{C_1}(x,p) - \frac{C_0}{D_1} \qquad \text{Eq. (A.6)}$$

The flux at distance l_1 and its Laplace is ($\overline{J_0}$ is the Laplace of J_0) is as follows:

$$\frac{d}{dx}C_1(l_1,p) = \frac{J_0}{D_1}$$

$$\frac{d}{dx}\overline{C}_1(l_1,p) = \frac{\overline{J_0}}{D_1}$$

We now formulate this differential equation as:

$$\frac{d^2}{dx^2}\overline{C}_1(x,p) = \frac{p}{D_1}.\overline{C_1}(x,p) - \frac{C_0}{D_1}$$

For $q_1 = \sqrt{\frac{p}{D_1}}$

and the solution is as follows:

$$\overline{C}_1(x,p) = s_1 e^{-q_1 x_1} + s_2 e^{q_1 x_1} + \frac{C_0}{p} \qquad \text{Eq. (A.7)}$$

s_1 & s_2 are to be determined

Applying the derivative of the Laplace solution and set to:

$$\frac{d}{dx}\overline{C}_1(l_1, p) = -\frac{\overline{J_0}}{D_1}$$

We get:

$$-\frac{\overline{J_0}}{D_1} = q_1 s_1 e^{-q_1 l_1} + q_1 s_2 e^{-q_1 l_1} \qquad \text{Eq. (A.8):}$$

We recall the following boundary condition and applying the Laplace transform we get:

$$C_1(l_1, t) = C_s$$

$$\overline{C}_1(l_1, p) = \frac{C_s}{p} = \overline{C}_s$$

Now we have the following two equations and we solve for s_1 & s_2:

$$\overline{C}_1(x, p) = \overline{C_s} = s_1 e^{-q_1 l_1} + s_2 e^{q_1 l_1} + \frac{C_0}{p} \qquad \text{Eq. (A.9):}$$

Rewritten as:

$$\overline{C}_s - \frac{C_0}{p} = s_1 e^{-q_1 x_1} + s_2 e^{q_1 x_1}$$

$$-\frac{\overline{J_0}}{D_1} = q_1 s_1 e^{-q_1 l_1} + q_1 s_2 e^{-q_1 l_1} \qquad \text{Eq. (A.10):}$$

We get the following solution:

$$s_1 = \frac{(\overline{C}_s - \frac{C_0}{p}) + \frac{\overline{J_0}}{q_1 D_1}}{2}.e^{-q_1(x-l_1)}, s_2 = \frac{(\overline{C}_s - \frac{C_0}{p}) - \frac{\overline{J_0}}{q_1 D_1}}{2}.e^{q_1(x-l_1)}$$ Eq. (A.11)

We now replace the value of s_1 & s_2 and apply the derivative to the solution to get value of the Laplace for the flux J which needs to be determined and is shown below:

$$\overline{C_1}(x,p) - \frac{C_0}{p} = \left(\overline{C_1}(l_1,p) - \frac{C_0}{p}\right)\cosh q_1(x-l_1) - \frac{\overline{J_0}}{q_1 D_1}\sinh q_1(x-l_1)$$ Eq. (A.11):

Eq. (A.12):

$$\overline{J_1}(x,p) = -D_1\frac{d}{dx}\overline{C}_1 = -q_1 D_1\left(\overline{C}(l_1,p) - \frac{C_0}{p}\right)\sinh q_1(x-l_1) + \overline{J_0}\cosh q_1(x-l_1)$$

Derivation: Layer #2:

For the second Layer we develop similar equations as shown:

$$\overline{C}_2(x,p) = L(C_2(x,p)) = \int_0^\infty C_2(x,p)e^{-pt}dt$$

$$q_2 = \sqrt{\frac{p}{D_2}}$$

$$\frac{d^2}{dx^2}\overline{C}_2(x,p) = \frac{p}{D_2}.\overline{C_2}(x,p) - \frac{C_0}{D_2}$$

$$C_1(l_2,t) = C_2(l_2,t)$$

Eq. (A.13):

$$\overline{C_2}(x,p)-\frac{C_0}{p}=\left(\overline{C_1}(l_2,p)-\frac{C_0}{p}\right)\cosh q_2(x-l_2)-\frac{\overline{J_1}}{q_2D_2}\sinh q_2(x-l_2)$$

Eq. (A.14):

$$\overline{J_2}(x,p)=-D_1\frac{d}{dx}\overline{C}_1=-q_1D_1\left(\overline{C}(l_1,p)-\frac{C_0}{p}\right)\sinh q_1(x-l_1)+\overline{J_1}\cosh q_1(x-l_1)$$

Derivation: Layer #3:

For the concrete Layer we develop similar equations as shown:

$$\overline{C}_3(x,p)=L(C_3(x,p))=\int_0^\infty C_3(x,p)e^{-pt}dt$$

$$\frac{d^2}{dx^2}\overline{C}_3(x,p)=\frac{p}{D_3}.\overline{C_3}(x,p)-\frac{C_0}{D_3}$$

$$C_2(l_3,t)=C_3(l_3,t)$$
$$C_3(\infty,t)=C_0$$

$$\overline{C}_3(\infty,p)=\frac{C_0}{p}$$

For $q_3=\sqrt{\frac{p}{D_3}}$

Eq. (A.15):

$$\overline{C}_3(x,p)-\frac{C_0}{p}=\left(\overline{C_3}(l_3,p)-\frac{C_0}{p}\right)\cosh q_3(x-l_3)-\frac{\overline{J_3}}{q_3D_3}\sinh q_3(x-l_3)$$

Eq. (A.16):

$$\overline{J_3}(x,p) = -D_3 \frac{d}{dx}\overline{C}_3 = -q_3 D_3 \left(\overline{C_3}(l_3,p) - \frac{C_0}{p} \right) \sinh q_3 (x - l_3) + \overline{J_3} \cosh q_3 (x - l_3)$$

We notice that these equations have a relationship which is the fluxes in layers 1, 2 and 3. We can use this relation to substitute in the above equations to find the final solution as :

$$\overline{C}_3(x,p) = \frac{C_0}{p} + \left(\overline{C_s} - \frac{C_0}{p} \right) . \frac{e^{-q_3(x-l_3)}}{Z} \qquad \text{Eq. (A.17)}$$

Recalling that:

$$\overline{C}_1(l_1,p) = \frac{C_s}{p} = \overline{C}_s$$

$$\overline{C}_3(x,p) = \frac{C_0}{p} + \left(\frac{C_s}{p} - \frac{C_0}{p} \right) . \frac{e^{-q_3(x-l_3)}}{Z} \qquad \text{Eq. (A.18)}$$

Regrouping we get:

$$\overline{C}_3(x,p) = \frac{C_0}{p} + (C_s - C_0) . \frac{e^{-q_3(x-l_3)}}{p.Z} \qquad \text{Eq. (A.19)}$$

The solution (constant surface chloride concentration)

The solution requires setting p*Z=0. By definition, p must be large enough on Laplace space for a solution to converge. Since p=0 is one of the solutions and if we need to find another solution, then we need to check the value of Z as shown below:

Set

$p=-\beta^2 D$ to simplify the solution.

p is the transformation of time variable space to the Laplace space.

Substitute into Z, grouped terms for simplifying the equation, and set Z=0.

β is an arbitrary constant.

We get Eq. (A.20)

$$Z = \sqrt{\frac{D_3}{D_1}}\sinh q_1(l_2 - l_1)\cosh q_2(l_3 - l_2) + \sqrt{\frac{D_3}{D_2}}\cosh q_1(l_2 - l_1)\sinh q_2(l_3 - l_2) + \sqrt{\frac{D_2}{D_1}}\sinh q_1(l_2 - l_1)\sinh q_2(l_3 - l_2) + \cosh q_1(l_2 - l_1)\cosh q_2(l_3 - l_2)$$

$$\sigma_1 = \sqrt{\frac{D_1}{D_2}} \qquad \sigma_2 = \sqrt{\frac{D_2}{D_3}} \qquad \frac{1}{\sigma_1.\sigma_2} = \sqrt{\frac{D_3}{D_1}}$$

Set $p=-\beta^2 D$ to simplify the solution and using

$$Z = \frac{1}{\sigma_1\sigma_2}\sinh i\beta h_1.\cosh i\beta\sigma_1 h_2 + \frac{1}{\sigma_2}\cosh i\beta h_1.\sinh i\beta\sigma_1 h_2 + \frac{1}{\sigma_1}\sinh i\beta h_1.\sinh i\beta\sigma_1 h_1) + \cosh i\beta h_1.\cosh i\beta\sigma_1 h_2$$

If Z=0, then:

$$0 = i\frac{1}{\sigma_1\sigma_2}\sin\beta h_1.\cos\beta\sigma_1 h_2 + i\frac{1}{\sigma_2}\cos\beta h_1.\sin\beta\sigma_1 h_2 - i\frac{1}{\sigma_1}\sin\beta h_1.\sin\beta\sigma_1 h_1) + \cos\beta h_1.\cos\beta\sigma_1 h_2$$

Since there is no β satisfying this equation to make it equal to 0, the only point that will satisfy these conditions is p=0. Therefore since $Z \neq 0$, then p=0 is the only solution.

Applying the inverse Laplace Transform we get:

$$C_3(x,p) = L^{-1}[(\overline{C}_3(x,p)] = C_0 + (C_s - C_0).\frac{1}{2\pi i}\int_{\gamma-i\infty}^{\gamma+i\infty}\frac{e^{-q_3(x-l_3)}}{p.Z}.e^{pt}dt$$ Eq. (A.21):

Appendix B

$$F_3(x,t,u) = \frac{e^{-u^2 Dt}[\cos(\sigma_1\sigma_2 u(x-l_3))V_3(u) + \sin(u\sigma_1\sigma_2 u(x-l_3))W_3(u)]}{u(W_3{}^2(u) + V_3{}^2(u))}$$

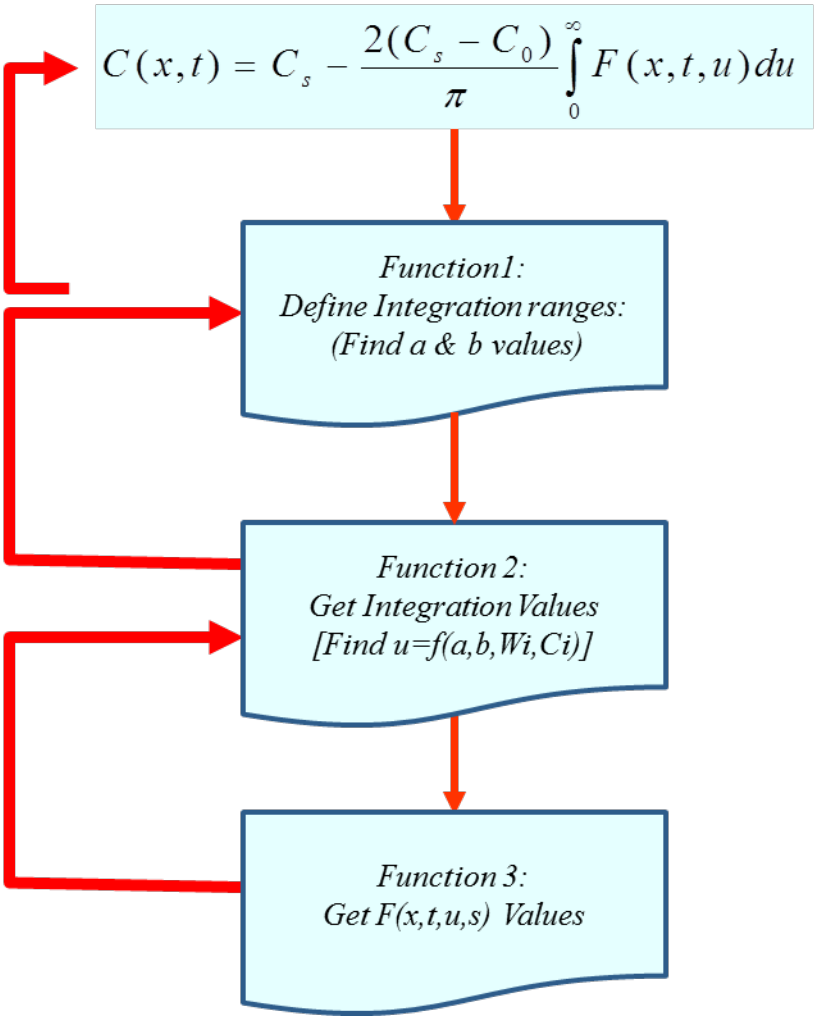

Figure-61 Program Flow Chart (Constant Boundary)